Summer 2016

A control algorithm for the solar village microgrid system

Hamad Ahmed Alharkan

Department:

A CONTROL ALGORITHM FOR THE SOLAR VILLAGE MICROGRID SYSTEM

by

HAMAD AHMED ALHARKAN

A THESIS

Presented to the Faculty of the Graduate School of the

MISSOURI UNIVERSITY OF SCIENCE AND TECHNOLOGY

In Partial Fulfillment of the Requirements for the Degree

MASTER OF SCIENCE IN ELECTRICAL ENGINEERING

2016

Approved by

Dr. M. Ferdowsi, Advisor
Dr. J. Kimball
Dr. P. Shamsi

ABSTRACT

In this thesis, the concept of microgrid system is introduced. Also, the major components of a microgrid will be discussed thoroughly. Both grid-connected and autonomous modes are explained. In addition, the control of a microgrid is defined for the following types: local, centralized and decentralized control.

As one of the nation's premiere research universities, the Missouri University of Science and Technology has built four inspirational solar houses (solar villages) for a competition in the US Department of Energy Solar Decathlon to allow students to research and improve different aspects of the microgrid system. Consequently, this thesis develops a computer model and displays the houses and the components of the Missouri S&T solar village. Also, it illustrated some technologies and techniques used in the solar village.

The simulation of the solar village system will be designed by MATLAB and is based on the data obtained from the real system. Energy management systems and the control scenarios of battery charging and discharging are provided along with an analysis of how effectiveness could be increased. Also, it proposed some specific algorithms to manage the power flow of the system based on the battery's state of charge (SOC), solar power generation, and load. The algorithms work to control SOC and operate under the following conditions: charging the battery, and discharging the battery, importing power from a utility, and exporting power to a utility. The primary focus in this thesis is to find a way to have the final SOC after a specific time be close to the initial SOC and maintain the SOC between reasonable range.

ACKNOWLEDGMENTS

I would like to express my sincere gratitude and appreciation to Dr. Mehdi Ferdowsi, my advisor during my master's program. He provided me with great guidance and advice throughout the program and generously gave of his time and knowledge. I would also like to thank Dr. Jonathan Kimball and Dr. Poura Shamsi for their time and advice.

I would like to thank the Saudi Arabian Cultural Mission (SACM) for providing me with financial assistance. I am also very grateful to Alqassim University for providing me with a full scholarship to allow me to pursue my master's degree. I truly appreciate their support and cooperation.

Also, I would like to thank my family. My parents, Ahmed Alharkan and Badrya Alqneeair, provided me with unending support throughout my master's program and always encouraged me to do my best, even when I doubted myself. I would also like to thank my wife, Hissah Almousa. She was extremely supportive, helpful, patient, and provided me with great motivation. Finally, I am grateful for the support that my brothers, sisters, and friends provided.

TABLE OF CONTENTS

LIST OF ILLUSTRATIONS

LIST OF TABLES

1. INTRODUCTION

1.1. MICROGRID

A microgrid is defined as a set of interconnected loads and distributed energy sources (microsources) throughout explicitly defined electrical restrictions that can be operated as a single controllable load. The general structure of micrgrid is shown in Figure 1.1. The microgrid is connected to the main grid through a common point of coupling, but can be separated from the main grid if there are disturbances with the power utility or problems with the power quality. Therefore, a microgrid provides local power generation for local loads. Microgrids can be powered by diverse energy sources including local and small distributed energy sources such as microturbines, wind turbines, fuel cells, and photovoltaic (PV) systems that are joined with storage devices that make the system highly efficient and able to supply continuous local loads. The local loads can be classified into two groups, the sensitive and non-sensitive load, based on the need to prevent power outages. Sensitive loads are defined as loads that are constantly supplied while non-sensitive loads are loads that can be shut down if there are disturbances in the main grid or problems in power equality. In addition, microgrids have features that allow extra power from the local generators to be sent to the utility grid, however, the main purpose of the microgrid is to avoid power outages that impact sensitive loads. In addition, one of the differences between a conventional grid and a microgrid is efficiency. A conventional grid has higher losses compared to a microgrid due to the large amount of energy that is wasted in a conventional grid as heat. Meanwhile, the power sources in a microgrid are small (microsources) and located in close proximity to the loads [1-4] which allow for more usable energy. The following are some of the advantages and disadvantages of a microgrid:

The advantages of a microgrid [201]:

- A main benefit of a microgrid system is its ability to island and isolate itself from a utility seamlessly with little or no interruption to the loads within the microgrid.
- A microgrid protects utility grid from any problems by decreasing the pressure on the grid during maximum peak hours.

- A microgrid uses low- or zero-emission generators which provide huge environmental advantages.
- A microgrid's generator is close to users which allows energy to be delivered with higher efficiency with less conduction losses.
- A microgrid reduces electricity costs by producing enough power to meet energy needs, but not producing excess energy.

The disadvantages of a microgrid:

- Voltage, frequency, and power quality are three main parameters that must be carefully considered and controlled using acceptable standards to maintain the proper power and energy balance.
- Electrical energy must be stored in battery banks which requires greater space and maintenance.
- If required, resynchronizing a microgrid with the utility grid is difficult.
- Microgrids must be properly protected.
- Issues such as standby charges and net metering may be problematic.

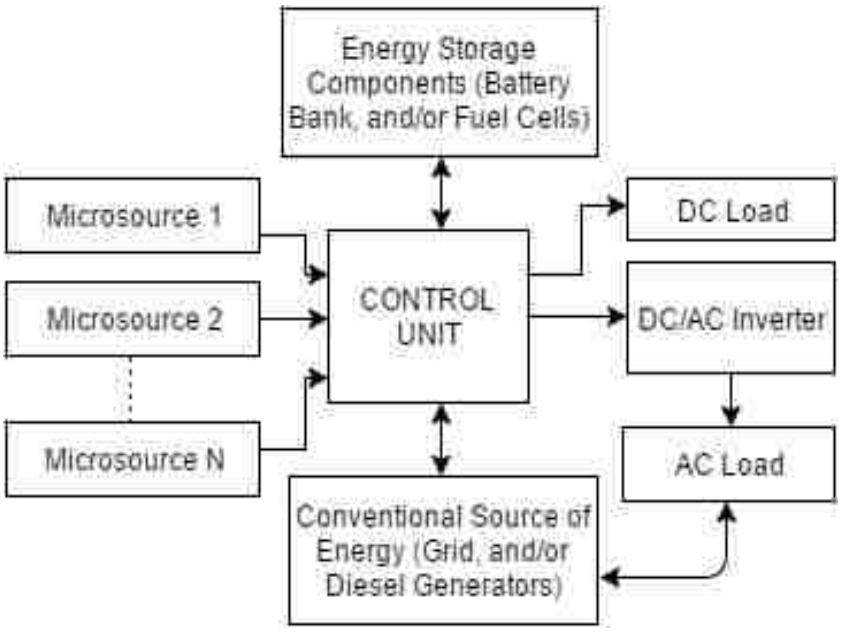

Figure 1.1. The general structure of microgrid.

1.2 COMPONENTS OF MICROGRID

In this section, some of the main components in a microgrid system will be discussed including the distributed generator or microsources such as the PV system, fuel cell, and wind turbine. Second, the power electronic elements in a microgrid will be discussed along with the storage system.

1.2.1. Distributed Generators. The following sections provide information about distributed generators.

1.2.1.1. PV system. A photovoltaic (PV) system, also called a photovoltaic power system or a solar panel, is one of the forms of sustainable energy. A solar panel uses sun rays to produce electricity. There are different types of the solar panels, which includes monocrystalline, polycrystalline and thin film. The solar village houses used monocrystalline and polycrystalline. Monocrystalline consists of silicon ingots. Four sides of cylindrical ingots are eliminated to make a slices of silicon ingots in order to optimize the function of a single monocrystalline solar cell. Monocrystalline solar panel have high efficiency rates, which is typically from 15% to 20%. Furthermore, since this type of solar panel produces a high power, they do not require a large space. It generates electricity as four times as thin-film solar panels. The maintenance of monocrystalline is low. However, the cost of monocrystalline is high. Figure 1.2 shows the shape of monocrystalline solar panel and cell.

Figure 1.2. The shape of monocrystalline solar panel and cell.

Polycrystalline solar panel consists of square silicon ingots. Since the complexity of making a polycrystalline solar panel is relatively simpler than monocrystalline, the cost of polycrystalline is low. Also, it has a typical efficiency from 13% to 16%, because the silicon purity is less than monocrystalline. Finally, it requires a large space to generate enough electricity comparing with monocrystalline. Figure 1.3 shows the shape of polycrystalline solar panel and cell.

Figure 1.3. The shape of polycrystalline solar panel and cell.

1.2.1.2. Fuel cell. A fuel cell is a dependable and sustainable energy source that can be traced back to 1839 when Sir William Grove created the first manmade fuel cell. A fuel cell generates electricity using many electrochemical reactions that result in the creation of electrical energy from chemical energy. The fuel that is used to produce the energy could be hydrogen, gasoline, methanol, ethanol, or natural gas. There are similarities between fuel cells and batteries excluding no need for recharging. However, fuel cells have to be supplied with high fuel and an oxidizer. Fuel cells generate low voltage DC electricity and require an inverter to convert the electricity from DC to AC to allow appliances to work properly. In addition, a fuel cell creates no emissions, only water and carbon dioxide. A fuel cell could convert approximately 80% of the energy stored to electricity with relatively low maintenance compared to other distributed generators and no noise. However, a fuel cell will produce extra heat. The heat could be

used for cogeneration to produce additional energy. The drawbacks of a fuel cell are cost and the need for a complicated control system. A fuel cell system is shown in Figure 1.4.

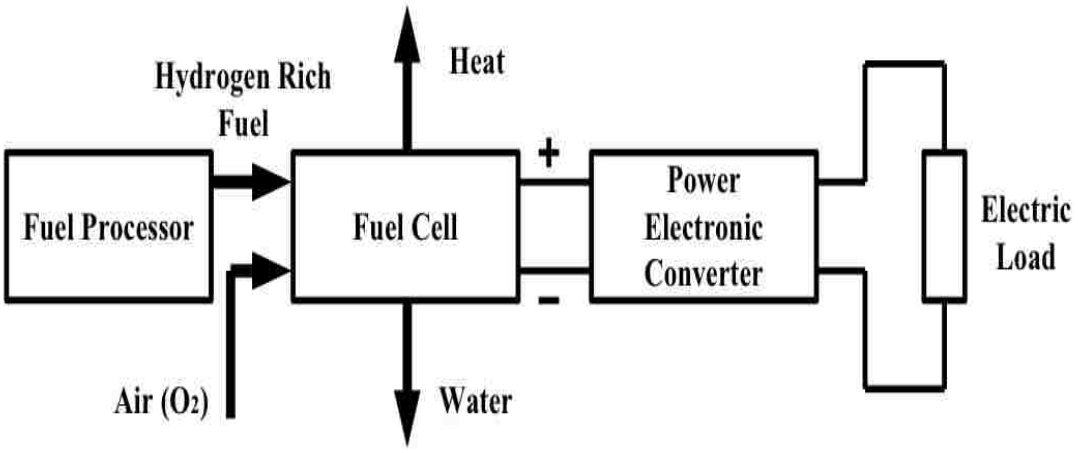

Figure 1.4. A fuel cell system [10].

There are 6 types of fuel cells as listed below:

- Proton Exchange Membrane.
- Direct Methanol.
- Alkaline.
- Phosphoric Acid.
- Molten Carbonate.
- Solid Oxide.

The different among the types of fuel cell is shown in Table 1.1. The operating temperatures of different fuel cells based on type, power density, efficiency rate, and possibility for cogeneration.

1.2.1.3. Wind turbine. A wind turbine system is a system that converts kinetic energy from wind into electrical power. A wind turbine uses energy from moving air by using the energy of the moving air to turn a shaft which then turns a generator to create power. The power generated by the wind relies on the wind speed and the way that the wind is caught by the sharpened pieces of steel called blades.

Table 1.1. The different among the types of fuel cell [10].

Fuel Cell Electrolyte	Temp. ^0C	Power Density	Efficiency	Cogen
Phosphoric acid	200 – 220	Moderate	40-45%	Yes
Alkaline	80 – 100	High	40%	No
Molten carbonate	600 – 650	Moderate	45-60%	Yes
Solid oxide	800 – 1000	High	50-65%	Yes
Proton exchange membrane	70 – 80	High	40-45%	No
Direct methanol (PEM)	70 - 80	Moderate	20%	No

There are two types of turbines, horizontal and vertical. The types of turbines are shown in Figure 1.5 (a & b). When a horizontal axis is used, the wind velocity is higher in the vertical hub and it has greater efficiency. However, this set up has low support and makes it difficult for technicians to access the generator to perform maintenance and upkeep procedures. When a vertical hub is used, the generator can be on the ground. However, there are weaknesses in the vertical pivot point. This set up has some drawbacks as the wind speed is lower at the ground level than at higher elevations and the efficiency of this system is low comparing with horizontal hub [11].

The horizontal axis components used in a wind turbine are depicted in Figure 1.6. The blades and rotor work to convert wind power into rotational mechanical power. The rotational mechanical power turns a generator and the generator converts the mechanical power into electrical power. In the gear box, the wind turbines will rotate between 40 and 400 rpm. The generators will rotate at 1,200 to 1,800 rpm. Several wind turbine models use a step-up gear box to efficiently operate the generator and produce efficient electricity. The rotor is a part of the wind turbine that harnesses the wind energy and usually consists of two or more wooden, fiberglass, or metal blades that rotate around a horizontal or vertical axes at a rate defined by the wind speed and the properties of the rotational blades. The rotational blades are connected to the hub which is connected to the main shaft.

(a) (b)

Figure 1.5. The types of turbines [11]. (a)Vertical axis, (b) Horizontal axis.

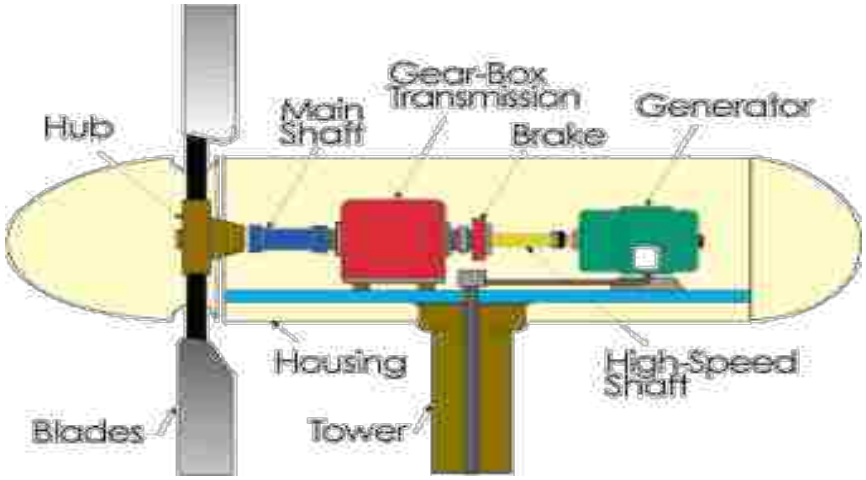

Figure 1.6. Wind turbine [11].

1.2.2. Power Electronic Elements. The following sections provide an overview of the major electric elements commonly used in a microgrid system.

1.2.2.1. Rectifier. A rectifier is an electrical device that converts alternating current (AC) to direct current (DC). The objective of a rectifier is to produce pure DC or generate a voltage or current waveform which can be considered a DC component [12].

There are different rectifier circuits that produce different waveforms as DC outputs. The following four items are the most common rectifier circuits:

- The half-wave rectifier.
- The full-wave rectifier.
- The three phase half-wave rectifier.
- The three phase full-wave rectifier.

1.2.2.2. Inverter. An inverter is a device which performs the opposite function of the rectifier. There have been many developments in static frequency conversion in power electronics and the conversion of AC power at one frequency to another AC frequency using solid-state electronics has become more popular. There are two methods used in static AC conversion:

- The cycloconverter.
- The rectifier-inverter.

The cycloconverter is a device that immediately converts AC power at a particular frequency to AC power at another frequency while the rectifier-inverter converts AC power to DC power and then converts the DC power to AC power again at different frequency [12].

1.2.3. Storage System. The use of renewable energy is associated with problems related to variability and intermittent energy production or instability. To reduce those problems, a suitable storage system must be installed in the local system. The perfect storage system would be fully equipped for technical or economical use and could store power produced by fossil fuels or nuclear technology. Storage systems have the ability to operate a system using a wide range of power densities. No particular storage system has the ability to handle all situations and a system will often employ multiple storage systems to perform tasks optimally. A system may use a combination of some or all of the following: super capacitors, batteries, super conducting magnetic energy storage, and kinetic energy storage in flywheels. The characteristics of compensation provided by the system determine the limits of energy storage. The type of stored energy and limit of the storage must be selected carefully. If there is a short-time voltage drop situation that may draw higher currents for only a few cycles, energy storage elements with smaller storage

capacities must be installed. However, a second backup source should be installed to handle situations in which the drop continues for a longer period of time and leads to the interruption of supply based on sensitive loads [13-16].

1.3. THE STRUCTURE OF THE MICROGRID

The microgrid structure consists of several components; the main components are distributed generation, loads, energy storage system, and static disconnect switch, controller, and mode switching device. These components are shown in Figure 1.5. Microgrid system contain a set of feeders, which might be located in the distributed system or a local electrical system. There are two types of feeder the sensitive load feeder (A-C) and nonsensitive load feeder (D). the sensitive load feeders have to be always supplied, therefore they must have at least one microsource to meet the requirements of the sensitive demands. During the fault on the main grid, the static switch will be opened, and then all sensitive load feeders are supplied by the microsources. On the other hand, the nonsensitve feeder might be de-energized during the fault on the utility. Once the fault is cleared, the main grid will reconnect to the microgrid. The point of common coupling (PCC) is used to determine the connection and disconnection of common coupling points. Connection or disconnection with main grid relies on the control of the microgrid and energy managements. In addition, the system will use distributed energy sources such as a distributed generator to supply the local sensitive load after the microgrid separates from the main grid for any reason. The microgrid will begin working autonomously after the static switch is opened. The arc of the system involves using power electronic interfaces such as an inverter or rectifier to properly handle power output and convert from AC to DC or from DC to AC. An energy storage system in the microgrid architecture will help the system avoid variability and intermittency of electricity supplying the sensitive load [17,18].

1.4. MICROGRID MODES OF OPERATION

There are two modes of operation for the microgrid, grid-connected mode (on grid) and islanded mode (off grid).

1.4.1. Grid-connected Mode (On Grid). In this mode, the static switch in the microgrid system is closed and all feeders are supplied by the main grid. Microgrid architecture is shown in Figure 1.7. Therefore, the microgrid is connected to the main grid and there are no disturbances in the utility and no power outages. In this case, the microgrid will support the main grid (utility) by either importing or exporting power based on the total generation of local distributed generators. The frequency in this mode is maintained by the main grid [1,2].

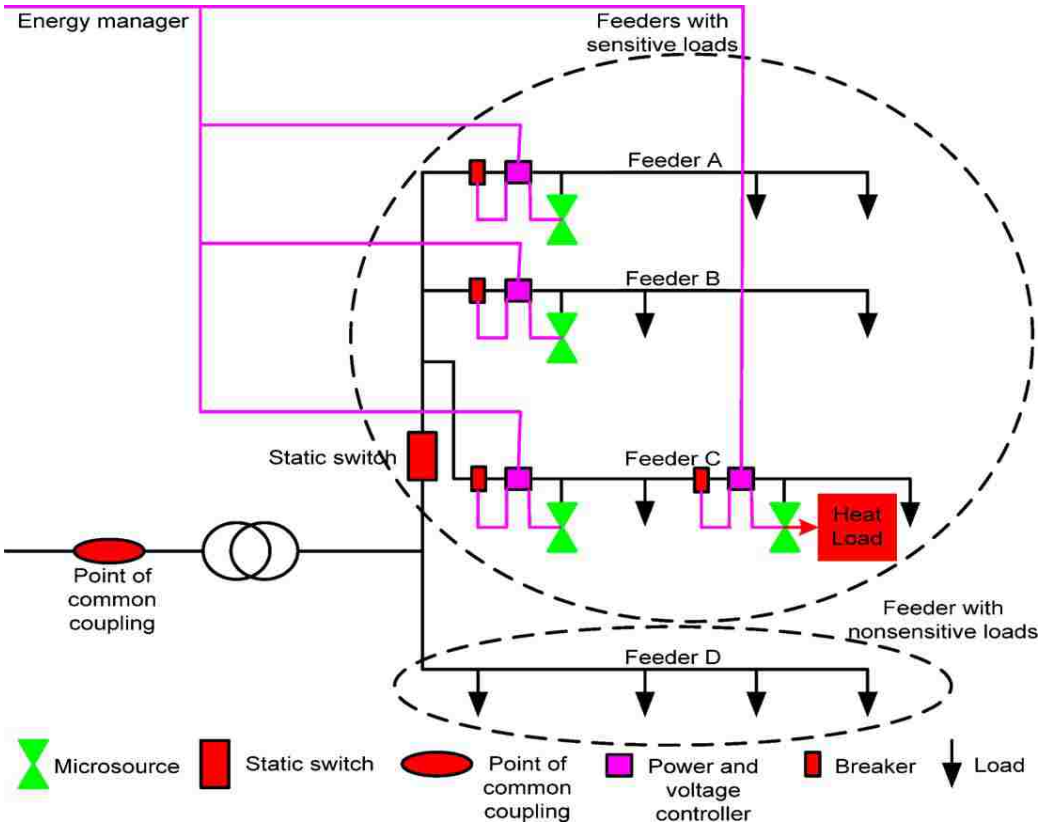

Figure 1.7. Microgrid architecture [4].

1.4.2. Islanded Mode (Off Grid). In this mode, the static switch of the microgrid is open and all feeders that connect to the distributed generators and sensitive local load are being supplied by distributed generators (microsources) as illustrared in Figure 1.5. The microgrid will work autonomously and has to generate enough power to cover all sensitive loads. Non-sensitive loads will not have power when the microgrid is in

islanded mode because these loads depend entirely on the main grid. When the main grid has recovered and is once again operating normally, the static switch will be reconnected and the microgrid will resume working in grid-connected mode [19-21].

1.5. CLASSIFICATION OF MICROGRID

Microgrids are classified into three different categories based on the type of voltage provided by distributed generators. The three types of microgrids are the AC Microgrid, High-frequency Microgrid, and DC Microgrid.

1.5.1. AC Microgrid. The AC microgrid contains a group of distributed generators and some energy storage systems that are connected to the microgrid. The distributed energy generators either produce a DC output voltage or have an electrical output at a frequency that is not compatible with the main grid's frequency. For example, a PV system or fuel cell generates DC voltage while distributed generators such as wind turbines generate output voltage at a frequency that is not compatible with the main grid. To make the frequency compatible, the distributed generator output is rectified and charges a battery that then feeds power to the microgrid through the inverter [20]. The other way is to use an inverter without batteries. Figure 1.8 provides an image of an AC microgrid configuration that has three radial feeders. In the image, A and B are connected to the sensitive loads and controllers while the C feeder is connected to the non-sensitive loads and is not impacted by any power outage or problems in the main grid. The microgrid can operate in either the grid-connected mode or islanded mode. The following sections will provide greater detail about the various modes [17,20].

1.5.1.1. Grid-connected mode of the AC microgrid. The power generated in the local distributed generator will be either imported or exported to/from the main grid based on the local load demands. In this way, the microgrid will work as a controllable load for the utility grid while the microgrid would maintain its frequency within a particular mode.

1.5.1.2. Islanded mode of the AC microgrid. When there are issues related to the quality of the fundamental network, the microgrid will disconnect from the main grid. One or more of the distributed generators are obligated to ensure that the voltage and frequency are kept at a particular level. When the frequency falls below acceptable

levels, the loads begin to restore the frequency of the microgrid. When this occurs, the microgrid will encounter the problem outlined in the following points.

- Generation and Demand Balancing**:** In the grid-connected mode, power is made accessible using the utility to meet the prerequisite loads of the microgrid. However, when the microgrid islands itself, power balance is achieved and demand is maintained at the microgrid level. This issue requires a legitimate control action involving demand side administration. The microgrid should have enough storage capacity to adequately address unexpected issues in between generation and load [3,18].
- Power Quality: Microgrids are designed to provide power quality in response to touchy or sensitive loads. The microgrid must have sufficient reactive power compensation to allow the system to handle voltage faults. In addition, a satisfactory harmonic decrease ability ensures that the harmonic created by nonlinear loads on the microgrid do not impact the sensitive loads [17].

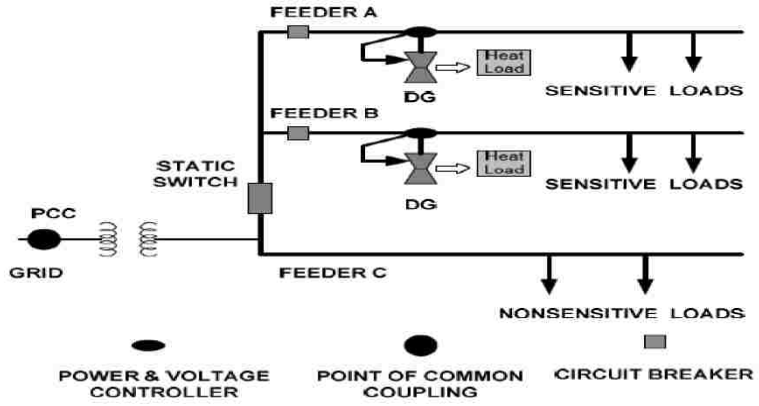

Figure 1.8. An AC microgrid configuration [1].

1.5.2. Microgrid with HFAC Link. A high-frequency AC power distribution system is typically found in aerospace applications including aircrafts or space crafts. The system can also be found in hybrid electric vehicles. The most significant advantage provided by the HFAC system involves in the system's smaller size and high power density and modularity [22,23].

1.5.3. DC Microgrid. The majority of home appliances operate using DC. The DC voltage can be provided by either a battery or by converting AC to DC using a rectifier. Some appliances which operate using DC have an adapter to convert it to DC. Figure 1.9 provides an image detailing the configuration of the DC microgrid [1,24].

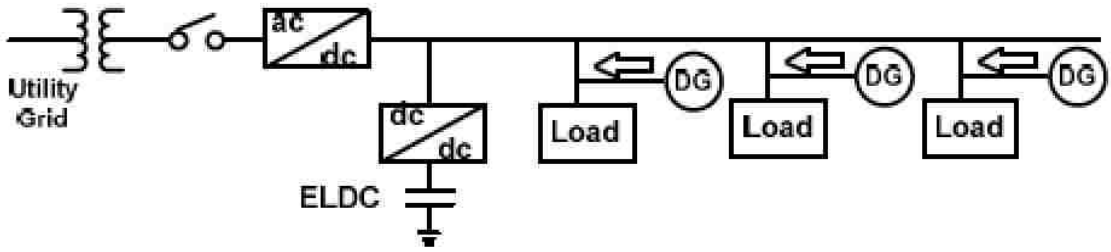

Figure 1.9. The configuration of the DC microgrid [1].

The advantages of a DC microgrid are as follows [25-27]:

- High efficiency in the DC microgrid as a result of the reduction of losses of the inverter between DC output and loads [28]
- No need for synchronization with utility and reactive power compensation
- Ability to overcome faults in the main grid with no effect on the DC microgrid directly as the energy is stored in the battery or capacitor.

The disadvantages of DC microgrids are as follows [28]:

- Need for special DC lines to be laid to distribute microgrid DC power
- Requires complicated protection system
- Requires loads that are suitable for DC power supply.

1.5.3.1. Grid-connected mode of the DC microgrid. In this mode, the rectifier handles the voltage distribution and the supervising algorithm will provide alerts regarding the amounts of power being provided by the running cogeneration system or fuel cell. A cogeneration system connected to the dc bus and its power generation will be distributed between the loads. In this mode, no power generated by the running cogeneration system will flow into the main grid [29].

1.5.3.2. Islanded mode of the DC microgrid. In this mode, the extra power in the microgrid will be continued by capacitors. The energy stored in the capacitor and the loads in the microgrid will determine the number of running cogeneration systems. If the energy stored in capacitors exceeds the limits of the capacitor, one of the cogeneration systems will be stopped as the total load of the microgrid will be greater than the total generation of the cogeneration system. The capacitor will discharge until it reaches that level right above the minimum limit. In cases where the capacitor discharges past the minimum limit, the cogeneration system will begin to run again. At this time, the total load of the microgrid will be less than the total power generation of cogeneration system and the capacitors will begin charging. The charging will continue until the capacitors reach a level that is greater than the maximum value [29-31].

1.6. MICROGRID CONTROLS

Microgrid controllers must be able to meet the certain performance standards and ensure the following [17]:

- That microsources work appropriately at predefined working points or are marginally unique in relation to the predefined working point yet are able to be filled as much as possible;
- That active and reactive power are exchanged by the microgrids and/or the distribution system;
- That disconnection and reconnection techniques are very easy;
- That market support is advanced by optimizing the generation of local microsources and power in combination with the utility;
- That heat usage for nearby establishments is optimized;
- That sensitive loads for items such as medical machinery and computer servers are supplied without interruption;
- That in instances where there is a general fault, the microgrid has the ability to work through the black-start; and
- That energy capacity of the storage system can bolster the microgrid and create overall system reliability and efficiency.

Depending on the above obligations and the controller coordination, the microgrid controls can be considered local controls, centralized controls, and decentralized controls. More detail regarding these terms will be provided in the following sections.

1.6.1. Local Controllers. Local controllers are an essential class of microgrid controllers. The principle utilization of local controllers is to control microsources. This sort of controller is intended to control the operation of microsources and their power electronic interfaces without using a communication system. Yet, it may have easy system or simple software. The system must be able to provide data regarding local controllers via the local voltages and current [17, 18]. For the majority of microgrid applications, local controllers will work with other types of controllers in islanded mode of microgrids where the local controllers are the main obliged controllers [20, 32, 33]. The local controllers should guarantee the "plug and-play" mechanism of microsources; a few microsources should be have the ability to consistently connect or separate from the main grid when and where required [34, 35].

The majority of microsources need power-electronic interfaces to convert the power from AC to DC or from DC to AC. Figure 1.10 contains a model of microsources connected to a microgrid. The image contains three fundamental components: the prime mover, the DC interface, and the voltage source inverter (VSI). The microsource connects to the microgrid through an inductor. The magnitude and phase of its output voltage are handled by voltage source inverter to control real and reactive powers. The voltage regulation is vital for a microgrid which is integrating a huge number of microsources to prevent intermittency that can be caused by a high number of microsources. Voltage regulation is used to guarantee that there is no extensive reactive current among distributed generators [17, 18].

Other than the voltage regulation, microsources must be able to manage active and reactive power. The most well-known systems that manage these forces include droop-based active and reactive controls. These droop controls are scaled-down forms of droop-based controls in the main grid. The droop-based controls comprise of voltage reactive power and frequency of active power droop controls [36, 37].

A form of voltage-reactive power droop control is shown in Figure 1.11. As the reactive current created by the microsource becomes more capacitive, the working

voltage will increase. Hence, the local voltage set-point is decreased to maintain the voltage at or close to its original set-point. In contrast, the local voltage set-point is expanded if the reactive current gets to be more capacitive. Q_{max} is shown to present the limit of reactive current increase and decrease, factors that are controlled by the volt-ampere (VA) rating of the inverter and the power created by the prime mover [17, 18].

When in grid-connected mode, the microgrid receives power from the grid from microsources as determined by the agent's situation. If the grid is interrupted for any reason, the microgrid can easily move to islanded mode. In addition, the microgrid is sometimes constructed in a way that allows it to work properly in islanded mode and allows it to disconnect from the main grid for certain reasons even if there are no issues or problems with the main grid. After the main grid is disconnected from the microgrid, the voltage phase angles of the distribution sources will change and cause the local frequency relying on the power mismatch to diminish. The frequency of the microsources will diminish if the microgrid receives power from the utility in grid-connected mode, but will increase if the microgrid provides energy to the utility in grid-connected mode. The reliance on the frequency allows each microsource to give its appropriate portion of load without a quick new power dispatch from the energy administrator [38, 39].

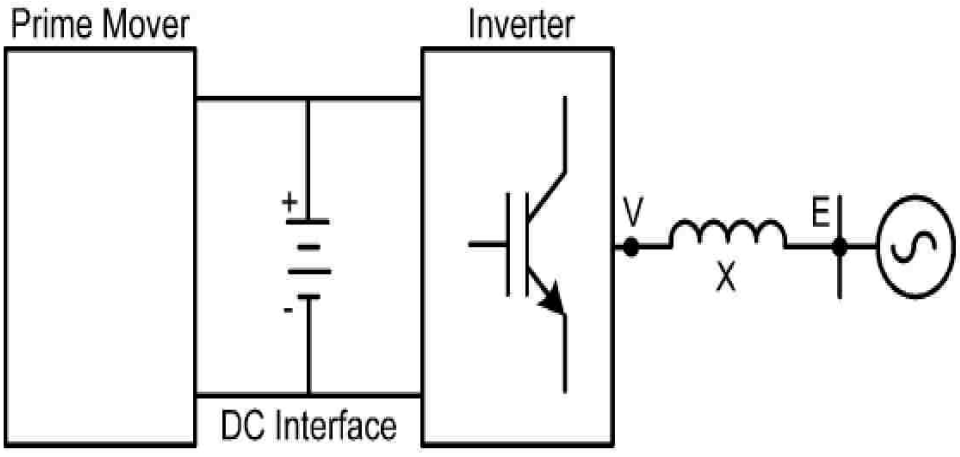

Figure 1.10. A model of microsources connected to a microgrid.

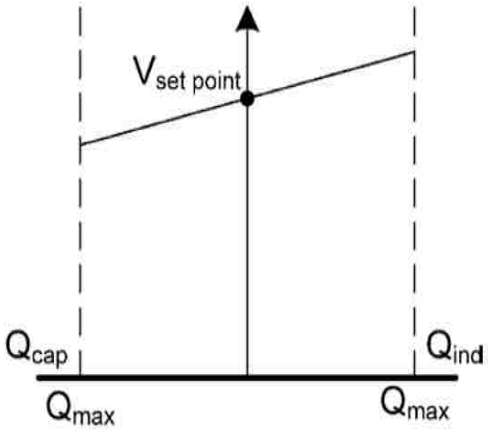

Figure 1.11. A form of voltage-reactive power droop control.

Figure 1.12 provides droop-based power-frequency control. The illustration shows how the sources have certain expected ratings, $P_{1\,max}$, and $P_{2\,max}$. The dispatched power in grid-connected mode (P_{10} and P_{20}) is characterized at base frequency, ω_0. The droop is characterized to guarantee that two systems are at the rated power at the same lowest frequency. During an adjustment in power demand, the two sources will work at different frequencies that may lead to a difference in the power angle between sources. When this change occurs, the two frequencies have a tendency to float toward a lower, single estimation of ω_1. Unit 2 will have higher increment in its aggregate power needs than Unit 1. Because of droop regulation, every controller must have ability to handle decreases in microgrid frequency.

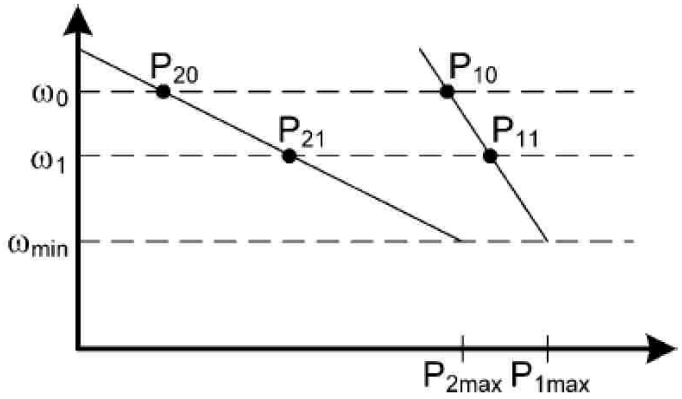

Figure 1.12. Droop-based power-frequency control [4].

1.6.2. Centralized Controllers. In the hierarchical system, either centralized or decentralized controllers can be used. The hierarchical system is shown in Figure 1.13 and consists of local controllers including Microsource Controllers (MCs), Load Controllers (LCs), Microgrid Central Controllers (MGCCs), Distribution Management System (DMS), and Market Operator (MO) [40-43].

In every microgrid, there is an MGCC that connects the distribution management system to the microgrid. The MGCC performs distinctive tasks that involve the base coordination of the local controllers that work to enhance microgrid operation. The contrast of the centralized and decentralized controls is characterized by the centralization tasks provided by the MGCC. The level of decentralization varies depending on the demands of the MGCC and the MCs and LCs. In a centralized control, the MCs and LCs apply the requests of the MGCC throughout the grid-connected mode and have the ability to independently operate on their own in islanded mode [43].

A distribution management system or distribution network operator (DNO), to which a few MGCCs can be connected, has the obligation to handle the operation of medium and low voltage zones which have more than one microgrid. In addition, one or more market operators may be part of the system to determine how the microgrids will share in a business operation. The DNO and MO do not include microgrids, but, instead, are delegates of the main grid. Centralized control is very good in utilizing microgrids and their associated features as listed below [43, 44]:

- The proprietors of microsources and loads have the same targets and search for a coordinated effort to meet their targets.
- It is practical to use it in small micogrid system with existence of an operator.

1.6.3. Decentralized Controllers. Decentralized controllers and centralized controllers are characterized in a similar way and are shown in Figure 1.13. In decentralized controllers, the principle obligation is given to MCs that work to expand their power generation to meet the requirements of the load and provide the most extreme transmission to the grid based on the consideration of business sector costs. A decentralized control is planned to increase the independence of microsources and burdens. Some of the ways to increase the independence of microsources depend on specific logic [45, 46].

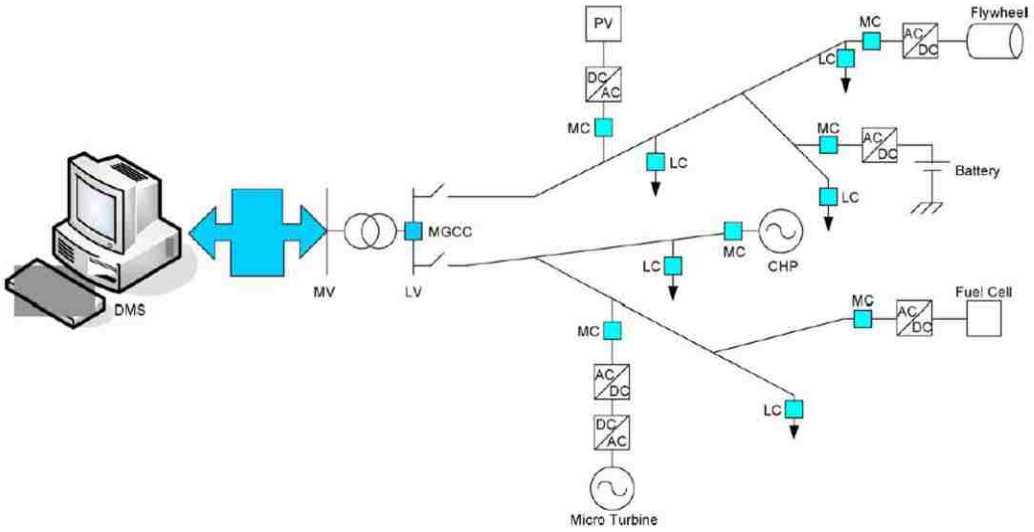

Figure 1.13. The hierarchical system [4].

A decentralized control can be utilized effectively in microgrids and contain some or all of the following attributes [43]:

- Microsources can have distinctive properties which allow a few choices to be made locally.
- Microgrids that are used in business situations assume that the controllers of all units in the business sector have a particular level of knowledge.
- Local microsources have different duties outside of generating energy for the local grid. The duties could involve creating warmth for nearby equipment, ensuring voltage remains at a certain level, or providing reinforcement to a system that provides local basic loads to serve as a backup for that system.

1.7. EXAMPLES OF MICROGRID

There are many examples of projects that use a microgrid system. The following sections are the best examples of microgrid use in Canada and America.

1.7.1. Hartley Bay. Hartley Bay located in British Columbia, Canada, is a remote seaside town that is accessible via air or water. An overview of Hartley Bay picture is provided in Figure 1.14. A total of 170 people rely on a remote microgrid in the town to provide them with power. With the developments in microgrid technology, areas such as

Hartley Bay have benefited greatly through the enhanced power control and cost reductions. Hartley Bay depends on three diesel generators which consists of two 420 kW generators and a single 210 kW generator which provides power for the town's 62 houses and 20 commercial business buildings.

Between 2008 and 2009, Harley Bay enhanced its vitality system by placing smart meters throughout the town to provide power readings that have information about the current fuel stream. This information can be analyzed to assess the effectiveness of the generators.

Figure 1.14. An overview of Hartley Bay picture [47].

The 210 kW generator is relatively wasteful and a loads reaction system has been installed which will better utilize the generator's meager power contributions and upgrade the diesel dispatch. The loads reaction system has been placed in business structures and consists of 20 variable indoor regulators and 12 controllers. The system has the capacity to lessen the greatest demand on the system, 61.3 kW, by 15%. The microgrid was expected reduce its diesel use by 77,000 liters per year. The individuals at

Harley Bay worked to enhance the town's energy by creating future projects which could help to reduce yearly fuel costs by 5% [47].

1.7.2. New York University. New York University (NYU) is one of the biggest colleges in the United States and has generated power on its campus since the 1960s. The University built its own very large oil-fired cogeneration plant in 1980. The University later transitioned from energy that is produced using the oil-fired method to a system that employs advanced natural gas techniques. This new system combined the heating and power center and used microgrid capabilities to create a plant that is more dependable and has greater control of energy use. The capital expense of the system overhaul was $126 million. However, tax excluded bonds masterminded through the Initiative of the state of New York and through increases in NYU's tuition worked to ease the financial burden. The combined heat and power system has a yield limit of 13.4 MW, a limit that is twice as the limit of the old plant's yield. The system has also been completely operational since 2011 and produces power that is used by 22 buildings and heat that is used by 37 buildings. The microgrid at NYU is made up of two 5.5-MW gas turbines that deliver power through the connection with heat steam generators and a 2.4 Megawatt steam turbine. The NYU microgrid is associated with the Con Edison grid and buys power when the loads are greater than the on-site producing limit. The NYU grid has reached a point where it could be disconnected from the main grid. Figure 1.15 provides an image of the NYU microgrid [47]. The ability to disconnect from the rest of the grid was tested when Hurricane Sandy hit the New York City area and the NYU microgrid was able to disconnect from the local network and continue to provide dependable energy to a significant part of the campus. The renovation of the system has resulted in significant improvements both economically and environmentally. The University has assessed the reserve funds relating to aggregate energy expenses to be $5 to $8 million annually. The new office has radically diminished NYU's emissions with an expected 68% lessening in EPA criteria pollutants (Nitrogen Oxide, Carbon Monoxide, and Sulfur Dioxide missions) and 23% decline in gas emissions. The reduction in these levels is a significant step toward the promise that NYU made to the City of New York to reduce greenhouse gas emissions by 30%.

Figure 1.15. An image of the NYU microgrid [47].

1.7.3. University of California, San Diego (UCSD). The UCSD microgrid venture generates power, heating, and cooling for 450 hectares on the UCSD campus and serves 45,000 people daily. Figure 1.16 provides an image of the USCD microgrid [47]. The microgrid is made up of two 13.5-MW gas turbines, one 3-MW steam turbine, and a 1.2 MW solar panel that generate enough combined energy to cover 85% of the University's power demands, 95% of the warming demands, and 95% of the cooling demands.

The turbines create 75% less emissions than traditional gas power plans. For HVAC services, the plant utilizes 140,674 kW/hour and provides 14,385 cubic meters of heat energy in addition to powering three cooling systems that power five chillers. A 2.8 MW liquid carbonate energy unit works to process waste methane which is supported by the California self-generation motivator project and take advantage a 30% government project tax credit. The University is associated with San Diego gas and electric through a single 69 kV substation. A "straight supervisory control and data acquisition framework" is utilized in the facility's system to guarantee that the energy supply corresponds with the rest of the grid. UCSD is currently introducing another top-of-the-line expert controller of Paladin hat is designed to handle all plant issues relating to hourly generation, storage, and burdens to enhance working conditions. The system is

able to receive more than 260,000 information inputs/second. To bolster the effectiveness of Paladin, UCSD will use V-Power software to process business sector value signs, weather forecasting, and the accessibility of resources. There are approximately 200 meters of primary lines at the facility's principle circuit breakers that track the facility's performance at all times. The UCSD system has been constructed with power meters built into all fundamental electrical lines and into all of the facility's primary circuit breakers. The Department of Energy recently gave UCSD an award to model the impact of the distribution system on the sloping throughout the production of the solar PV system.

Figure 1.16. An image of the USCD microgrid [47].

2. SOLAR VILLAGE

2.1. OVERVIEW

The solar village is comprised of four solar-powered buildings that are supplied using renewable energy. The village was built by the solar house team from the Missouri University of Science and Technology for a competition hosted by the US Department of Energy, the Energy Solar Decathlon. The solar house team works to inspire future generations to construct renewable energy buildings. The team is comprised of students from different majors and is advised by individuals from MST and other companies. The team began to build the solar houses in 2002 when it built the first structure called the "2002 house." The team has built a new home every two years. Outside of the research involving the microgrid system, the village is a location that allows for the testing and improvements of real world, sustainable energy generation and storage. In addition, one of the solar house's main objectives is to reduce the level of dangerous emissions from conventional generators and are released into populated areas such as cities. Figure 2.1 provides a picture of the solar village houses at Missouri S&T [48].

Figure 2.1. A picture of the solar village houses at Missouri S&T [48].

2.2. SOLAR VILLAGE OBJECTIVES

The Solar Village Microgrid Project will provide researchers with the opportunity to engage in hands-on exploration, training, and demonstrations that aim to accomplish the following goals [48]:

- Determine the relationships between different components of the microgrid scale including the burden of installing and measuring power generation, capacity, and heat and to determine the optimal loads for capacity, storage, and generation.
- Find the ways in which utilities could stabilize generation, storage, and load at particular voltages while keeping voltage and frequency at reasonable and safe levels.
- Improve and develop the designs of microgrids, controllers, and other operational equipment.
- Discover how microgrids can simplify the distribution of solar photovoltaics and determine if dividing the national power grid into smaller grids is feasible and could be the future of electric utilities. Some of the issues that will be studied will involve determining if microgrids will be viable power options, if they will provide users with more independence, if community-scale microgrids are sensible for electric utilities for future generations, and how the techno-economics of the microgrids will work and impact users and communities.

2.3. ARCHITECTURE OF SOLAR VILLAGE

Each of the four solar homes are different from one another due to changes in technology and the general evolution of the field. The homes are built to meet all expectations related to providing sustainable energy that meets the daily needs of the homes at all times. Originally, all four houses were wired individually to the main grid which was powered by Rolla Municipal Utilities. Each house is now wired to the shed. The village also includes an electric vehicle charging station. The following sections provide a brief description about each of the four houses to provide greater detail about the solar capacity of houses [48].

2.3.1. 2002 House. 5 kW of electricity is generated by 32 solar panels on the roof. Evacuated tubes are shown on the roof. It contains a vacuum to increase the energy absorption from the sun as heat. This heat converted to hot water in a tank by heat exchanger and use it as local hot water supply [48]. Figure 2.2 depicts the 2002 house.

Figure 2.2. The 2002 house [48].

2.3.2. 2005 House. 3 kW of electricity is generated by solar panels on the roof. In addition, the structure used insulated panels to reduce the energy costs associated with heating the house. The roof of the house was designed using the "step" technique which included solar panels and thermal systems in one panel and made the roof more efficient and more aesthetically pleasing. The home's appliances were all smart and energy efficient. Figure 2.3 shows an image of the 2005 solar house [48].

Figure 2.3. An image of the 2005 solar house [48].

2.3.3. 2007 House. This solar house uses appliances that had smart energy ratings and would use less energy than the comparable conventional appliances. The 2007 house also used a subfloor system which consisted of conductive aluminum boards that would conduct heat and work to warm the house. The solar panel on the roof had a 7 KW capacity and the electrical system includes battery bank. One of the new features in this home involved a home automation system that would remotely control the lights, windows, and the thermostat for high-voltage alternating current (HVAC), which actually should be heating, ventilation, and air conditioning. Figure 2.4 provides an image of the 2007 solar house [48].

Figure 2.4. An image of the 2007 solar house [48].

2.3.4. 2009 House. The automation system used in the 2009 house was very advanced and was able to interact with ambient conditions. The washer and dryer were a single entity and the home automation system was able to control the washer, dryer, and dishwasher. The addition of these appliances into the automation system showed that smart home technologies were viable. Figure 2.5 provides an image of the 2009 house and shows some of the home's 40 monocrystalline solar panels that had a maximum production ability of 8 KW. Since 8 KW is not enough power to meet the needs of an ordinary home, all appliances in the 2009 house were designed to use less energy. In addition, evacuated tube collectors on the roof used sunlight to heat water and provide the energy for the radiant floor heating system [48].

Figure 2.5. An image of the 2009 house [48].

2.3.5. Shed. The shed is shown in Figure 2.6 and plays the main role of the microgrid system in the solar village. This structure contained the batteries, bi-directional inverter, fuel cell, and switches. All four houses in the village were directly wired to the shed and a computer in the shed monitored all houses and their associated components. This computer could be accessed remotely to obtain information regarding the function of the homes and their components at any time using a software called SynapSuite. This software illustrated the power generation from distributed generation and main grid. In addition, the program provided the load volume in kilowatts for each house.

Figure 2.6. The shed [48].

The total power generation of the solar panels was 21 KW for both the monocrystalline and polycrystalline panels used in the houses. In addition, the ability to combine the power and heating capabilities was accomplished using a 5 KW natural gas fuel cell which was able to interact with a hydrogen reformer to produce electricity and low levels of heat. The electricity was connected to the microgrid and the heat in two of the houses was supplied using heat from the hydronic system fuel cell. Two racks of lithium ion batteries that accounted for a total energy storage capacity of 60 kwh were installed and provided a nominal voltage of 960 V DC. The village's bi-directional inverter was responsible for charging and discharging the batteries and primarily functioned to convert DC to AC to allow it to be used in the microgrid system. The system's switchgear consisted of six intelligent switches which interacted with one another to allow the microgrid system to work effectively. The solar village's microgrid is shown in Figure 2.7 (a, b). It shows how the components in the solar village were wired along with the village's microgrid. Each solar panel system for each four houses connected to inverters. And, they are connected to the switch A8 in Synap6 (number 1) by grid tie.

2.3.5.1. A123 Lithium ion batteries. Two racks of lithium ion batteries provided roughly 30 kwh of storage capacity per rack with a nominal voltage about 960 DC voltage. Figure 2.8 shows the grid battery rack which consists of eight modules. In addition, the battery management system is placed based on the industry-specific standard. In the Figure 2.8, the top two modules are assigned for cooling and management wires. Table 2.1 provides the operating parameters of the grid battery system rack.

Table 2.1. Operating parameters of the grid battery system rack [49].

Parameter	Range
Energy rating	22 KWh
Rack voltage range	563 V to 788 V
Cell voltage range	22.2 V to 3.8 V
Maximum charge / discharge	88 KW
Recommended average charge / discharge rate	Less than or equal to 22KW

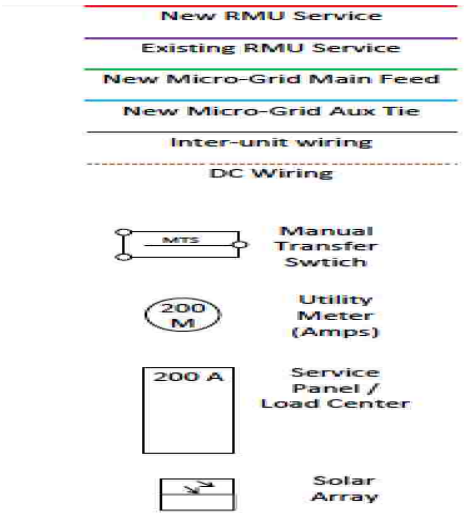

(a)

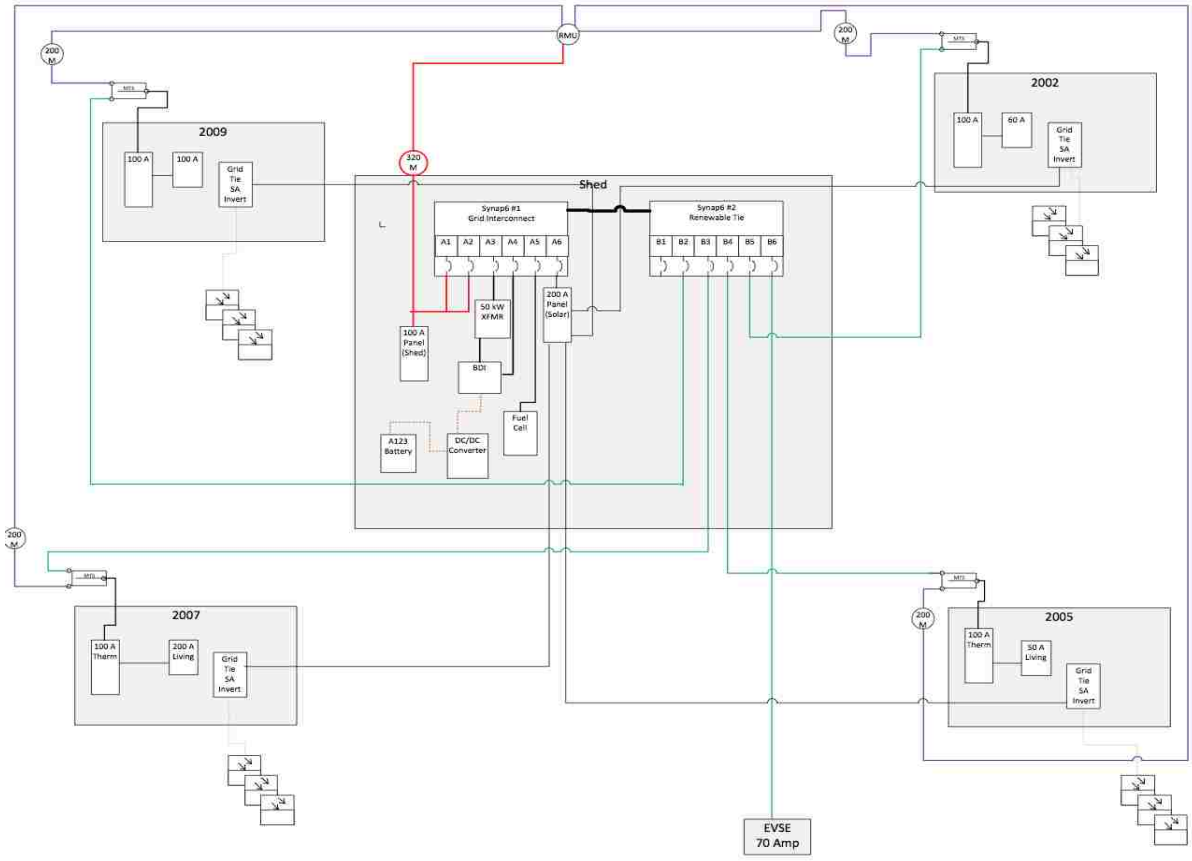

(b)

Figure 2.7. The solar village's microgrid [53]. (a) definition and illustrations of the lines and equipment, (b) layout of the Solar Village

Figure 2.8. The grid battery rack [49].

Lithium is the lightest of all metals, has the greatest electrochemical potential, and provides the largest energy density per weight. The following list provides some brief advantages and disadvantages of the lithium ion battery [51].

Advantages of lithium-ion batteries:

- Cell voltage = 3.7 V
- High specific energy 100-160 Wh/kg
- High specific power 250-340 W/kg
- High energy efficiency
- Good high-temperature performance
- Relatively low self-discharge (5%-10% per month)
- Low maintenance and no periodic discharge is needed; no memory.

Disadvantages of lithium-ion batteries:

- High internal resistance
- Requires a protection circuit which limits voltage and current; battery is safe if not provoked
- Liable to aging; storing the battery in a cool place at 40% state of charge can reduce the aging effect

- Subject to transportation regulations and larger shipments of lithium-ion batteries can be subject to specific regulations. This constraint does not apply to personal carry-on batteries.
- Relatively expensive.

2.3.5.2. Bi-directional inverter. The power conversion system is a bi-directional inverter specifically created for an energy storage system. A bi-directional inverter for the solar village is shown in Figure 2.9 and includes many items including a 240V AC split phase grid interconnection, a 50 KW inverter (maximum 50 KVA), and a DC input designed at 60 amps. The DC side of the inverter is connected to the batteries while the AC side is connected to the main grid. Therefore, the batteries will be in charging mode if the system has excess energy available. And, it will be in discharging mode if the system does not have enough energy. Consequently, a bi-directional inverter is critical when the system is in islanded mode. Also, it could be used for economic purposes while grid-tied [57].

.

Figure 2.9. A bi-directional inverter for the solar village [50].

2.3.5.3. Solar village fuel cell. The manufacturer of the fuel cell in solar village is Clear Edge power. They designed advanced, safe, and reliable fuel cell, called Model 5. It is a constant phosphoric acid fuel cell (PAFC) system prepared for combining heat and power applications. It is able to produce 5 kW of ultra-clean, continuous electric power and 6,15 kW of useful thermal energy. This heat is very often used for local hot water, procedures for hot water, and places heating applications. The fuel cell system can also provide continuous, uninterruptible power when the main grid fails. As long as natural gas is available, electric power and heat can be produced. Figure 2.10 shows the basic operation of the fuel cell system. First of all, in the process called catalytic steam reformation, natural gas is converted to hydrogen in the fuel processing system. And then, Hydrogen and air are supplied to a phosphoric acid fuel cell stack in which hydrogen and oxygen combine electrochemically to produce direct current (DC) electricity, heat, and water. Finally, alternating current (AC) electricity is produced through DC to AC inverter. Useable heat is delivered to a local water source through heat recovery heat exchanger [56].

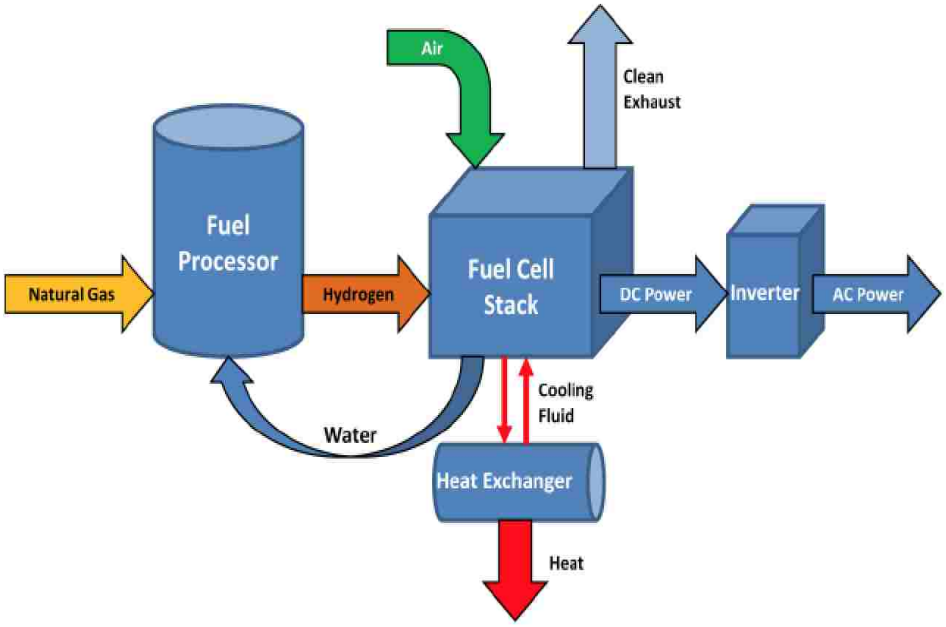

Figure 2.10. The basic operation of the fuel cell system [56].

2.3.5.4. Switchgear of the system and energy management. The switchgear of the system consists of six intelligent switches which communicate with one another to allow the microgrid system to work effectively using a power management system called Synap6. The Synap6 system consists of two switchgear units that provide real-time load and generation management for the microgrid. It is the same hardware that is used in the SynapsSuite web portal that allows for the tracking of a microgrid. Figure 2.11 provides an image of the SynapsSuite home page. The hardware at the site functions as an intelligent switchgear and ensures that power and energy demands are met along with ensuring that the system is energy efficient, cost efficient, and capable of islanding. The batteries are managed by a code called SNTBatt, a code that is not related to the IATS code. IATS is a code that works to manage the individual Synap6 modules. There are 12 modules in the solar village system that can switch the batteries on and off safely. The solar village system is created by Milbank and is closed source. SNTBatt was a custom software program that was written specifically for Missouri S&T and works to manage the batteries and the inverter. IATS can give commands to SNTBatt by writing to a named pipe that SNTBatt creates at its startup. This pipe may or may not be a good interface for the system. In addition, the SNTBatt software does not allow users to easily query it regarding the battery's state of charge (SOC). The manufacturer could add this capability to the solar village. The information gathered is written into a main database. Charging is currently managed within SNTBatt, and IATS tells SNTBatt to charge or not charge when the system is in islanded mode. The batteries can automatically disconnect from the DC bus if a fault is observed or if the charge or discharge limits are not respected. The SynapSuite provides input on when the batteries will charge or discharge using commands sent to the inverter.

2.3.6. EV Charging Station. The EV charging station in this village is not a standard EV charging station as it is bi-directional. The EV charging station is provided by Milbank and the station is located at the front of the solar houses. Figure 2.12 provides an image of the EV charge station in the solar village.

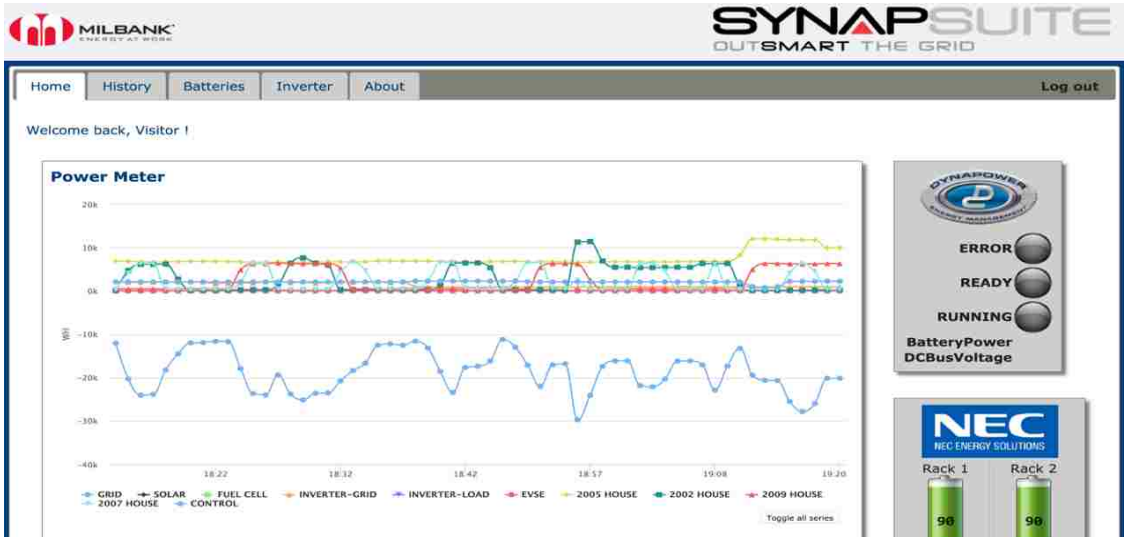

Figure 2.11. An image of the SynapsSuite home page.

Figure 2.12. An image of the EV charge station in the solar village.

3. SIMULATION OF MICROGRID SYSTEM

3.1. INTRODUCTION

This project will use MATLAB Simulink to simulate the solar village microgrid system. The simulation will use realistic data provided by Milbank. The realistic data include load profile for the houses and PV system generation profile. This chapter will illustrate the simulation approach for the houses of the solar village, PV generation, and batteries. At the end of the chapter, the simulation results will be described and analyzed. Figure 3.1 provides an illustration of the entire solar village microgrid simulation. The solar village uses AC and the simulation will use DC for all scenarios. The reason for the use of DC is to reduce the complexity of the simulation.

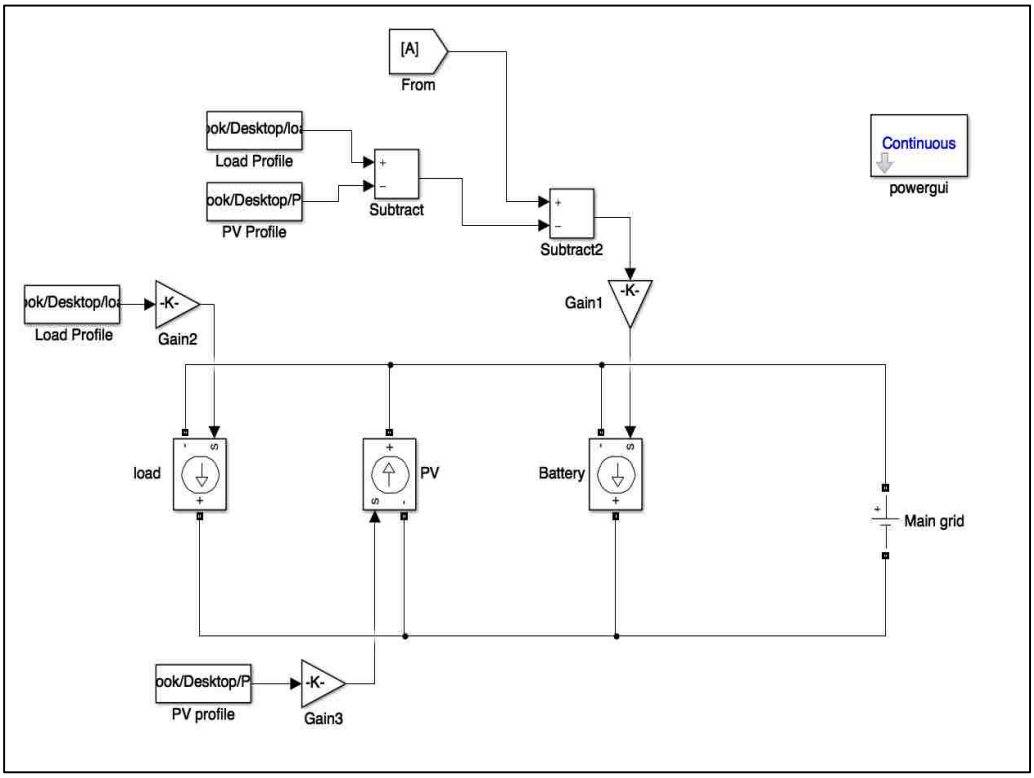

Figure 3.1. An illustration of the entire solar village microgrid simulation.

3.2. SOLAR PANEL

In this simulation, the solar panels will use a controlled DC source to provide the simulation with realistic values for the PV generation profile. The PV generation profile is considered after DC-DC converter in microgrid system. Therefore, there is no need for a DC-DC converter simulation on the design of microgrid. A block in MATLAB called the "From File" block is implemented in the model to use data from a MAT file and output the data as a signal. The data is a series of samples. Each sample contains a time stamp and an associated data value. The sample time is one minute and the data values will be the power generation of the PV system in watts. These values will be divided by the voltage in the "Gain" block and then inserted as signals into the controlled current source. Figure 3.2 illustrates the simulation of solar panel. A typical solar generation profile plot for one day (24×60 = 1440 minutes) is displayed in Figure 3.3. And, the average value of this solar generation profile is 3,722 w.

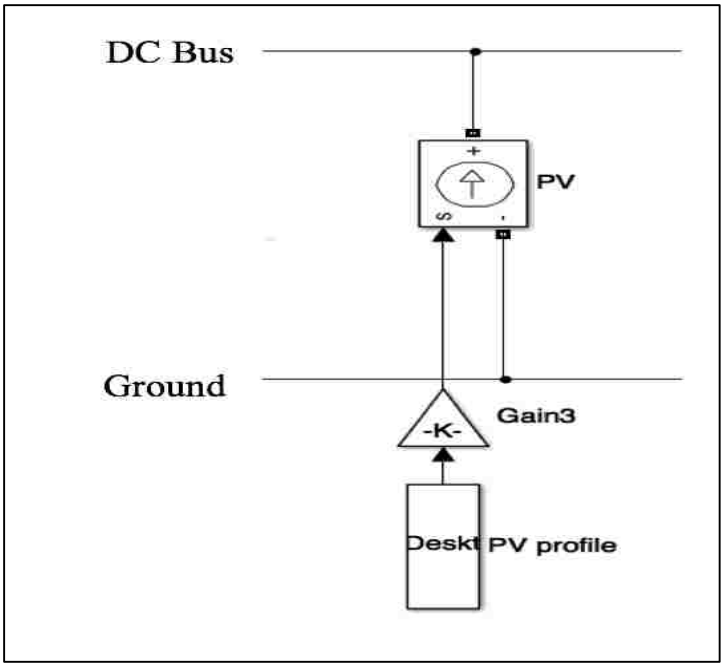

Figure 3.2. The simulation of solar panel.

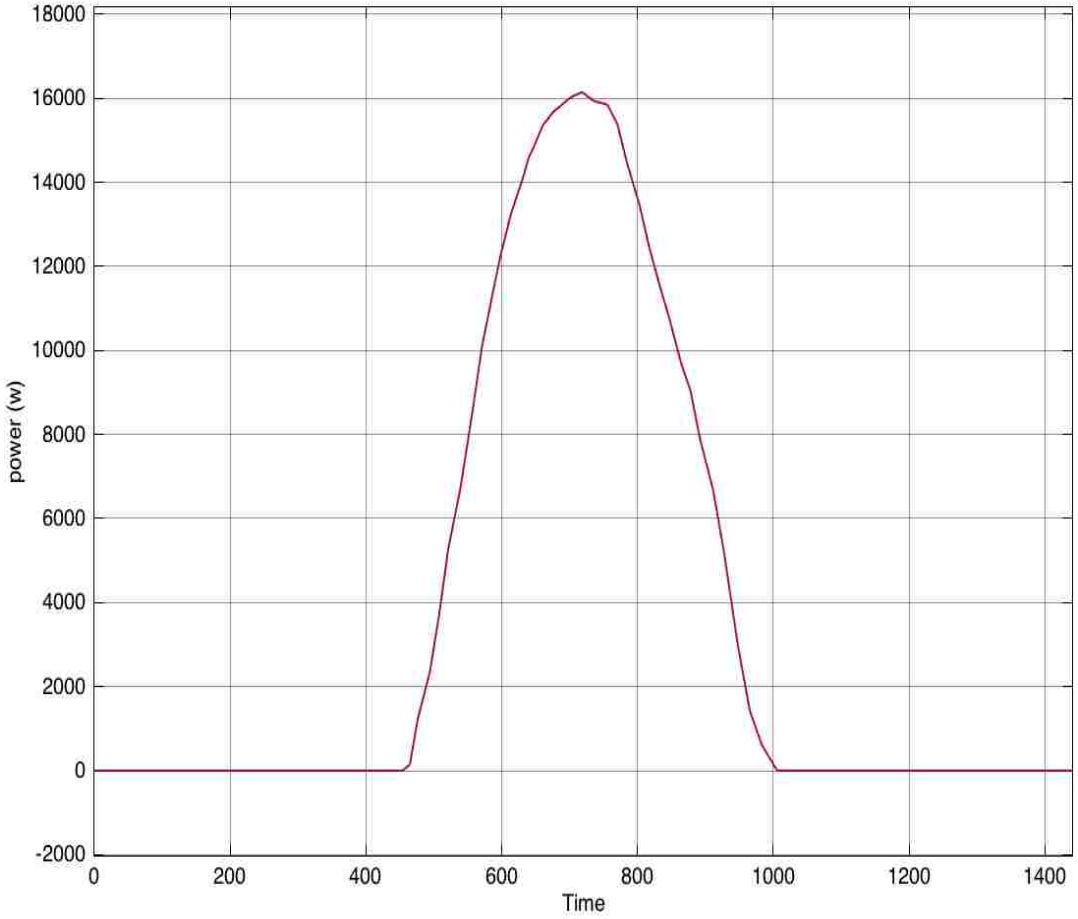

Figure 3.3. A typical solar generation profile plot for one day.

3.3. THE HOUSES OF THE SOLAR VILLAGE

In this simulation, the load profile is the total load power of all four solar houses. A controlled DC source simulates the total load profile for the houses in the solar village. The simulation of load profile uses similar approach of the PV profile to insert data into the simulation. Also, the data is a series of samples. Each sample contains a time stamp and an associated data value. The sample time is one minute and the values are the power load for the houses in watts. These values will be divided by the voltage in the "Gain" block and then inserted as signals into the controlled current source. Figure 3.4 provides an image of the simulation of the load. A typical load profile plot for one day (24×60 = 1,440 minutes) is displayed in Figure 3.5. And, the average value of this load profile is 10,061 w.

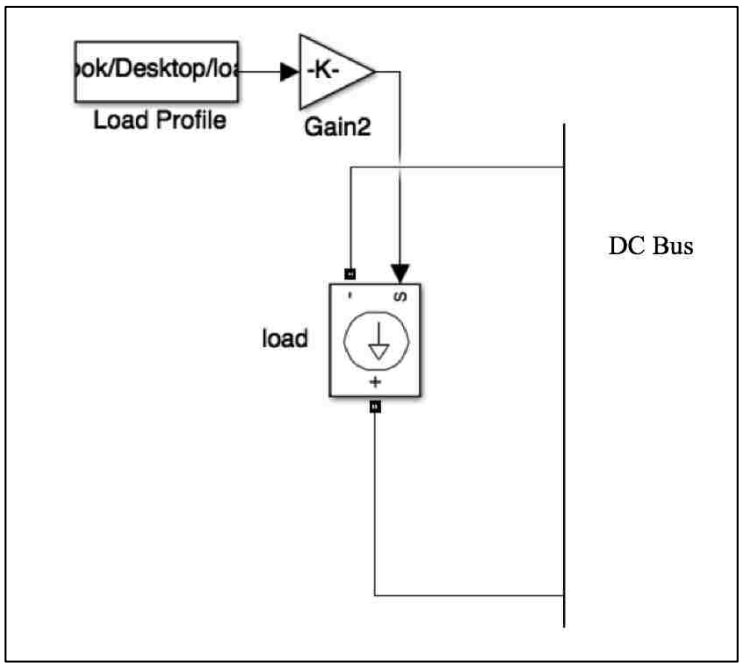

Figure 3.4. An image of the simulation of the load.

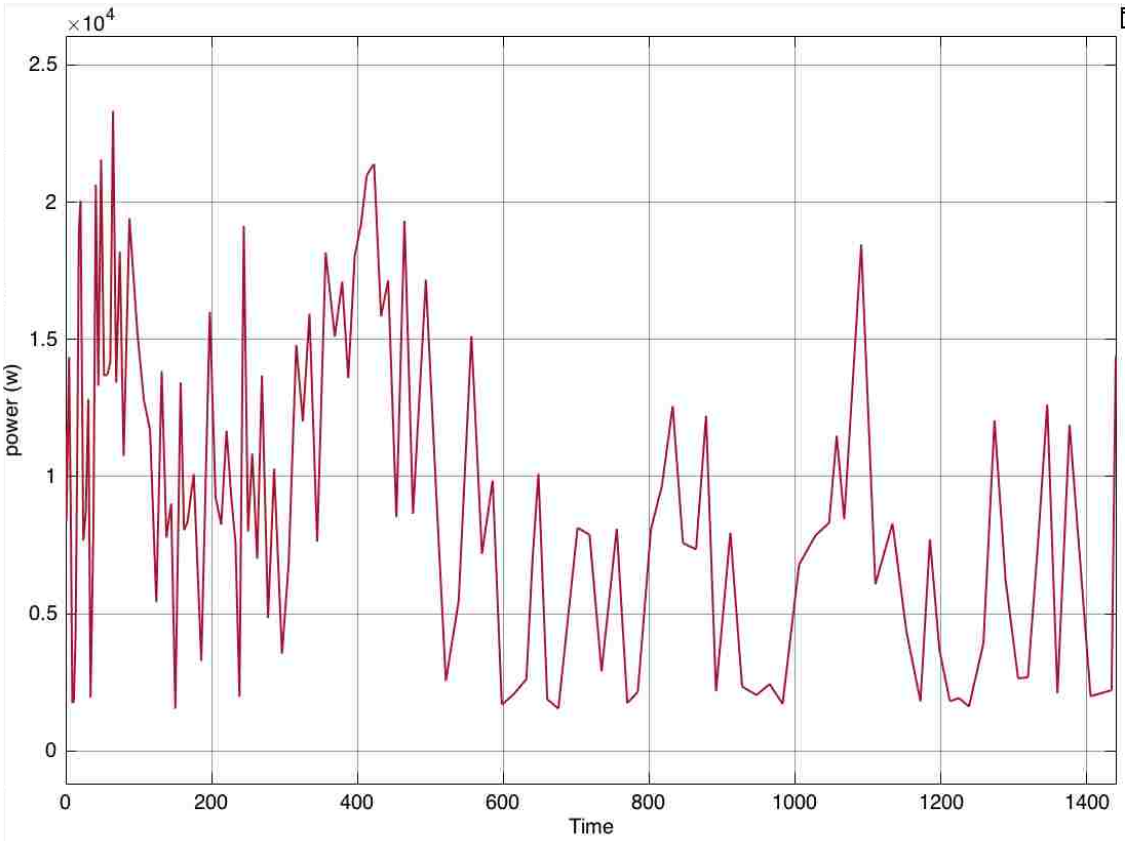

Figure 3.5. A typical load profile plot for one day.

3.4. THE BATTERIES

The simulation of batteries uses a current source. It is controlled by the difference between the load and PV profile. One of the main parameters of the battery is state of charge (SOC). The SOC of the battery is between 0% and 100%. The SOC for a fully charged battery is 100% and for an empty battery is 0%. The SOC is calculated as:

$$\mathrm{SOC} = 100\ (1 - \frac{1}{\mathrm{Q}} \int_0^{\mathrm{t}} \mathrm{i}\ (\mathrm{t}).\,\mathrm{dt}) \qquad (1)$$

where, SOC is state of charge (%), Q is maximum battery capacity (Ah), and i is battery current.

The simulation of SOC is shown in Figure 3.6. The input of the integrator block is the battery discharge current profile. The Integrator block outputs the value of the integral of its input signal with respect to time and the output is divided by time in seconds (3600 seconds) and the rated capacity for the batteries. The SOC will be the difference between the result of this equation and the initial SOC. The rated capacity of the battery is measured in amperes per hour. The rated capacity is the minimum effective capacity of the battery. The initial SOC parameter is used as an initial condition for the simulation and does not affect the discharge curve. Also, nominal voltage is an important parameter of the battery as it represents the end of the linear zone of the discharge characteristics.

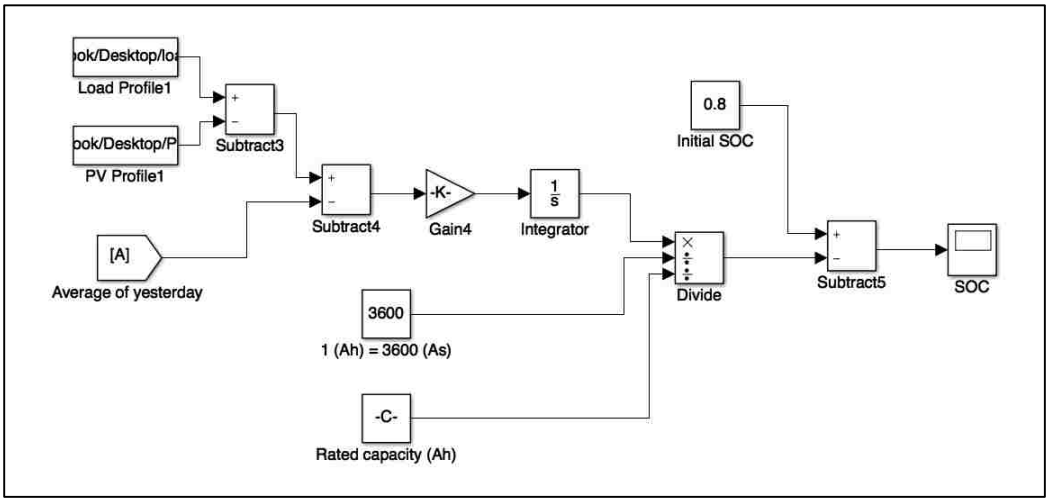

Figure 3.6. The simulation of SOC.

3.5. SIMULATION RESULTS

Energy management systems and the control of battery charging and discharging are discussed in this section. This section will show different scenarios for different seasons of the year. Each scenario has a specific control objective. One of the main goals in this chapter is to find a way to have the final SOC after 24 hours be close to the initial SOC and maintain the SOC between 40% and 70%. In addition, the chapter will provide information regarding the algorithm used in the simulation to manage and organize the energy in the microgrid system. The algorithm is designed and written by MATLAB. The scenarios of the simulations are flat grid power, SOC control algorithm, peak power shaving, and SOC control algorithm for peak power shaving scenario. Each one of these scenarios will be discussed individually.

3.5.1. Flat Grid Power Scenario. Since the average of the solar generation and load are provided in the simulation, the average of load for three days per seasons that are selected is greater than the average of solar generation. Therefore, the system is in need to import power from the grid. Consequently, the scenario is chosen to be constant power from the main grid. The control objective is to create a constant load to the main grid, and, therefore, the main grid provides constant power for the system. To accomplish this, the battery will be controlled depending on the load profile of the houses, PV profile, and average difference between the load profile and PV profile or the average power imported from the grid for the previous day. The battery simulation is shown in Figure 3.7.

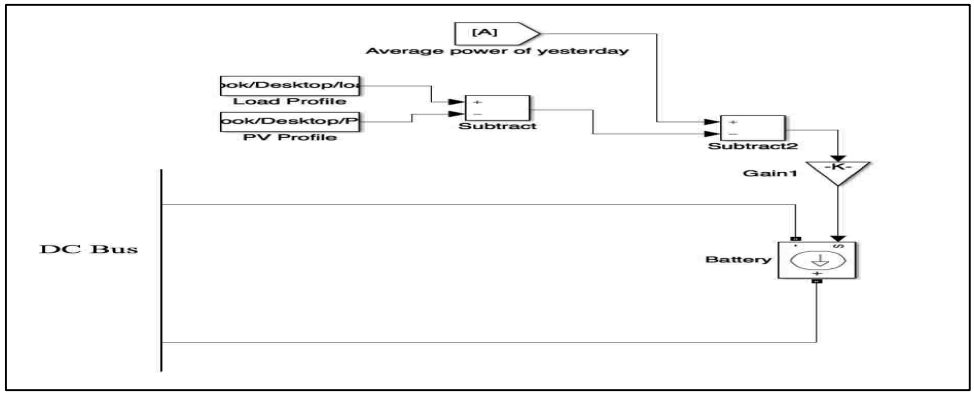

Figure 3.7. The battery simulation.

The logic of flat grid scenario is illustrated in Figure 3.8. The timeline is divided into segments. Each segment represents one day which is equivalent to 1,440 minutes. At the end of each day, the system will calculate the average difference between load and PV power to determine the grid power for the next day. The grid will receive constant power throughout the day. The following equation represent the average difference between load and PV power to determine the grid power for the next day:

$$\beta = \frac{1}{1{,}440}\sum_{j=1}^{1{,}440}[\,P_{\text{Load }(d-1),j} - P_{\text{PV }(d-1),j}] \qquad (2)$$

where, β is the average difference between load and PV power to determine the grid power for the next day, $P_{\text{Load }(d-1),j}$ is the power load profile for the day before the designated day (w), $P_{\text{PV }(d-1),j}$ is is the power load profile for the day before the designated day (w), j is the sample of a minute from each day $(1 \leq j \leq 24\ hourse \times 60\ minutes)$.

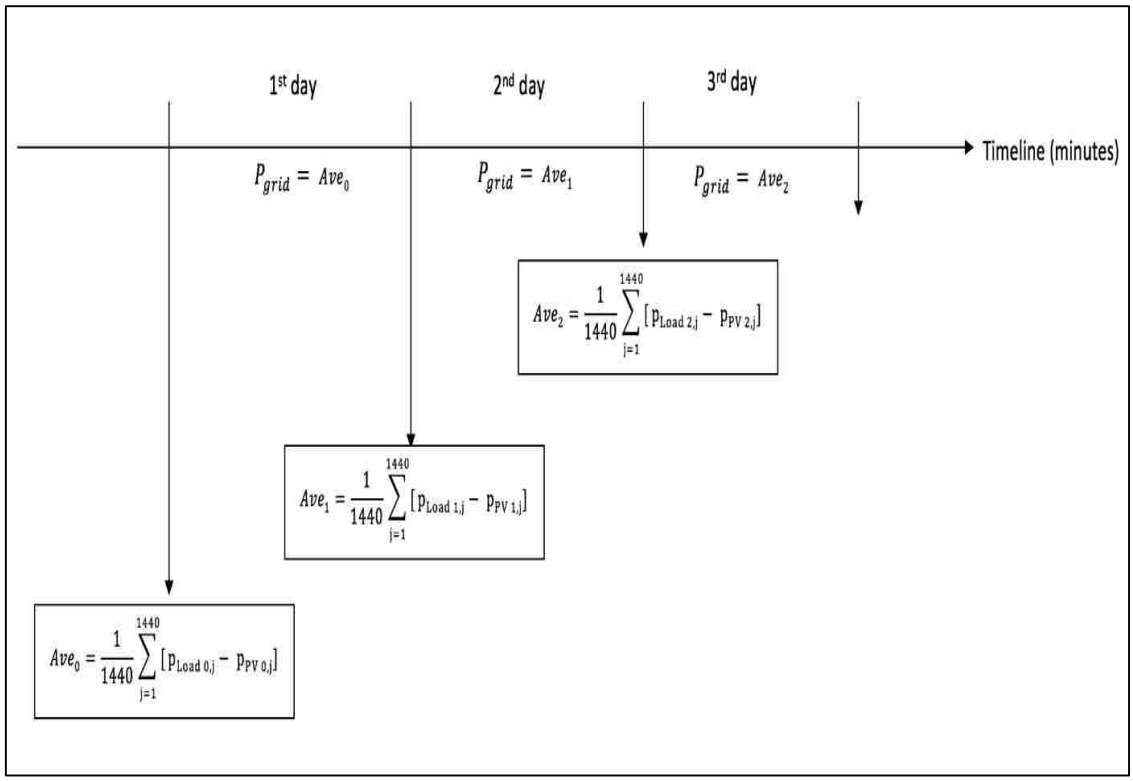

Figure 3.8. The logic of flat grid scenario.

Since the battery is simulated using a control current source, the following equation explains the total amount of charge and discharge current for the batteries in a day:

$$I_{Batt,j} = \left[\frac{1}{1,440}\sum_{j=1}^{1,440}[\, I_{Load\ (d-1),j} - I_{PV\ (d-1),j}]\right] - \left[I_{Load\ d,j} - I_{PV\ d,j}\right] \qquad (3)$$

where, I_{Batt} is the current of the battery (A), $I_{Load\ d,j}$ is the current load profile for specific day (A), d is the date for the particular day, j is the sample of a minute from each day ($1 \leq j \leq 24\ hourse \times 60\ minutes$), $I_{PV\ d,j}$ is the current PV profile for the same day of $I_{Load\ d,j}$ (A), $I_{Load\ (d-1),j}$ is the current load profile for the day before the designated day in $\left[I_{Load\ d,j} - I_{PV\ d,j}\right]$ (A), $I_{PV\ (d-1),j}$ is the current PV profile for the day before the designated day in $\left[I_{Load\ d,j} - I_{PV\ d,j}\right]$ (A), and $\left[\frac{1}{1440}\sum_{j=1}^{1440}[\, I_{Load\ (d-1),j} - I_{PV\ (d-1),j}]\right]$ is the average current for the previous day. If $I_{Batt,j}$ is greater than zero, the batteries are in charging mode. If $I_{Batt,j}$ is less than zero, the batteries are in discharging mode.

The scenario will be investigated during the four seasons each year, summer, fall, winter, and spring. Three consecutive days per season will be selected for the scenario. The average power values from each of the three days are shown in Table 3.1. In addition, the PV power profile and load power profile are provided in the simulation for each day. The time interval of the data is one minute. The total number of samples for three days is 4320. Based on this information, the following table has been constructed to display the average power for the three days used each season. This table shows that all the numbers are positive. So, in order to keep SOC between acceptable rang, the system need to get power from the grid. Furthermore, the small average power values such as 74 and 52 w indicates that most of the solar houses are empty or the solar generation is high during a day. If there is no body in most of the houses, the load power will be decreased. Also, the large average power values such as in winter indicates that the heating load is large during the day.

3.5.1.1. Summer. The load profile for three days in summer is shown in Figure 3.9. The PV profile for three days in summer is shown in Figure 3.10. The power of the main grid in the summer is shown in Figure 3.11. The power supplied by the grid is the average of the differences between the load and PV profile the previous day. Figure

3.12 provides the SOC of summer. Since β is high in the second day of summer, the overall SOC is high. Also, the SOC shows that the final SOC is lower than the initial SOC by approximately 1.5% ($\Delta SOC \approx -1.5\%$). Table 3.1 shows the average power values from each of the three days.

Table 3.1. The average power values from each of the three days.

Day	Average of Previous Day	Summer (w)	Fall (w)	Winter (w)	Spring (w)
1st day	$\frac{1}{1{,}440}\sum_{j=1}^{1{,}440}[p_{Load\ 0,j} - p_{PV\ 0,j}] = \beta_0$	714	47	6,339 w	1,544
2nd day	$\frac{1}{1{,}440}\sum_{j=1}^{1{,}440}[p_{Load\ 1,j} - p_{PV\ 1,j}] = \beta_1$	1,400	1,206	4,449	488
3rd day	$\frac{1}{1{,}440}\sum_{j=1}^{1{,}440}[p_{Load\ 2,j} - p_{PV\ 2,j}] = \beta_2$	593	439	6,418	52

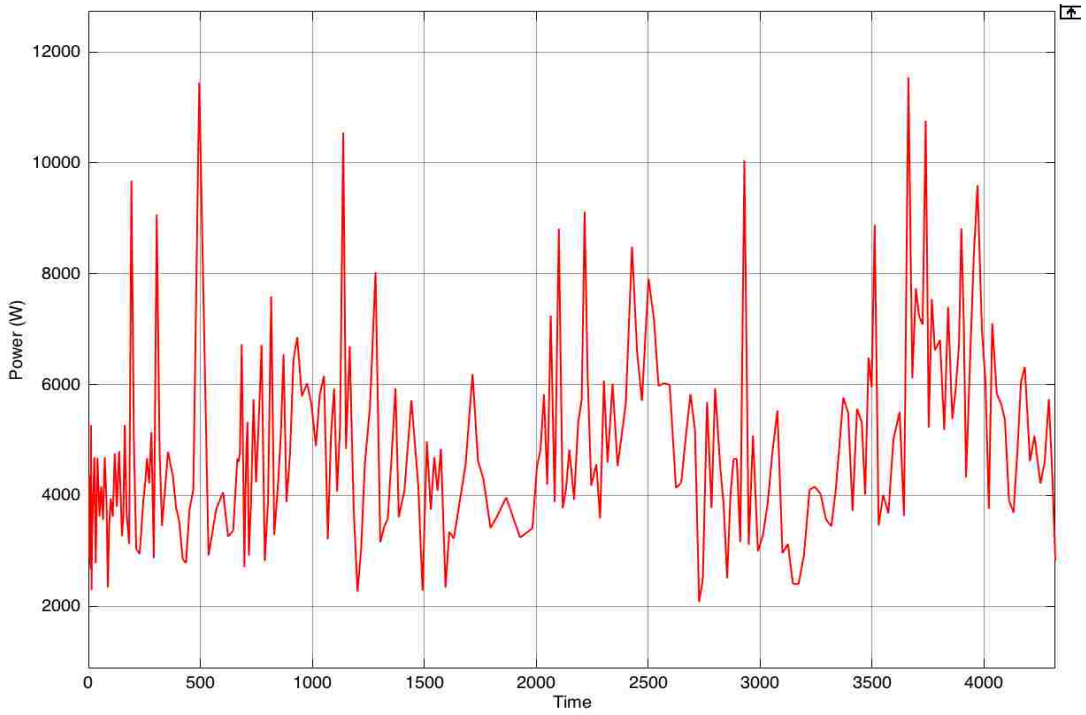

Figure 3.9. The load profile for three days in summer.

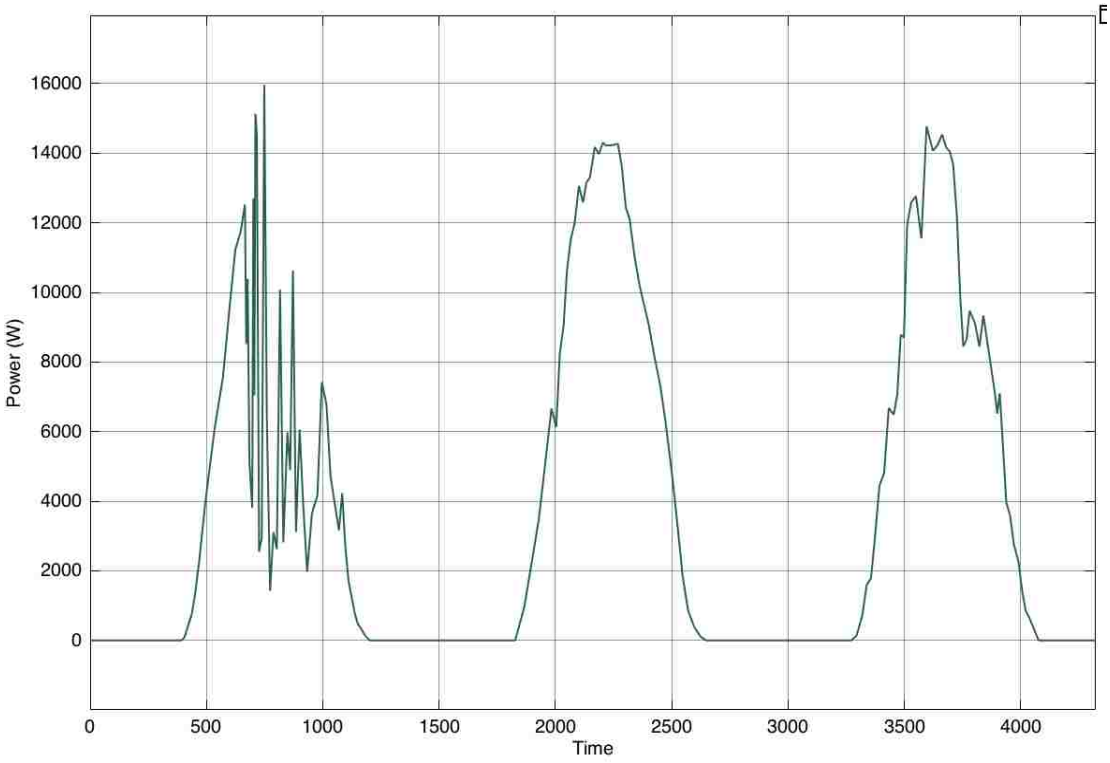

Figure 3.10. The PV profile for three days in summer.

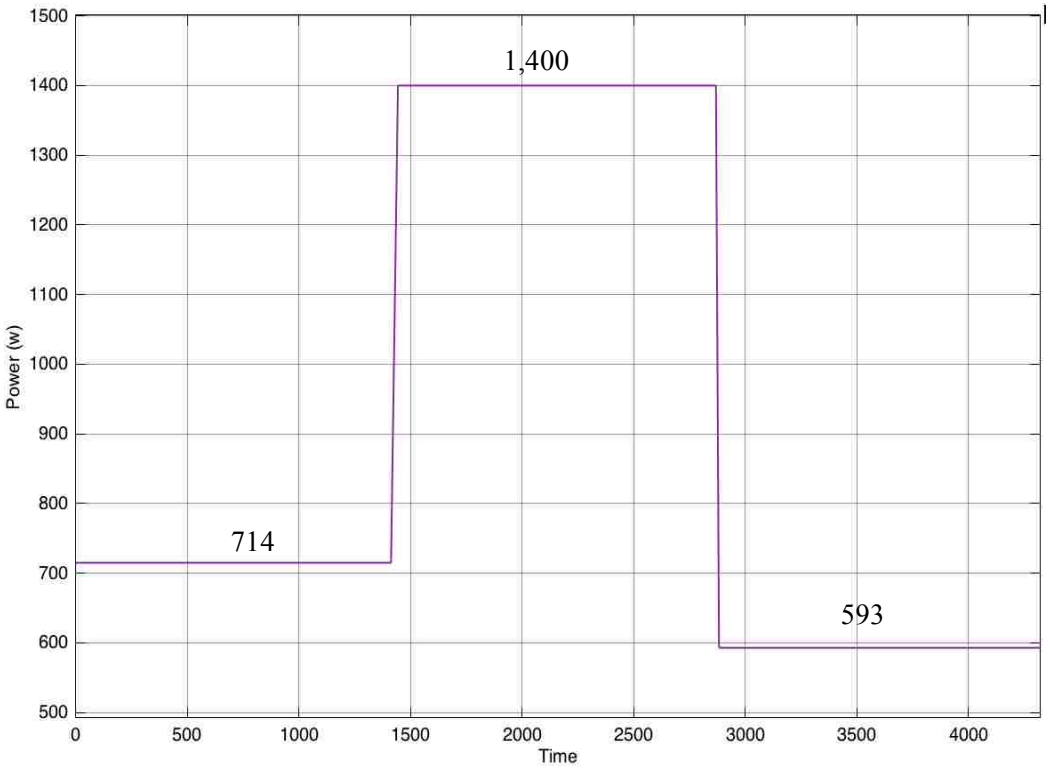

Figure 3.11. The power of the main grid in the summer.

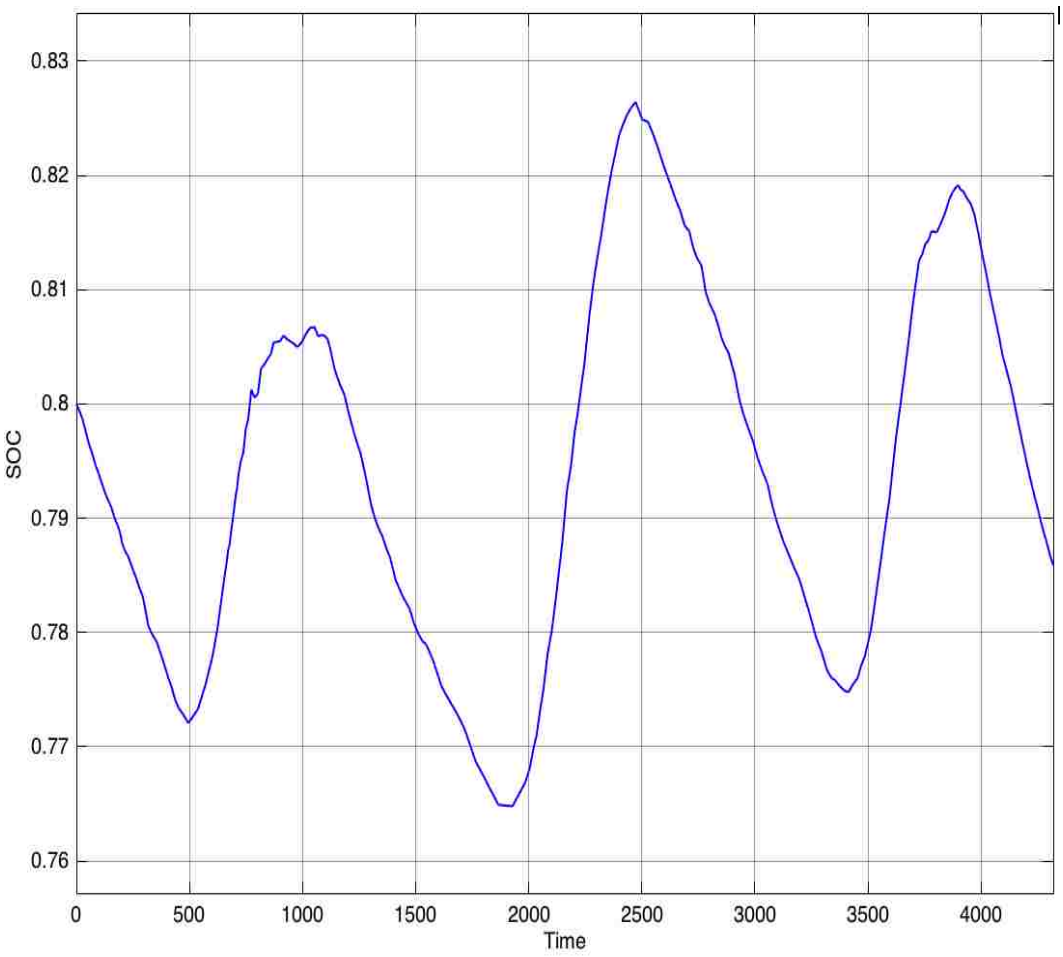

Figure 3.12. The SOC of summer.

3.5.1.2. Fall. The load profile for the three days in fall is shown in Figure 3.13. Figure 3.14 shows the PV profile for three days in fall and the power of the main grid during this season is displayed in Figure 3.15. The power supplied by the grid is the average of the differences between the load and PV profile the previous day. Figure 3.16 shows the SOC of the system. The difference between the final SOC and initial SOC is approximately 10% ($\Delta\, SOC \approx -10\%$). The PV generation on the third day is low and, therefore, the SOC for the third day shows considerable discharging to cover the demand of the load.

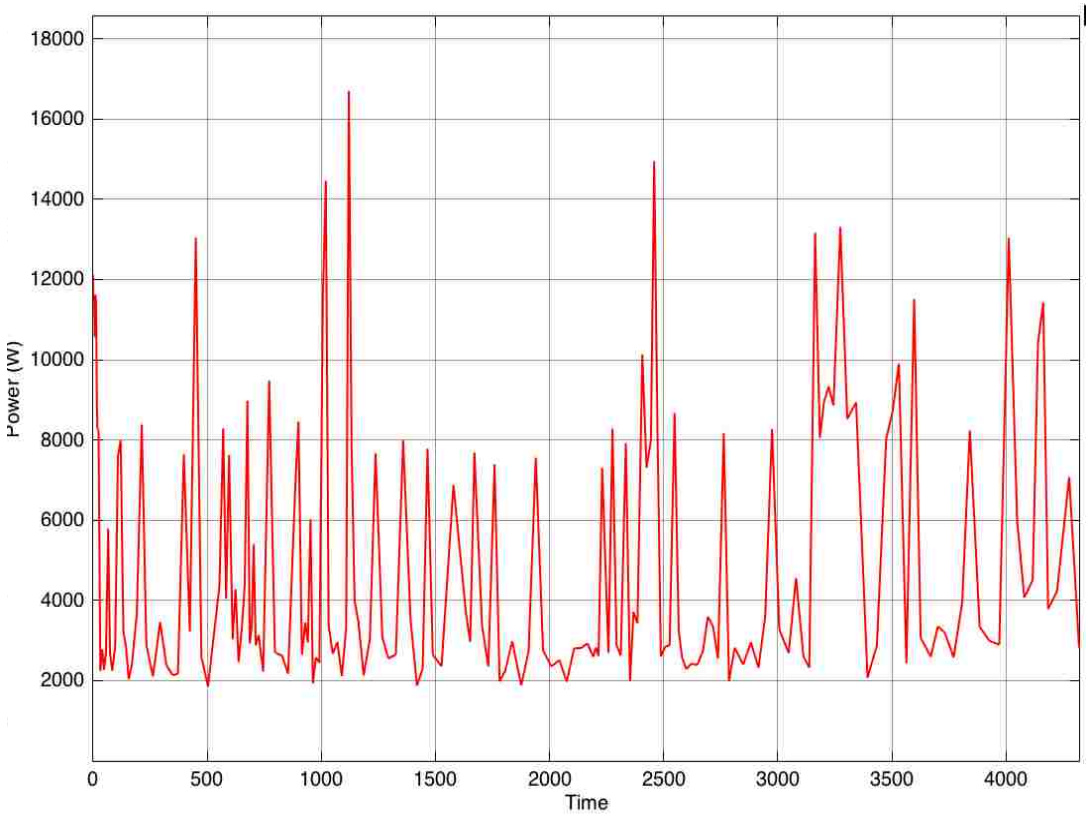

Figure 3.13. The load profile for the three days in fall.

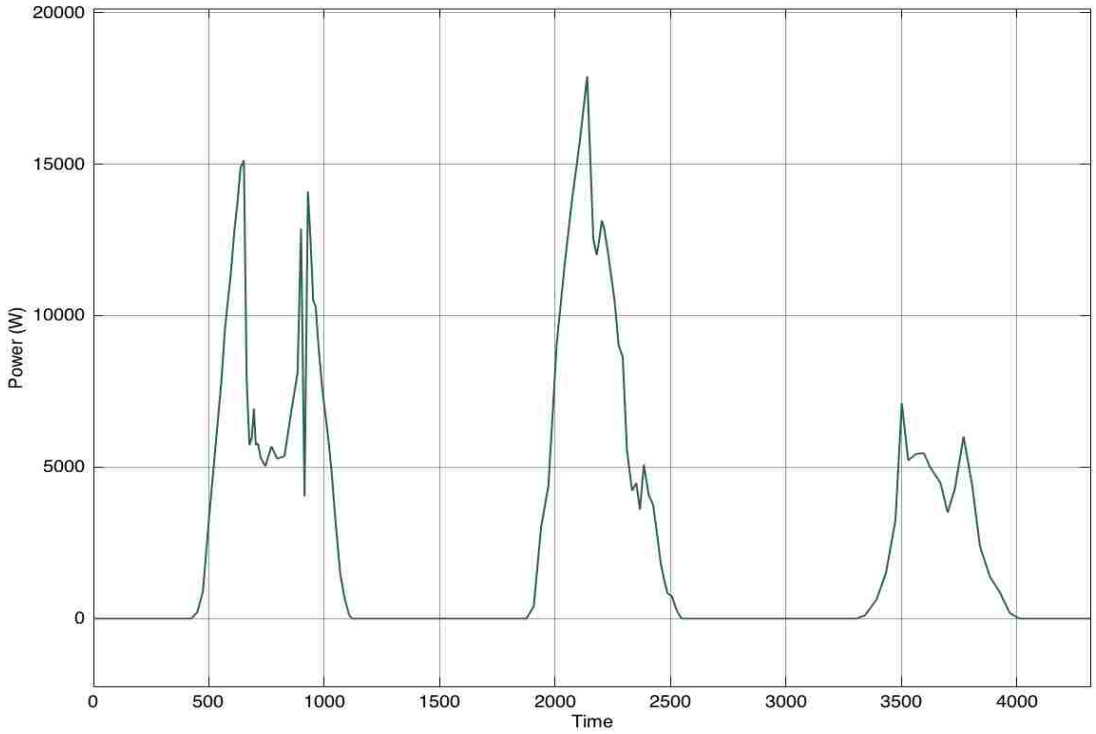

Figure 3.14. The PV profile for three days in fall.

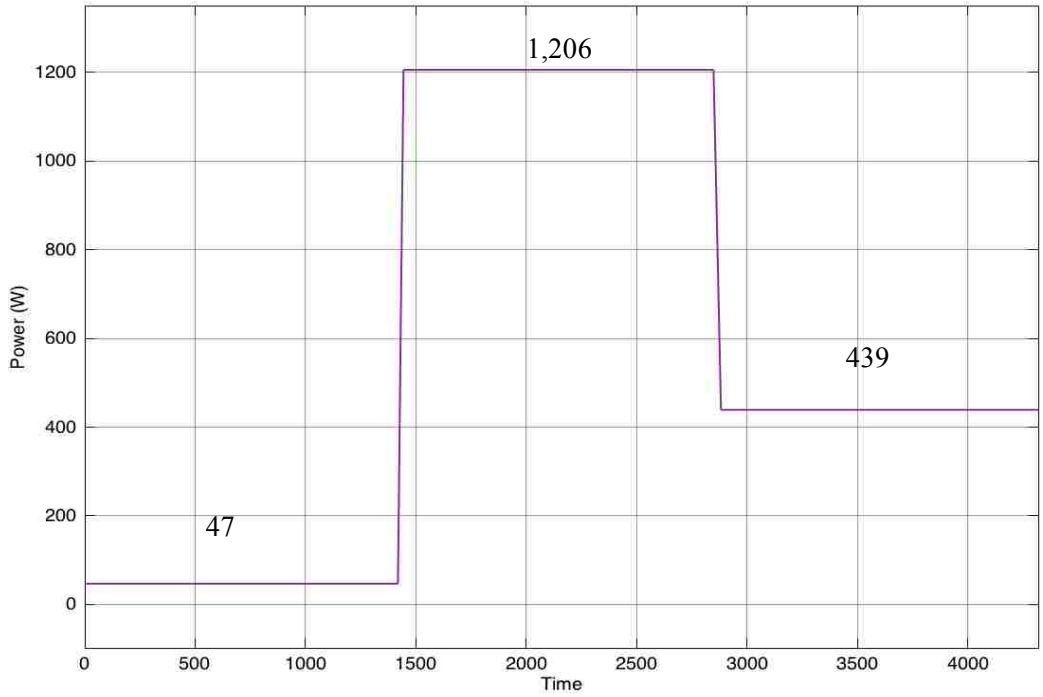

Figure 3.15. The power of the main grid during this season.

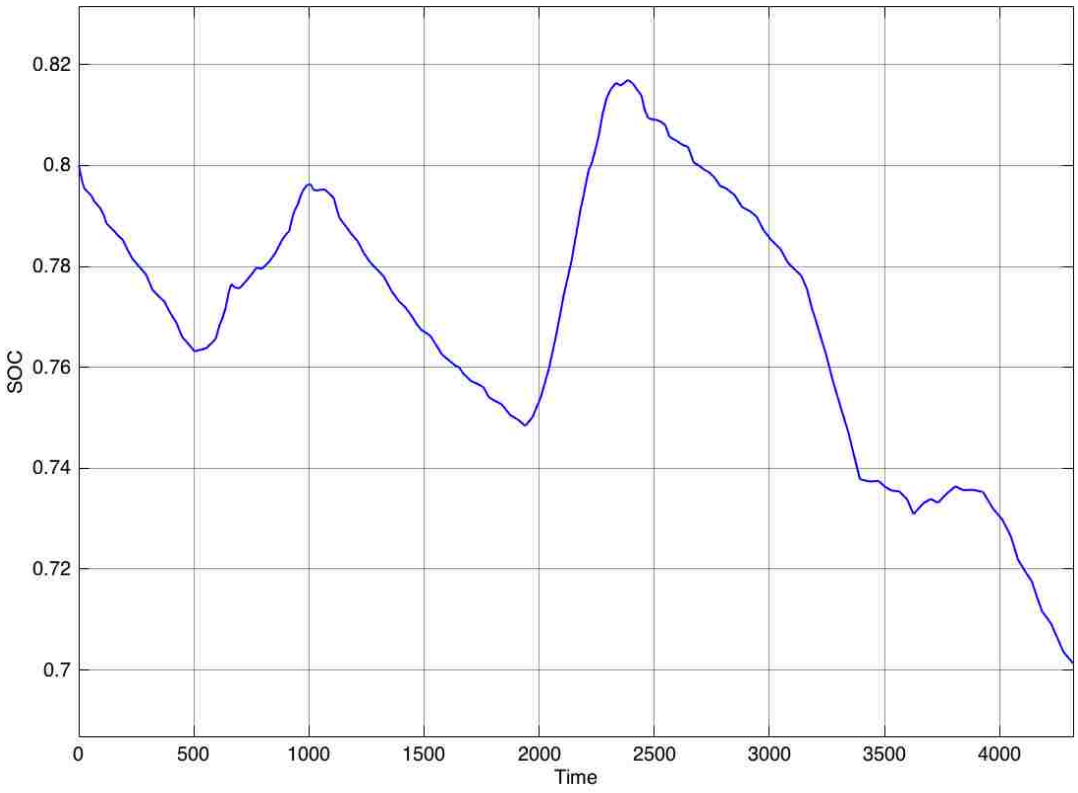

Figure 3.16. The SOC of the system.

3.5.1.3. Winter. The load profile for three days in winter is displayed in Figure 3.17. The PV profile for these three days is shown in Figure 3.18 while Figure 3.19 shows the power of the main grid in winter. The power supplied by the grid is the average of the differences between load and PV profile the previous day. The SOC in winter is shown in Figure 3.20. In winter, the β is high due to high load and low PV generation for all three days. The SOC shows that the final SOC is lower than initial SOC by approximately 2.5% ($\Delta\, SOC \approx -2.5\%$).

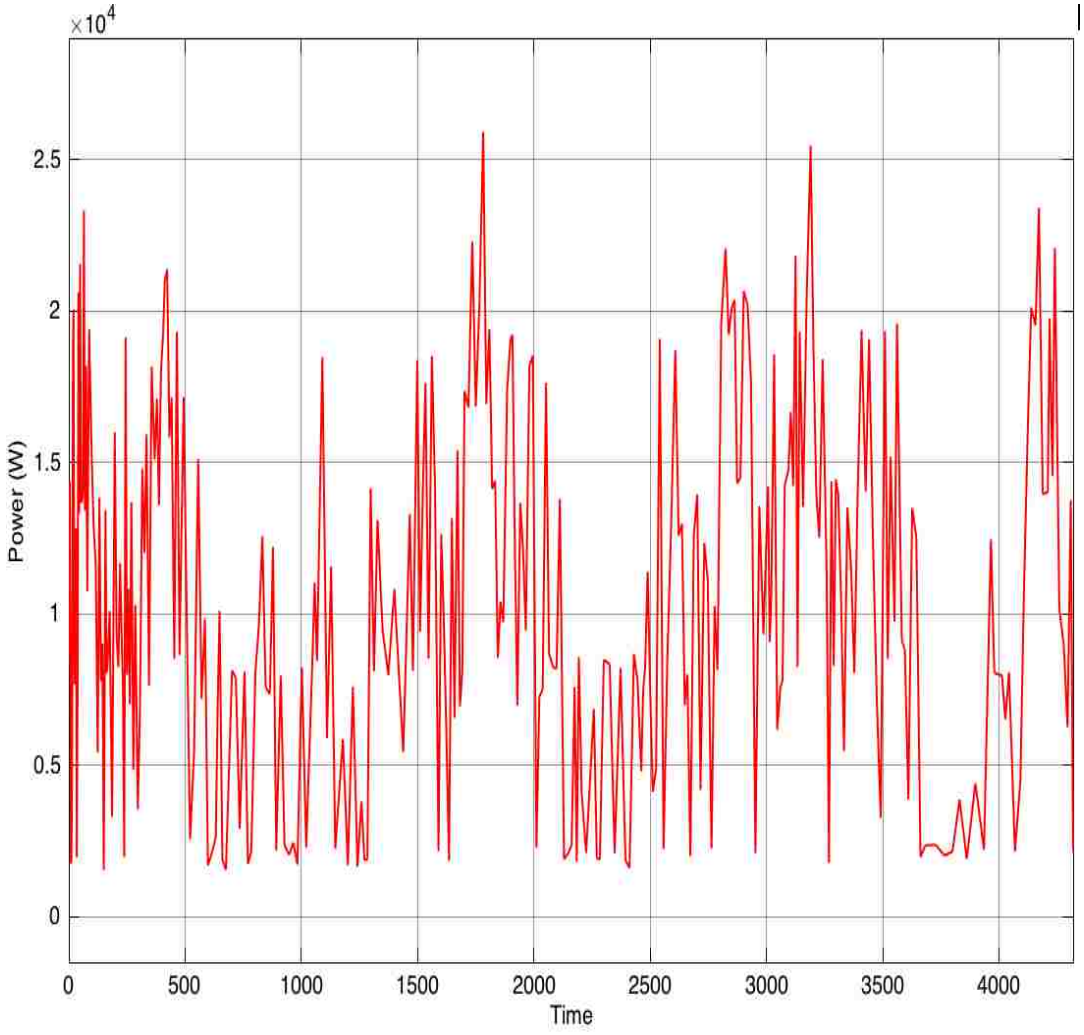

Figure 3.17. The load profile for three days in winter.

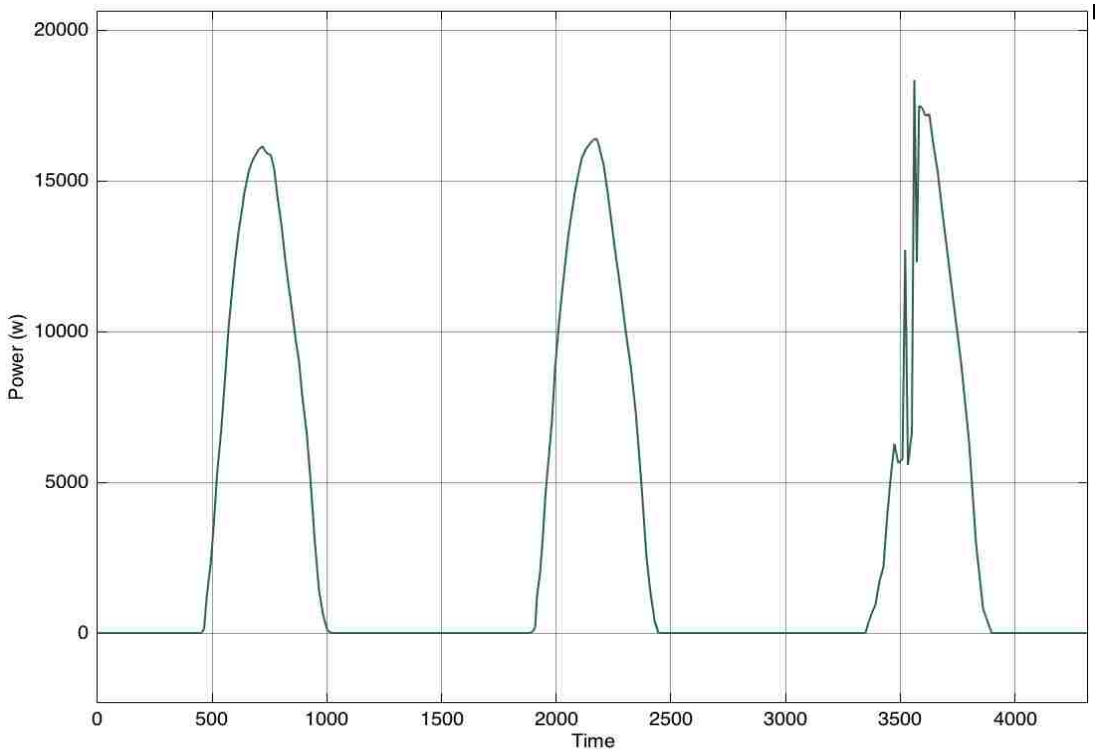

Figure 3.18. The PV profile for these three days.

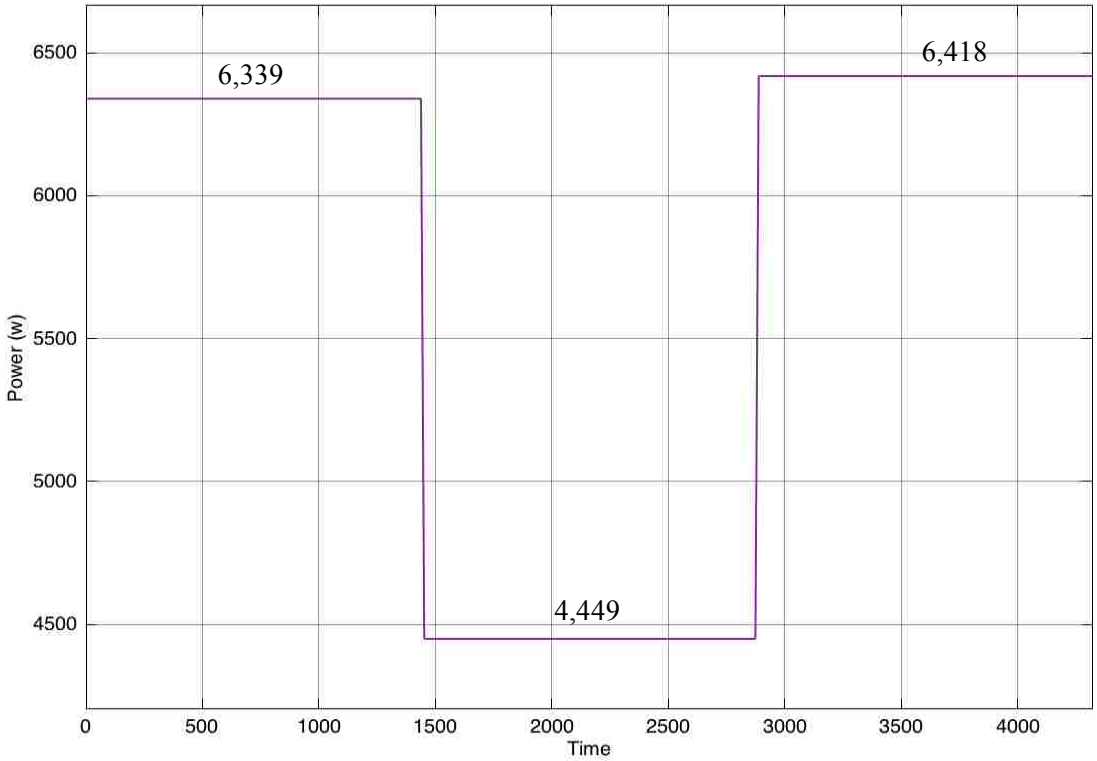

Figure 3.19. The power of the main grid in winter.

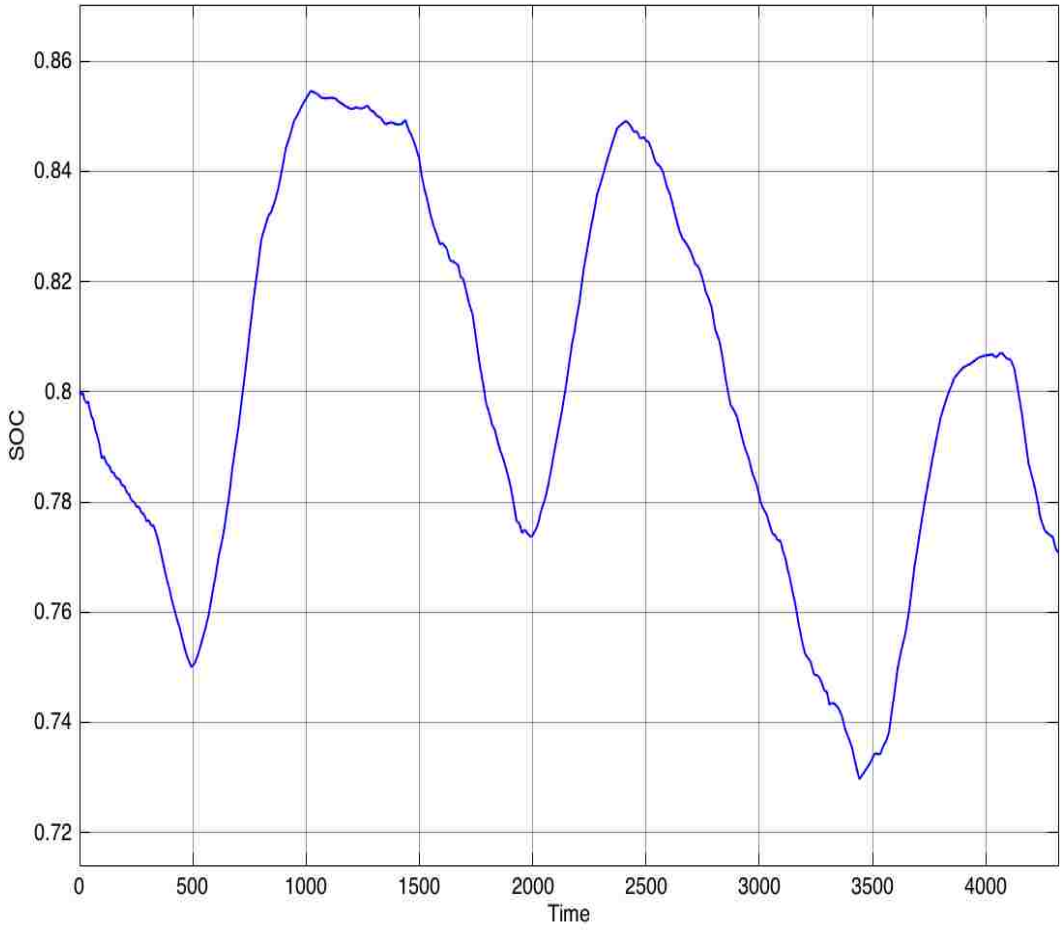

Figure 3.20. The SOC in winter.

3.5.1.4. Spring. The load profile for three days in spring is shown in Figure 3.21. Figure 3.22 shows the PV profile for these three days and Figure 3.23 shows the power supplied by the main grid in spring. The power of the grid is the average of the differences between the load and PV profile the previous day. The SOC in spring is shown in Figure 3.24. In this SOC, the final SOC is higher than the initial SOC which means that the battery will continue charging on the third day to reach a high level of charge due to increasing the PV generation and decreasing the load and β. The SOC shows that the final SOC is higher than initial SOC by approximately 8% ($\Delta\, SOC \approx 8\%$).

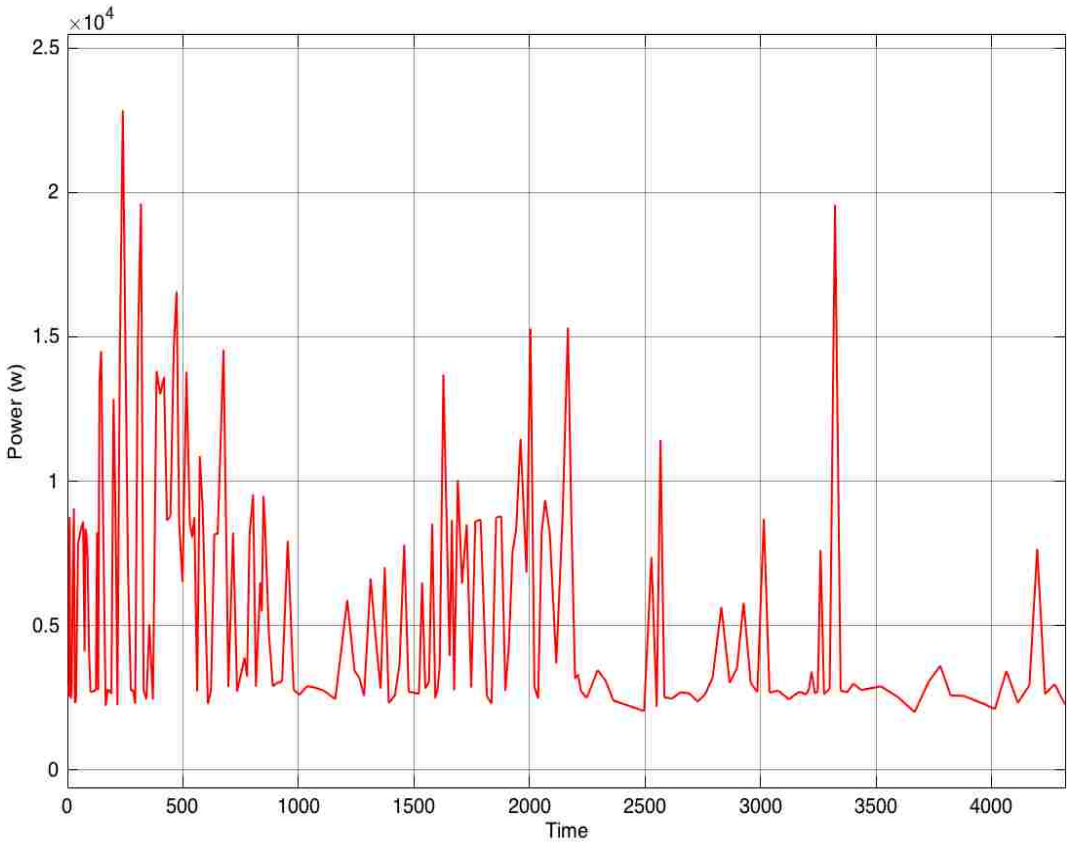

Figure 3.21. The load profile for three days in spring.

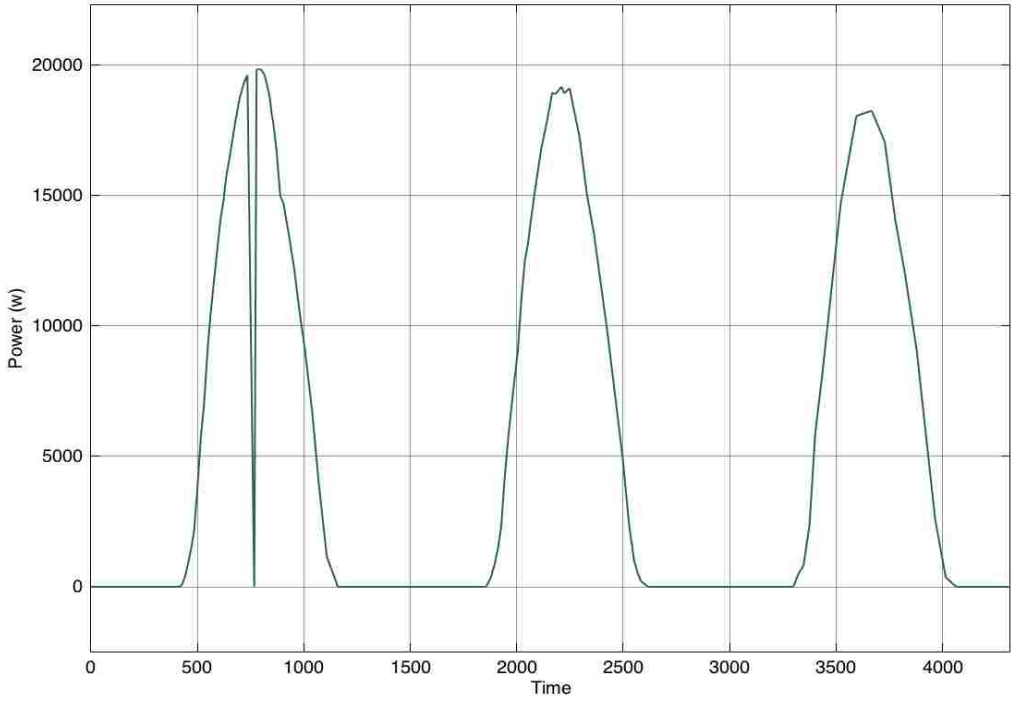

Figure 3.22. The PV profile for these three days.

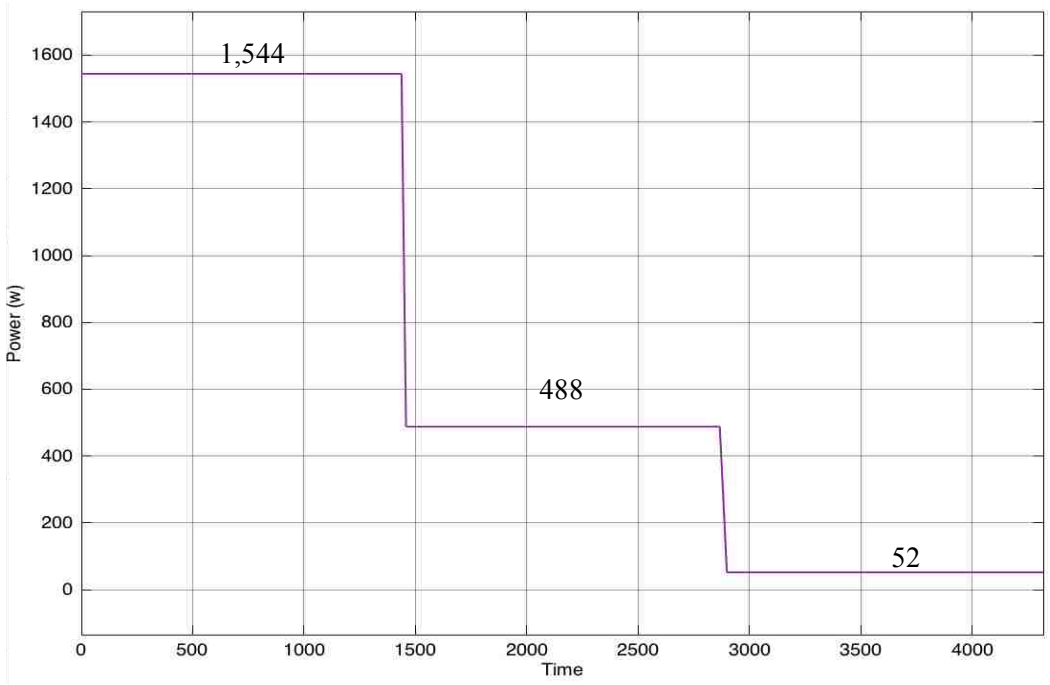

Figure 3.23. The power supplied by the main grid in spring.

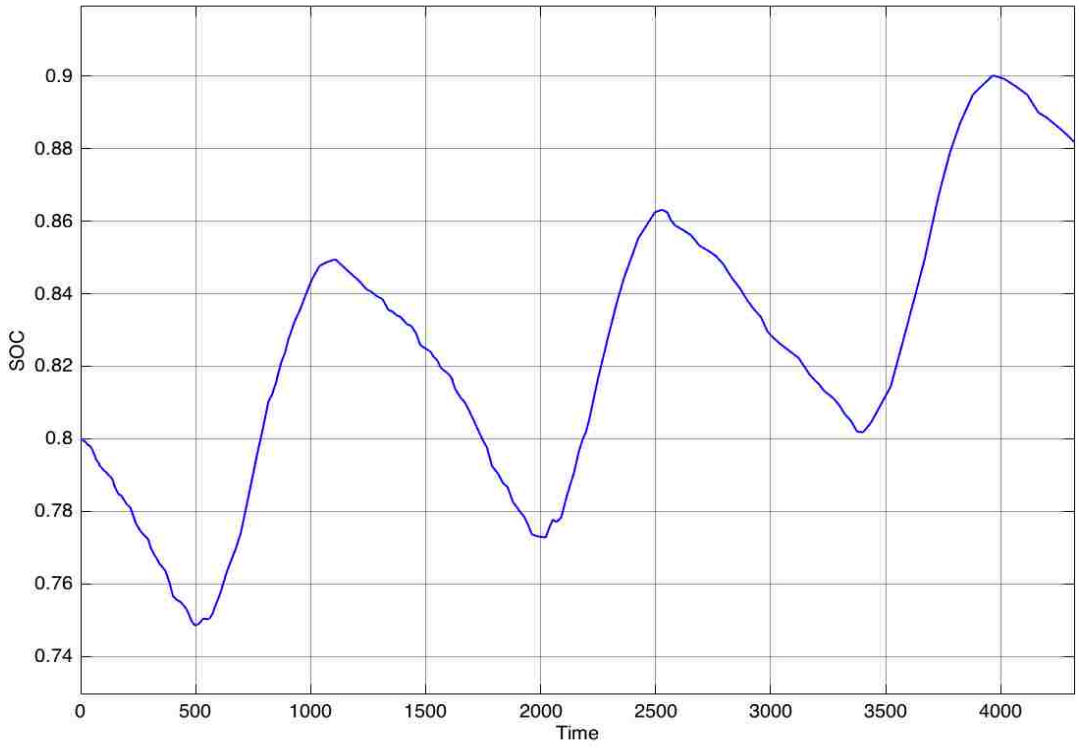

Figure 3.24. The SOC in spring.

3.5.2. SOC Control Algorithm Scenario. An algorithm is implemented to be added to the previous scenario to control the SOC. The algorithm is designed based on the SOC and variations between the solar panel generation and the load. The system can operate to charge or discharge the batteries and the algorithm's objective is to keep the SOC consistently in the 40% to 70% charge range to ensure that the batteries do not reach extremely high or low ranges. The algorithm will monitor the SOC. If the SOC passes either the upper or lower limit, the power supplied by the main grid will be adjusted to ensure that SOC stays within the established ranges. The logic of the algorithm is to check the SOC every two hours and adjust the system accordingly. The following actions of adjustments are taken based on the detected conditions:

- Decrease the power grid by 40% if:
  - SOC is between 80% - 90%; and
  - The power grid is greater than 200 w.
- Decrease the power grid by 40% and shift it down by 2,000 if:
  - SOC is between 80% - 90%; and
  - The power grid is less than 200 w.
- Decrease the power grid by 20% if:
  - SOC is between 80% - 90%.
- Leave the power grid as it is if:
  - SOC is between 40% - 70%.
- Increase the power grid by 20% if:
  - SOC is between 30% - 40%
- Increase the power grid by 40% if:
  - SOC is between 20%- 30%; and
  - The power grid is greater than 200 w.
- Increase the power grid by 40% and shift it up by 2,000 if:
  - SOC is between 20% - 30; and
  - The power grid is less than 200 w.
- Decrease the power grid 40% and shift it down by 2,000 if:
  - SOC is greater than 90%.

- Increase the power grid by 40% and shift it up by 2,000 if:
  - SOC is less than 20%.

Figure 3.25 provides a flowchart for the algorithm. The flowchart assumes the average difference between the load profile and PV profile for the precedent day as defined by β as in equation (2).

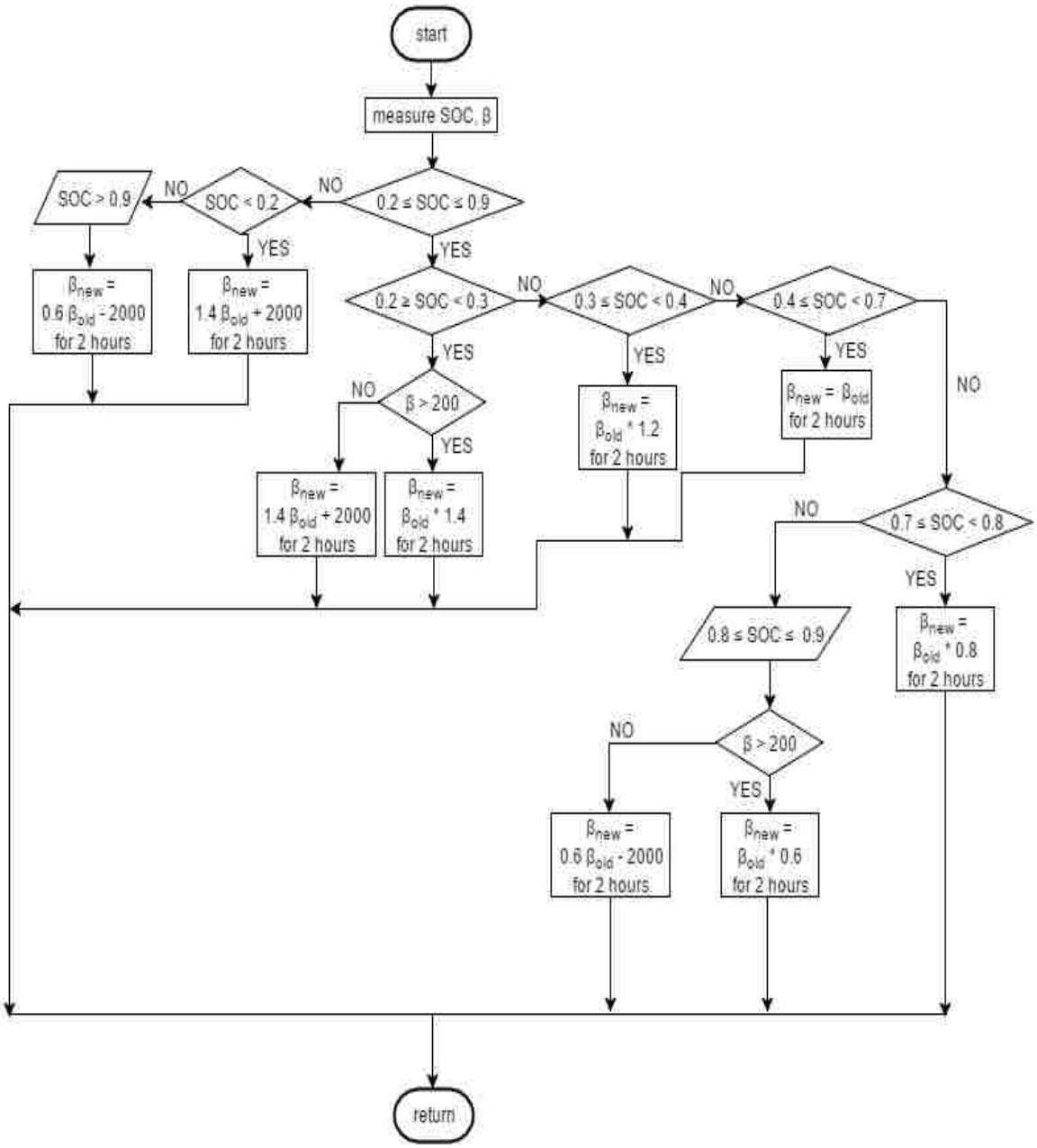

Figure 3.25. A flowchart for the algorithm.

The commands will involve either increasing or decreasing the power imported form the grid based on the range of the SOC. The code will be implemented using the MATLAB function as shown in Figure 3.26. The MATLAB function uses an input and output. The inputs of this function will be SOC and β and the output will be an adjusted numbers multiplied, added or subtracted by β to scale or adjust the power of main grid. The signals will be sent to the code using the "Tag" block, something which is responsible for receiving the input values from the simulation and sending them to the code. The "Goto" block will send the commands from the code back to the model.

```
1   function h  = fcn(soc,B)
2   %#codegen
3   h=1;
4   if (soc>=0.4)&&(soc<0.7)
5       h=B;
6   elseif (soc>=0.3)&&(soc<0.4)
7       h=1.2*B;
8   elseif (soc>=0.2)&&(soc<0.3)&&(B>200)
9       h=1.4*B;
10      elseif (soc>=0.2)&&(soc<0.3)&&(B<200)
11      h=1.4*B+2000;
12  elseif (soc>0.7)&&(soc<=0.8)
13      h=0.8*B;
14  elseif (soc>0.8)&&(soc<=0.9)&&(B>200)
15      h=0.6*B;
16      elseif (soc>0.8)&&(soc<=0.9)&&(B<200)
17      h=0.6*B-2000;
18  elseif (soc>0.9)
19      h=0.6*B-2000;
20  else h=1.4*B+2000;
21  end
22  return
```

Figure 3.26. The MATLAB function.

3.5.2.1. Summer. The load and PV profiles for three days in summer are shown in Figures 3.9 and 3.10. The power of the main grid during summer is shown in Figure 3.27. The power of the grid is the average of the differences between the load and PV profile the previous day. The SOC in summer is shown in Figure 3.28. The battery SOC starts discharging with 0.8 initial value. Since the SOC is within range 0.8 and 0.7, β will be 80% of its original value. Also, once the SOC exceeds 0.8 in the second day, the main grid power is reduced by 60% of β to avoid any overcharging. The SOC shows that the final SOC is lower than initial SOC by approximately 4% ($\Delta\, SOC \approx -4\%$). Also, it shows that applying the algorithm in this scenario was able to bring SOC back to the limits even though initial SOC was 80%.

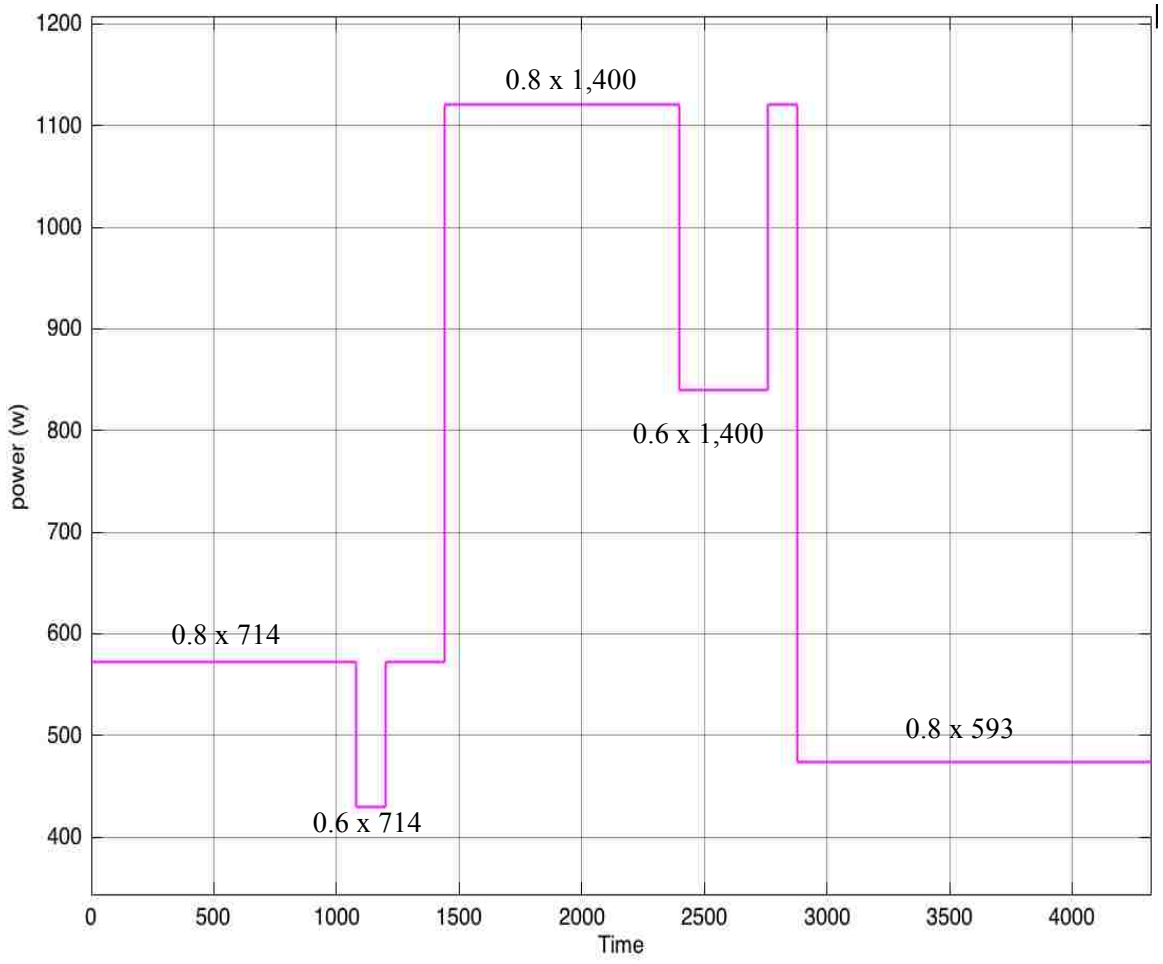

Figure 3.27. The power of the main grid during summer.

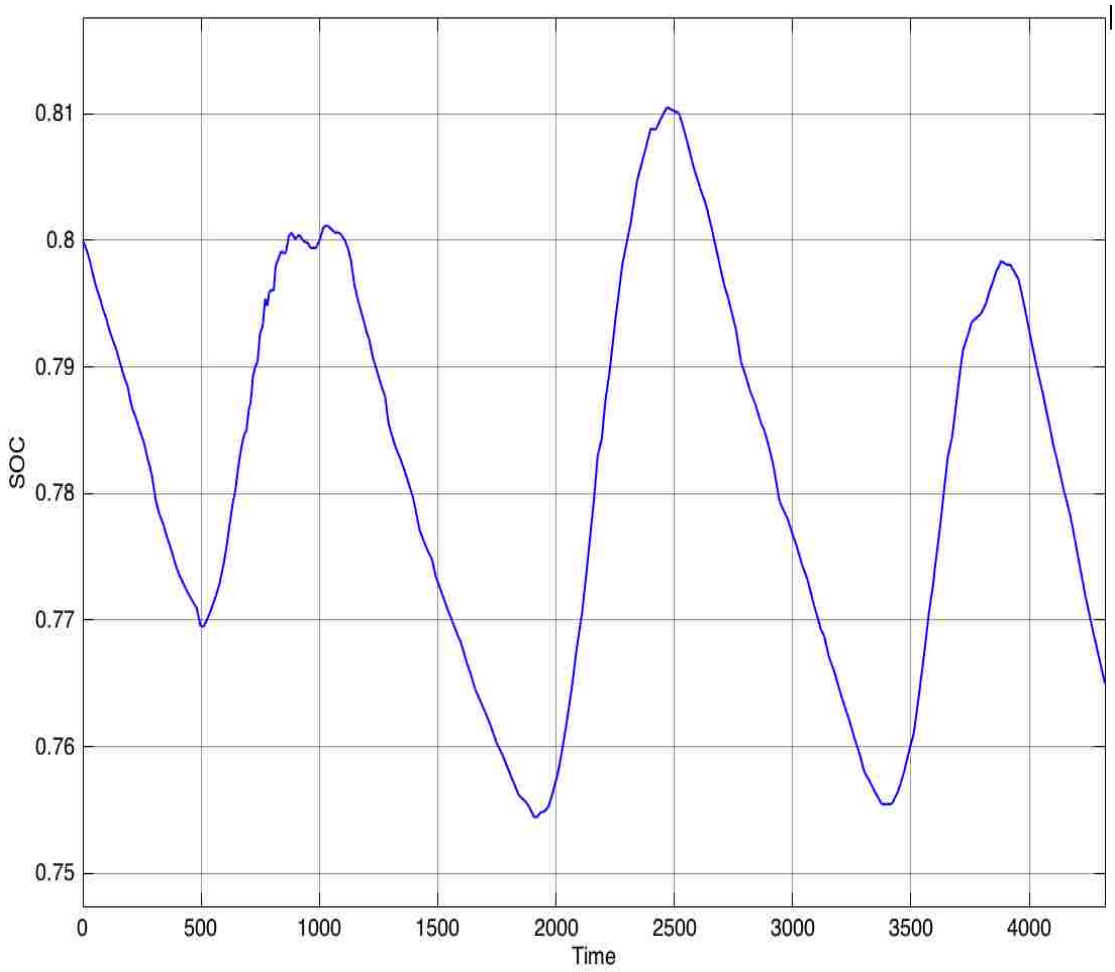

Figure 3.28. The SOC in summer.

3.5.2.2. Fall. The load and PV profiles for the three days in fall are shown in Figures 3.13 and 3.14. The power of the main grid in fall is shown in Figure 3.29. The power of the grid is the average of the differences between the load and PV profile the previous day. Figure 3.30 shows the SOC in fall. The SOC is maintained between 0.8 and 0.7 except for the middle of second day and at the end of third day. In the middle of second day, the power of the main grid reduced by 60% of β, because the SOC exceed the 0.8 level. At the end of the third day, the SOC decreased below 0.7 which means the grid power will go back to the original β. Also, The SOC shows that the final SOC is much lower than initial SOC by approximately 10% ($\Delta\, SOC \approx -10\%$).

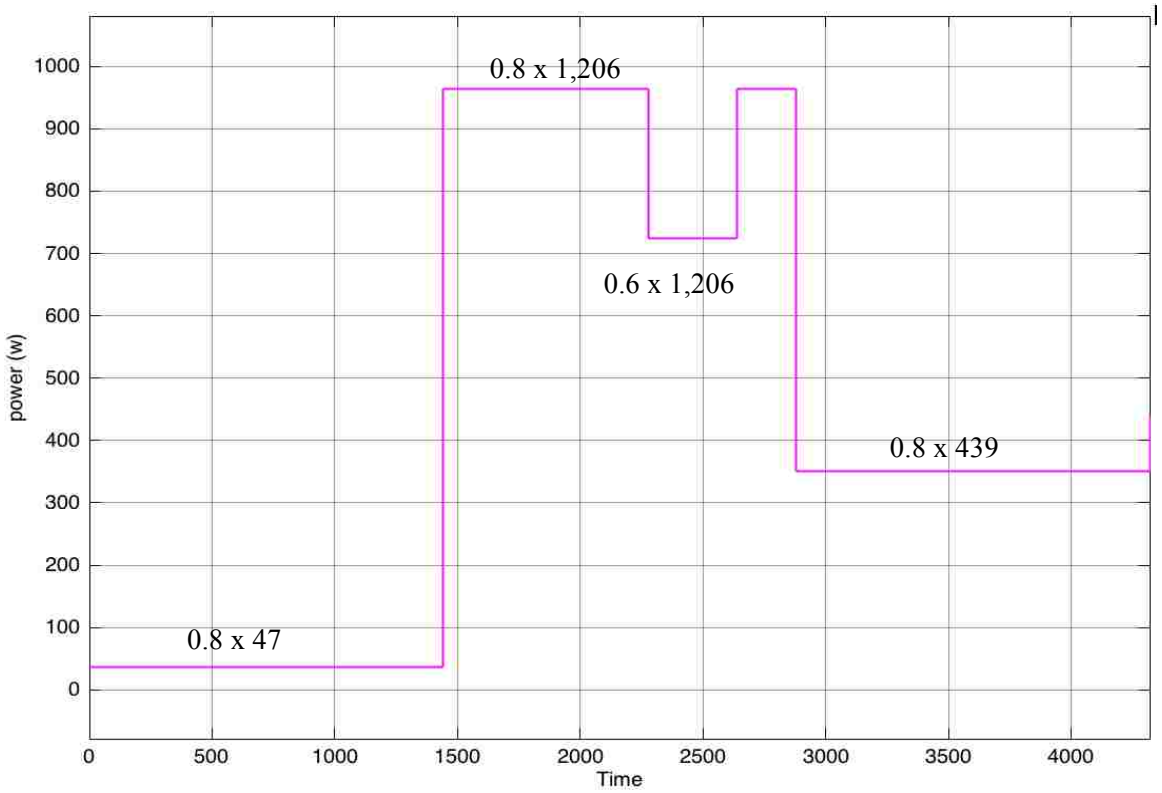

Figure 3.29. The power of the main grid in fall.

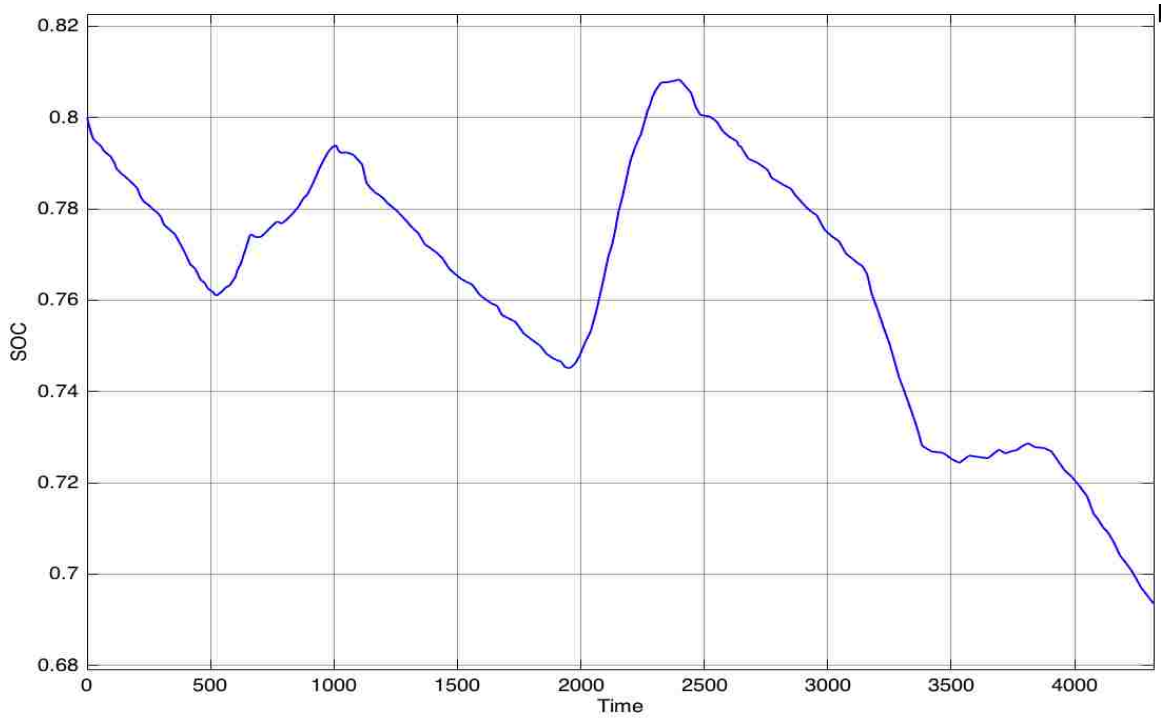

Figure 3.30. The SOC in fall.

3.5.2.3. Winter. The load and the PV profiles are shown in Figures 3.17 and 3.18. The power of the main grid during winter is shown in Figure 3.31. The power of the grid is the average of the differences between the load and PV profile the previous day. Figure 3.32 shows the SOC of winter. The battery SOC starts discharging with 0.8 initial value. Since the SOC within range 0.8 and 0.7, the β will be 80% of its original value. Also, once The SOC exceeds the 0.8 in the second day, the power of main grid reduced by 60% of β to avoid any overcharging. And, when the SOC below 0.7, the grid power will go back to its original value to ensure that the SOC of the battery is maintained within reasonable range. The SOC shows that the difference between the final SOC and initial SOC is around 12% ($\Delta\, SOC \approx -12\%$).

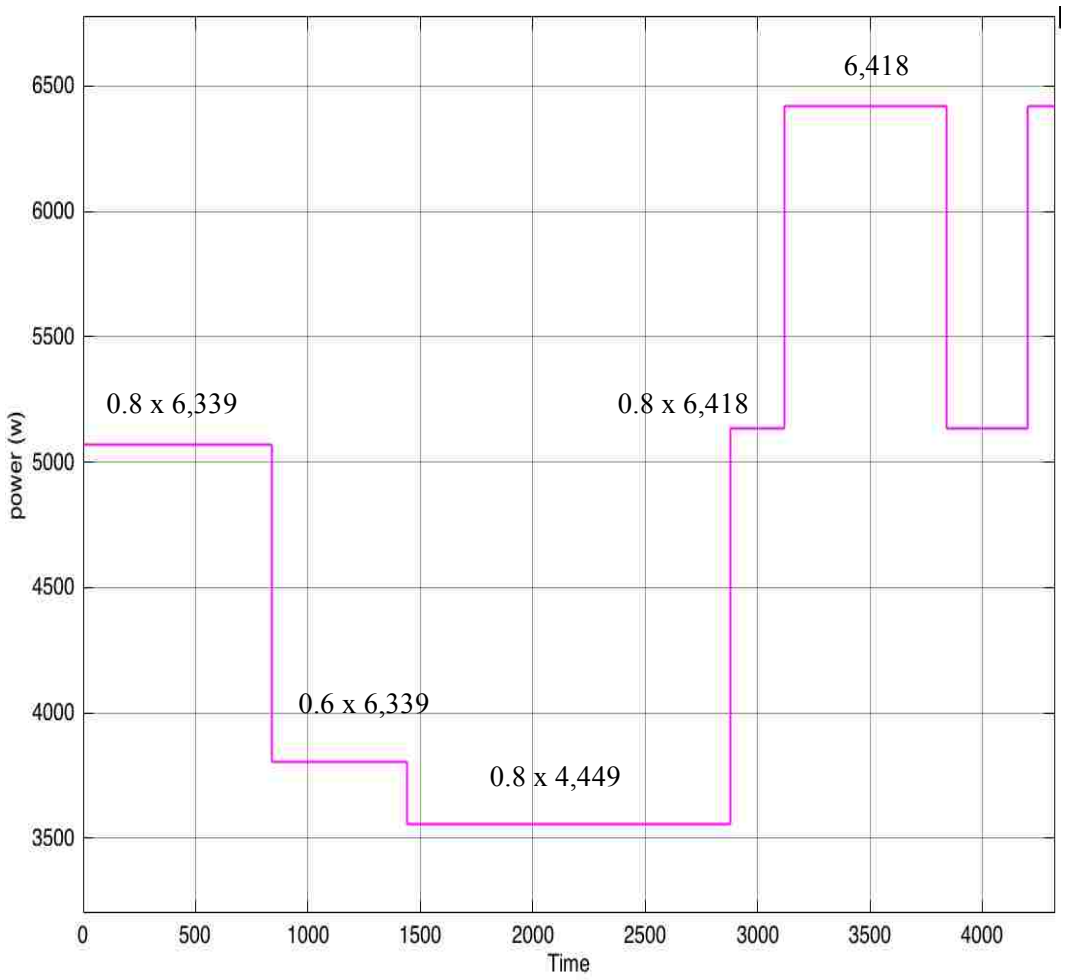

Figure 3.31. The power of the main grid during winter.

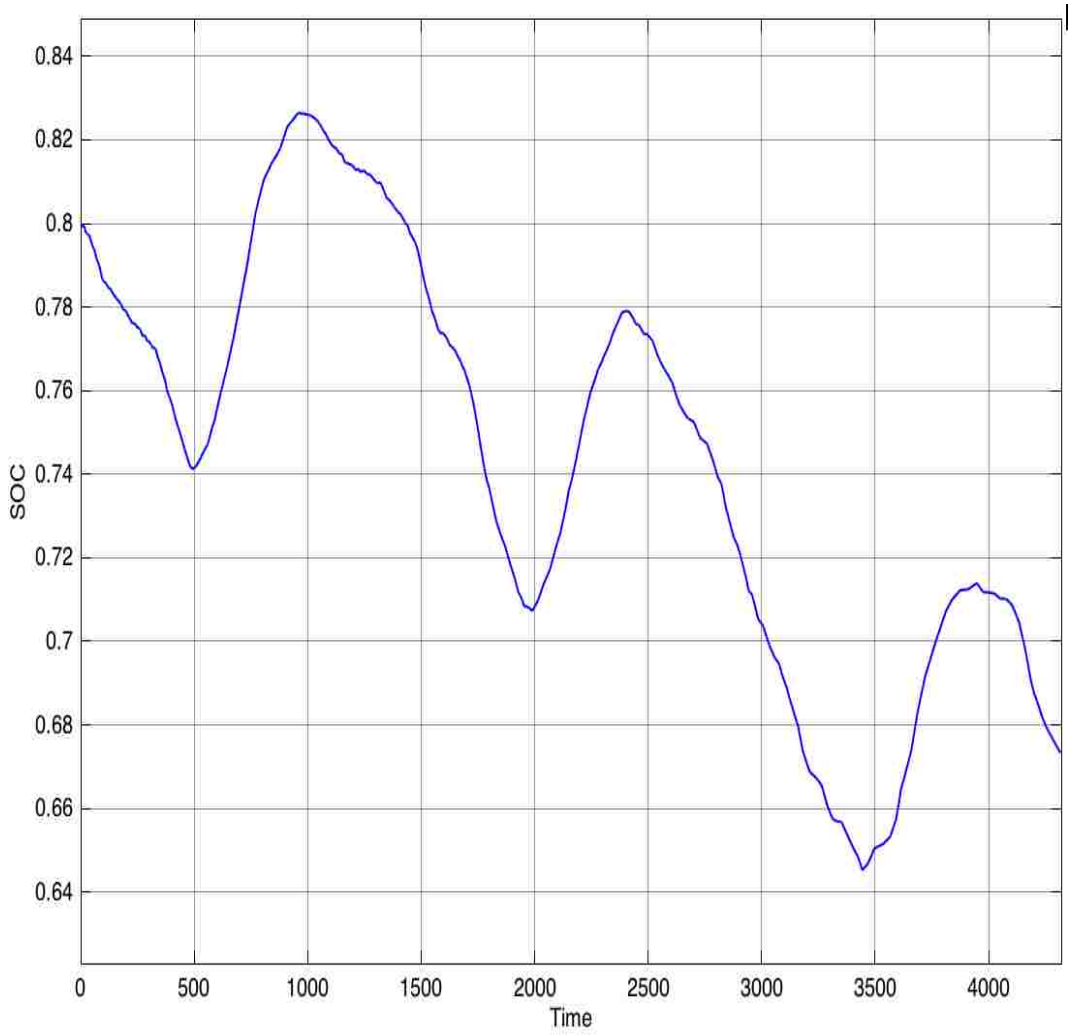

Figure 3.32. The SOC of winter.

3.5.2.4. Spring. The load and PV profiles for spring are shown in Figures 3.21 and 3.22. Figure 3.33 shows the power of the main grid in spring. The power of the grid is the average of the differences between the load and PV profile the previous day. The SOC of spring is shown in Figure 3.34. The battery SOC in the third day exceeds 0.8 and β is low. Therefore, the microgrid system will send power to the grid in order to avoid overcharging the battery. The exported power to the grid is 60% of the β subtracted by 2000. Also, The SOC shows that the final SOC is bit higher than initial SOC by around 3% ($\Delta\, SOC \approx 3\%$).

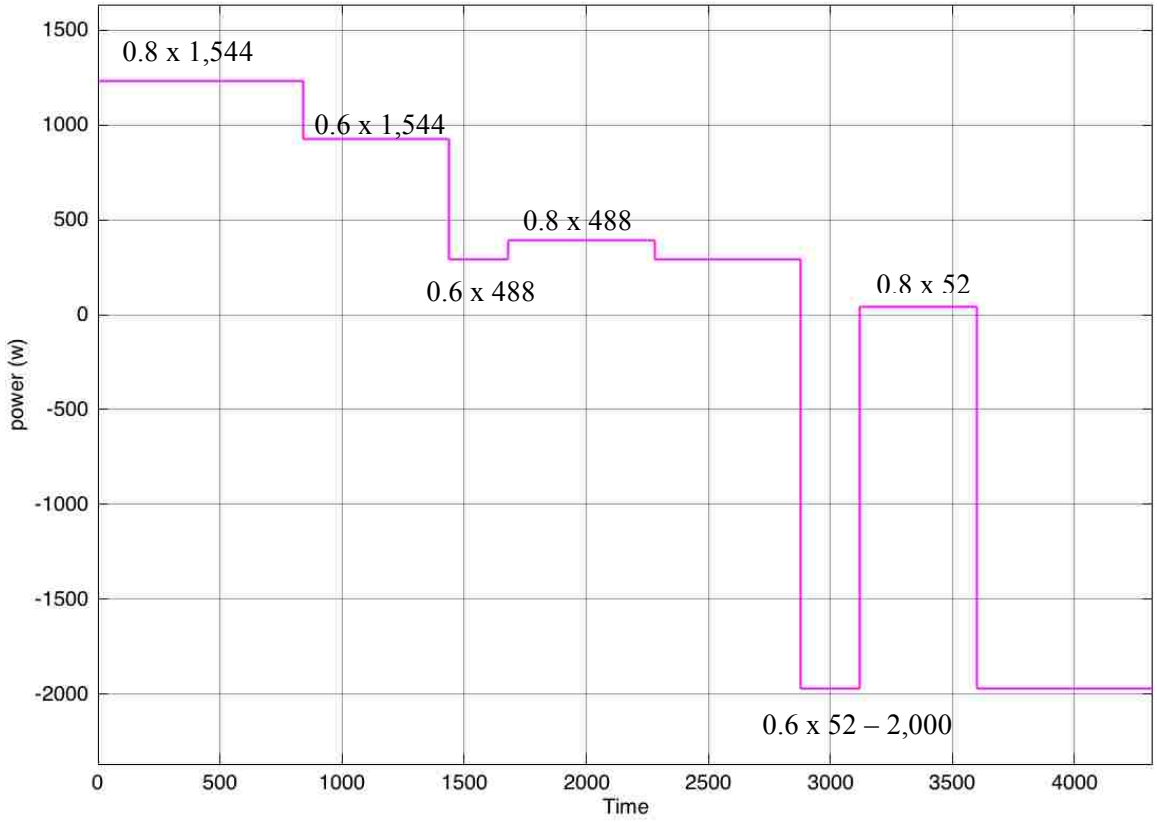

Figure 3.33. The power of the main grid in spring.

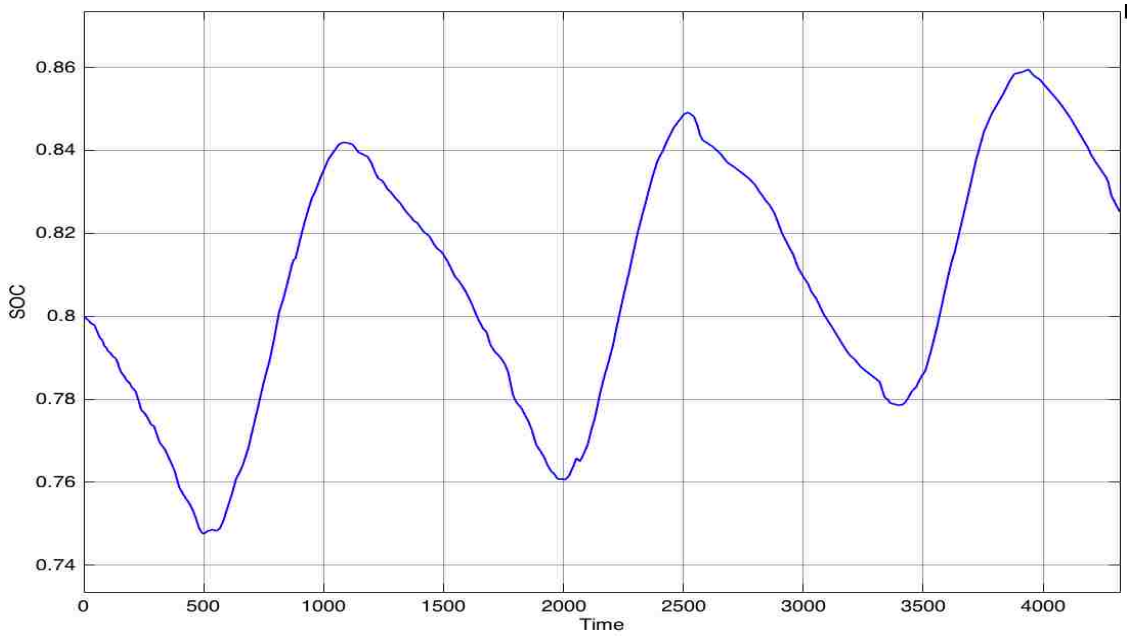

Figure 3.34. The SOC of spring.

3.5.3. Peak Power Shaving Scenario. The control objective for this scenario is to create a constant load for the main grid with the exception of the peak load power hours. The main grid will supply constant power for the system until a certain time at which point the system will slowly ramp down to zero and then increase power until a specified time point. The time that the system works to ramp up power will be the interval of maximum load demand. In this simulation, the chosen time interval is from 3:00 pm until 7:00 pm each day. The constant grid power in this scenario will be higher than in the flat scenario due to the ramp. The scenario will be investigated in three days selected during summer, fall, winter, and spring. In addition, a PV power profile and load power profile are provided in the simulation for each day. The time interval of the data is one minute and there will be 4,320 samples over the three-day sample, providing a sample for each minute of each day. The average values from each of the three days are shown in Table 3.2.

Table 3.2. The average values from each of the three days.

The day	Average of previous day except PV peak power time (3pm-7pm)	Summer (w)	Fall (w)	Winter (w)	Spring (w)
1st day	$\beta_{0,new} = \frac{\beta_{0,old} \times 24(houres)}{24 - 5\ (houres)}$	903	59	8,007	1,950
2nd day	$\beta_{1,new} = \frac{\beta_{1,old} \times 24(houres)}{24 - 5\ (houres)}$	1,768	1,523	5,619	616
3rd day	$\beta_{2,new} = \frac{\beta_{2,old} \times 24(houres)}{24 - 5\ (houres)}$	755	554	8,106	66

3.5.3.1. Summer. The load and PV profiles for three days in summer are shown in Figures 3.9 and 3.10. The power of main grid in summer is shown in Figure 3.35. The power of the grid is the average of the differences between the load and PV profile the previous day. The SOC in summer is shown in Figure 3.36. The SOC shows that the final

SOC is bit lower than initial SOC by around 1% ($\Delta\, SOC \approx -1\%$). The power of main remains constant except the PV peak power from 3pm until 7pm each day.

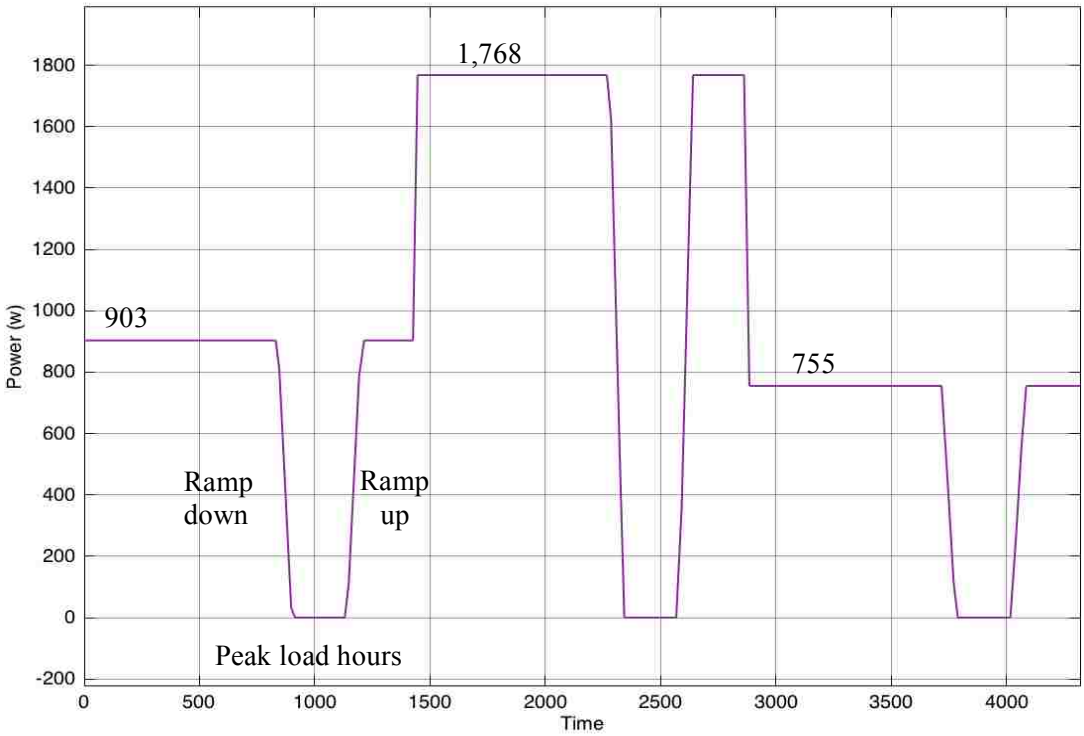

Figure 3.35. The power of main grid in summer.

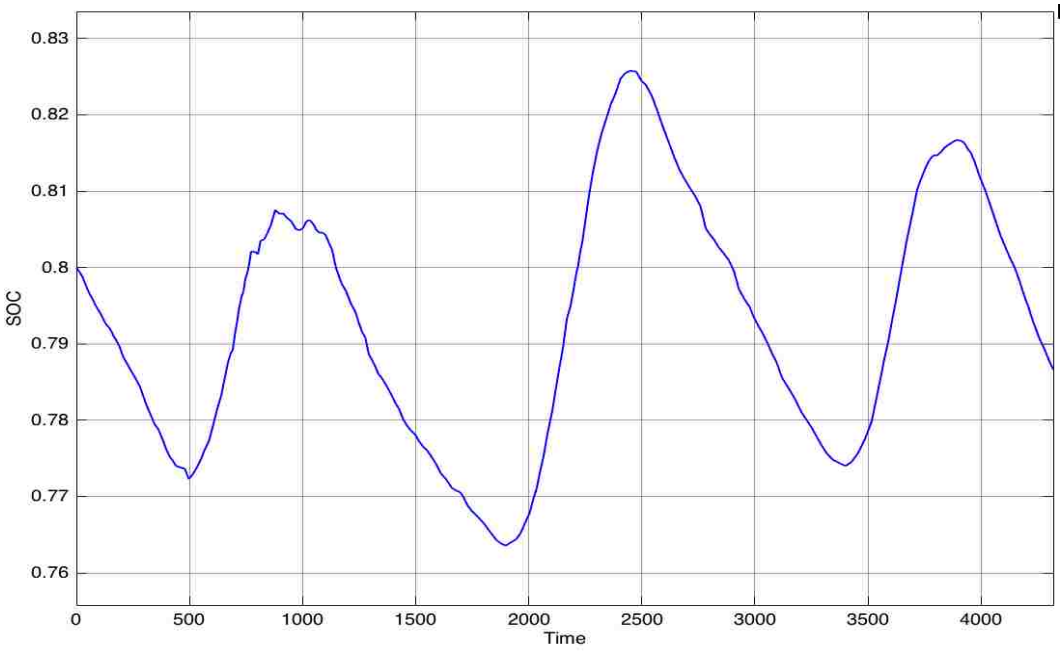

Figure 3.36. The SOC in summer.

3.5.3.2. Fall. The load and PV profiles for the three days in fall are shown in Figures 3.13 and 3.14. The power of the main grid in fall is shown in Figure 3.37. The power of the grid is the average of the differences between the load and PV profile the previous day. The SOC in fall is shown in Figure 3.38. The SOC shows that the final SOC is lower than initial SOC by 10% ($\Delta\, SOC \approx -10\%$). The power of main remains constant except the PV peak power time from 3pm until 7pm each day.

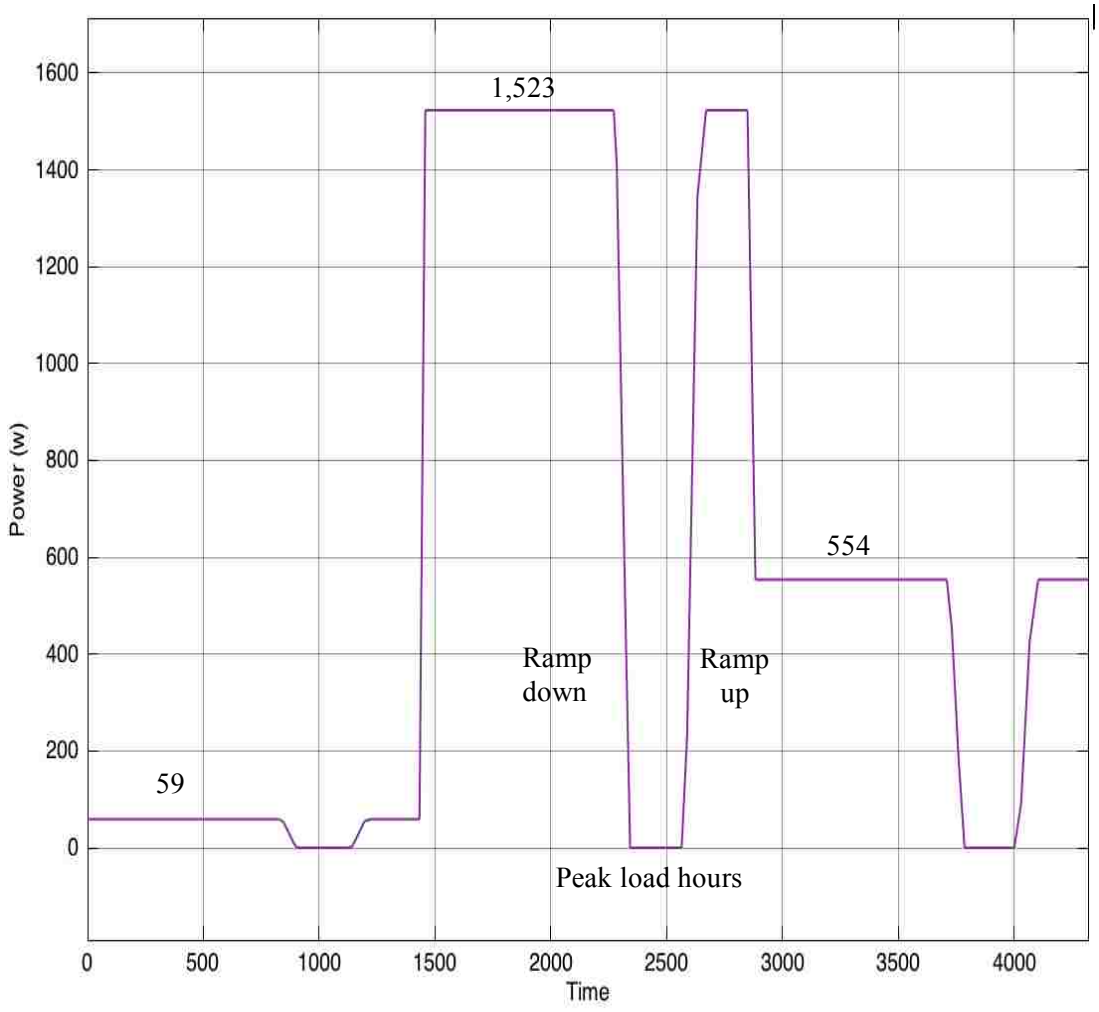

Figure 3.37. The power of the main grid in fall.

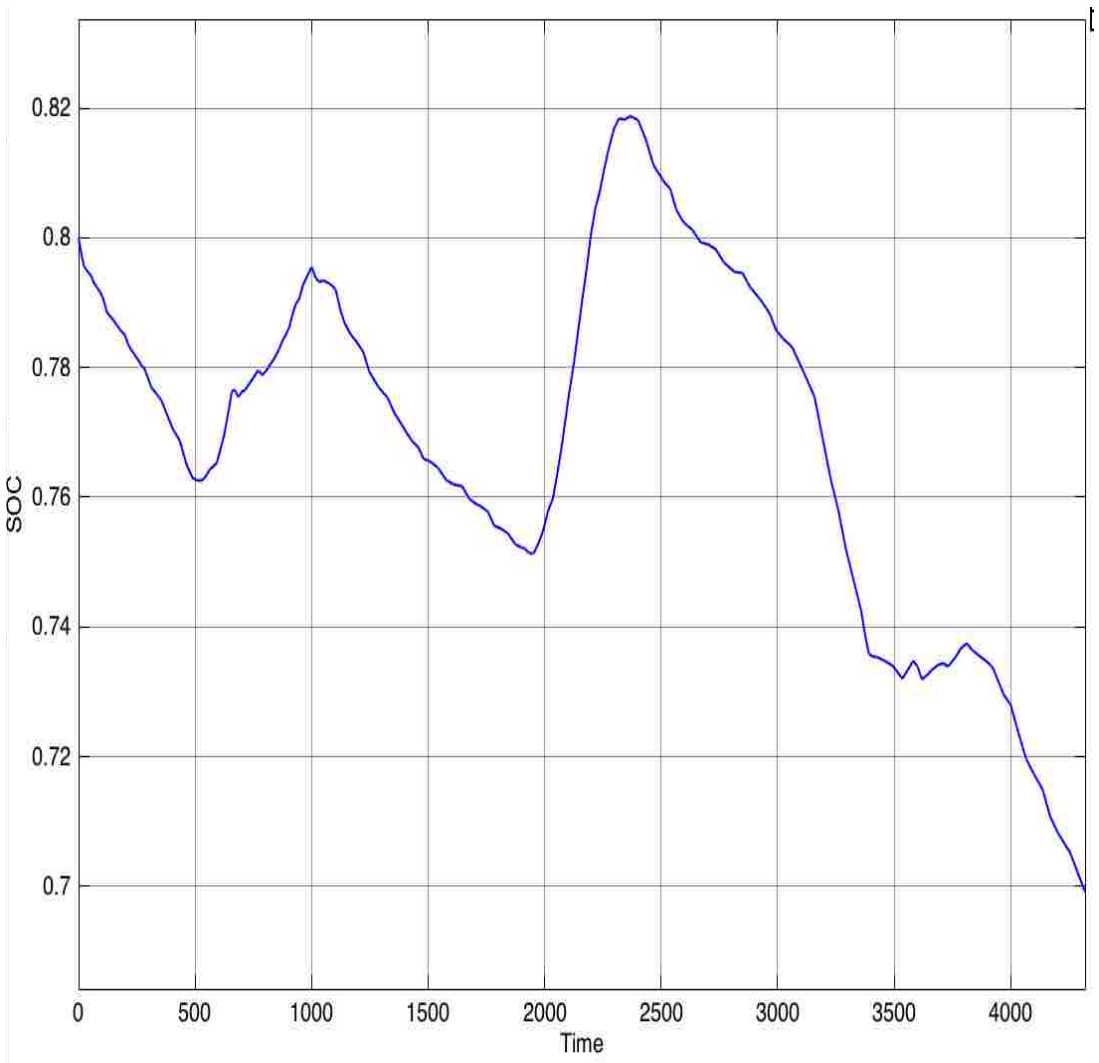

Figure 3.38. The SOC in fall.

3.5.3.3. Winter. The load and PV profiles for three days in winter are shown in Figures 3.17 and 3.18. The power of the main grid in winter is shown in Figure 3.39. The power of the grid is the average of the differences between the load and PV profile the previous day. The SOC in winter is shown in Figure 3.40. The SOC shows that the final SOC is bit lower than initial SOC by around 3% ($\Delta\, SOC \approx -3\%$). The power of main remains constant except the PV peak power time from 3pm until 7pm each day.

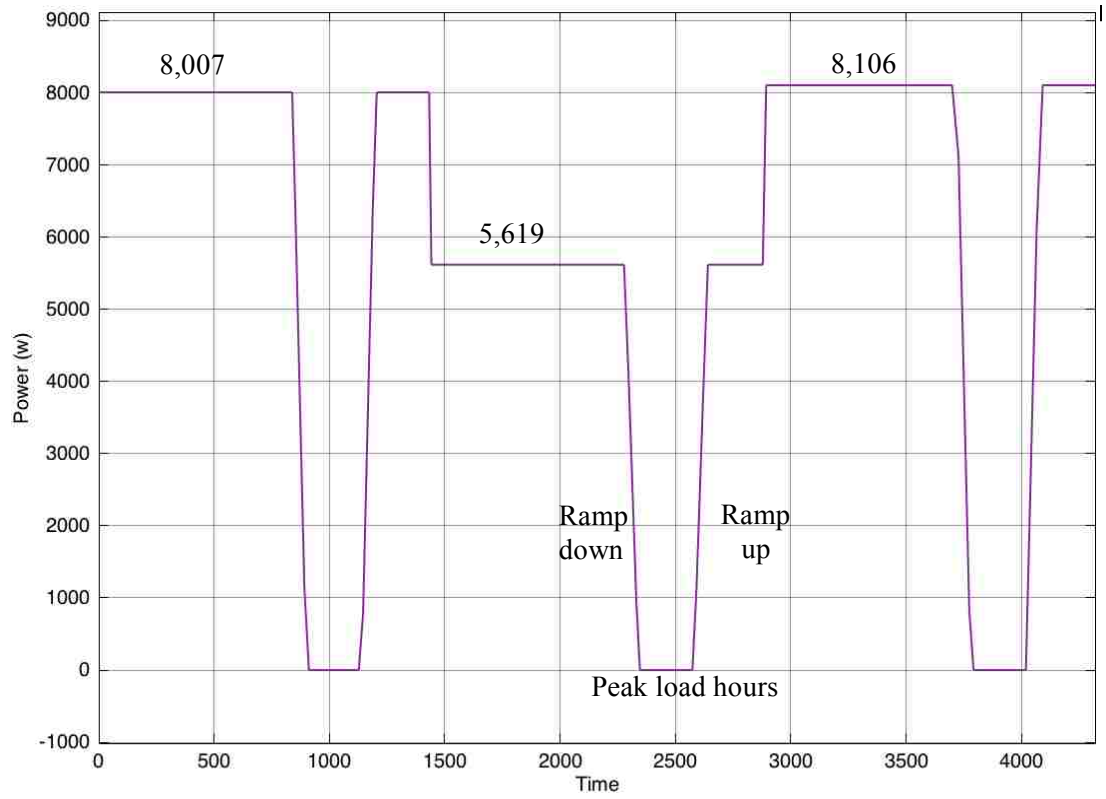

Figure 3.39. The power of the main grid in winter.

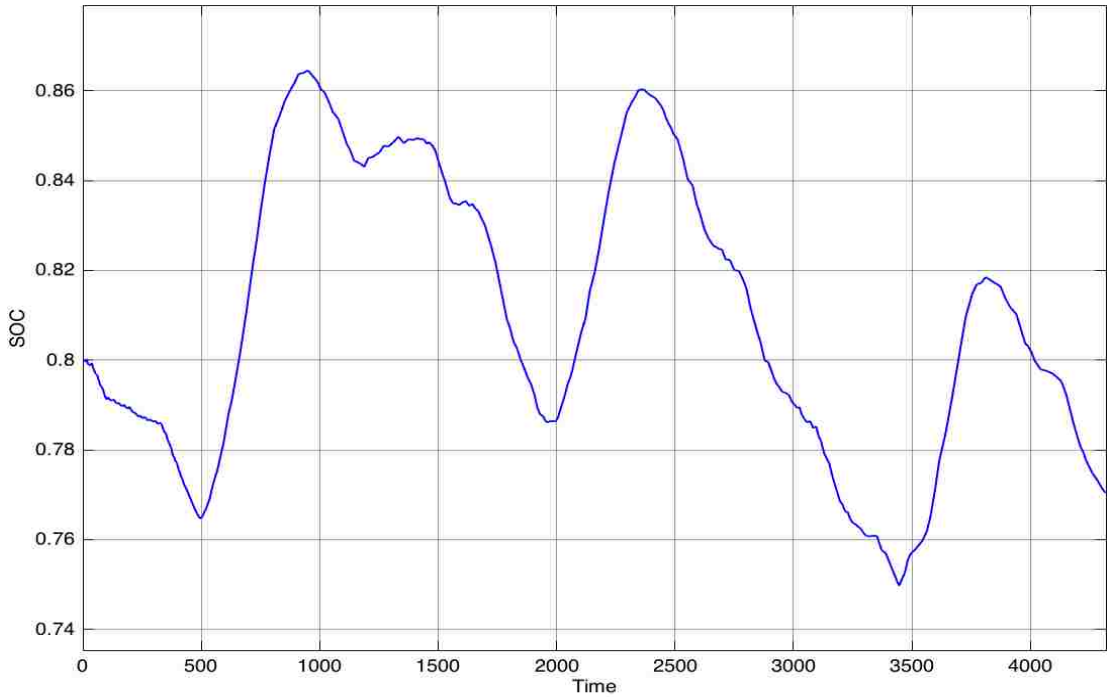

Figure 3.40. The SOC in winter.

3.5.3.4. Spring. The load and PV profiles for three days in spring are shown in Figures 3.21 and 3.22. The power of the main grid in spring is shown in Figure 3.41. The power of the grid is the average of the differences between the load and PV profile the previous day. The SOC in spring is shown in Figure 3.42. The SOC shows that the final SOC is higher than initial SOC by around 6% ($\Delta\, SOC \approx 6\%$). The power of main remains constant except the PV peak power time from 3pm until 7pm each day.

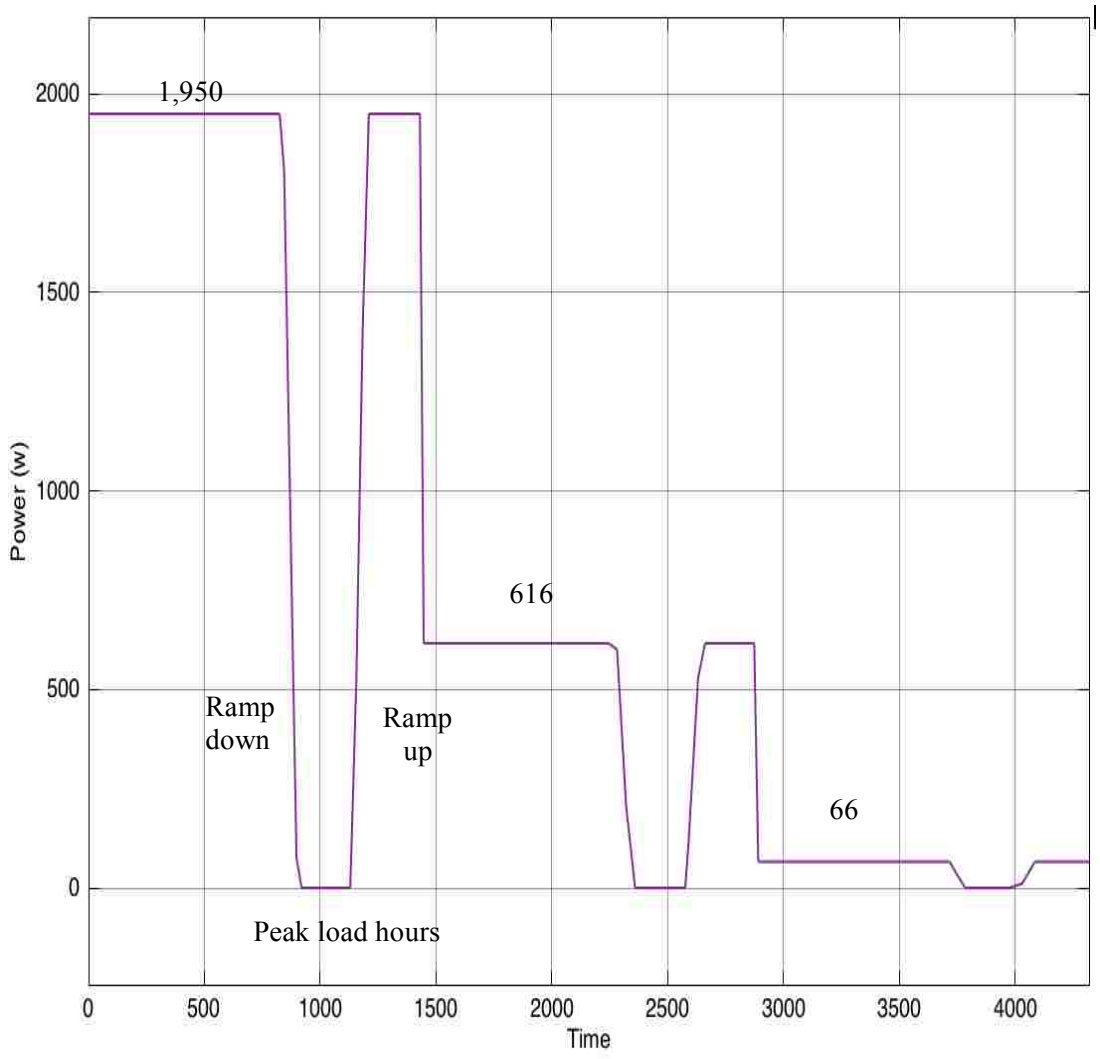

Figure 3.41. The power of the main grid in spring.

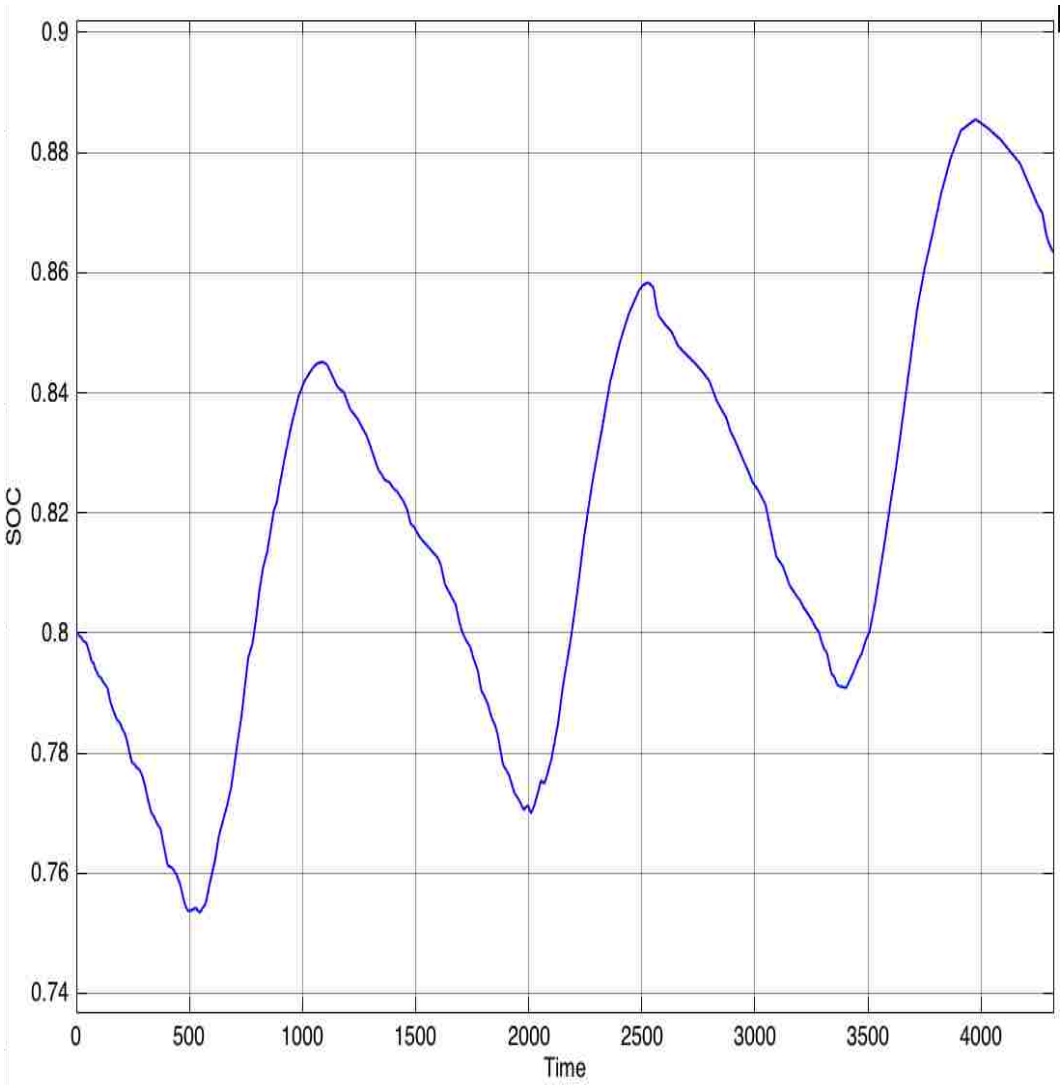

Figure 3.42. The SOC in spring.

3.5.4. SOC Control Algorithm for Peak Power Shaving Scenario. The control objective for this scenario is to demand a constant load to the main grid except for peak power demand hours. Also, the algorithm tries to control the SOC and keep it within acceptable range. The algorithm will be applied in the same way that it is used in the SOC control algorithm scenario. This scenario will be implemented for three days per season.

3.5.4.1. Summer. The load and PV profiles for three days in summer are shown in Figures 3.9 and 3.10. The power supplied by the main grid in summer is shown in Figure 3.43. The power of the grid is the average of the differences between the load and PV profile the previous day. The SOC in summer is shown in Figure 3.44. The battery SOC starts discharging with 0.8 initial value. Since the SOC within range 0.8 and 0.7, the β will be 80% of its original value. Also, in figures, once The SOC exceeds 0.8 in the PV peak power (β = 0), the system will send the power to the grid. That happened in the first and second day. The SOC shows that the final SOC is lower than initial SOC by approximately 4% ($\Delta SOC \approx -4\%$). Also, it shows that the algorithm in this scenario is controlling the SOC successfully and bringing it back to the limits.

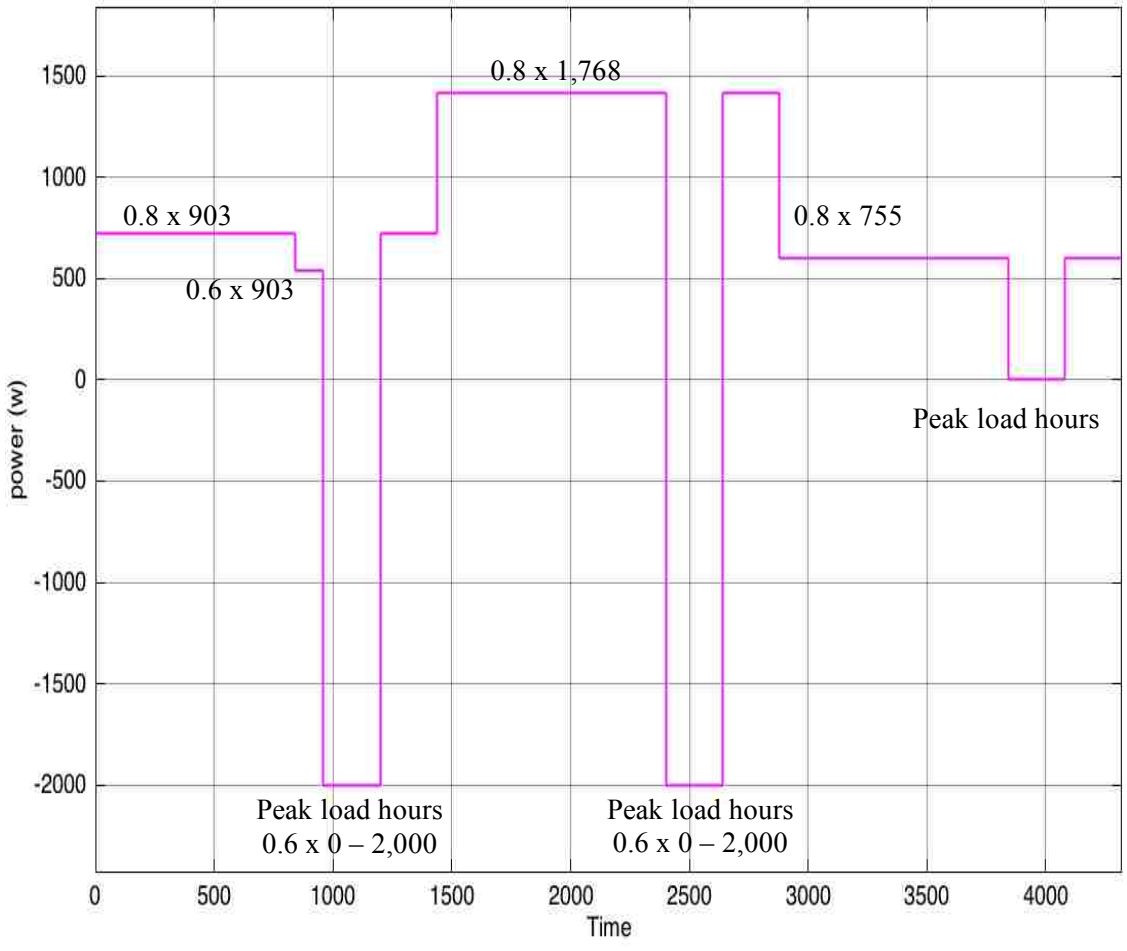

Figure 3.43. The power supplied by the main grid in summer.

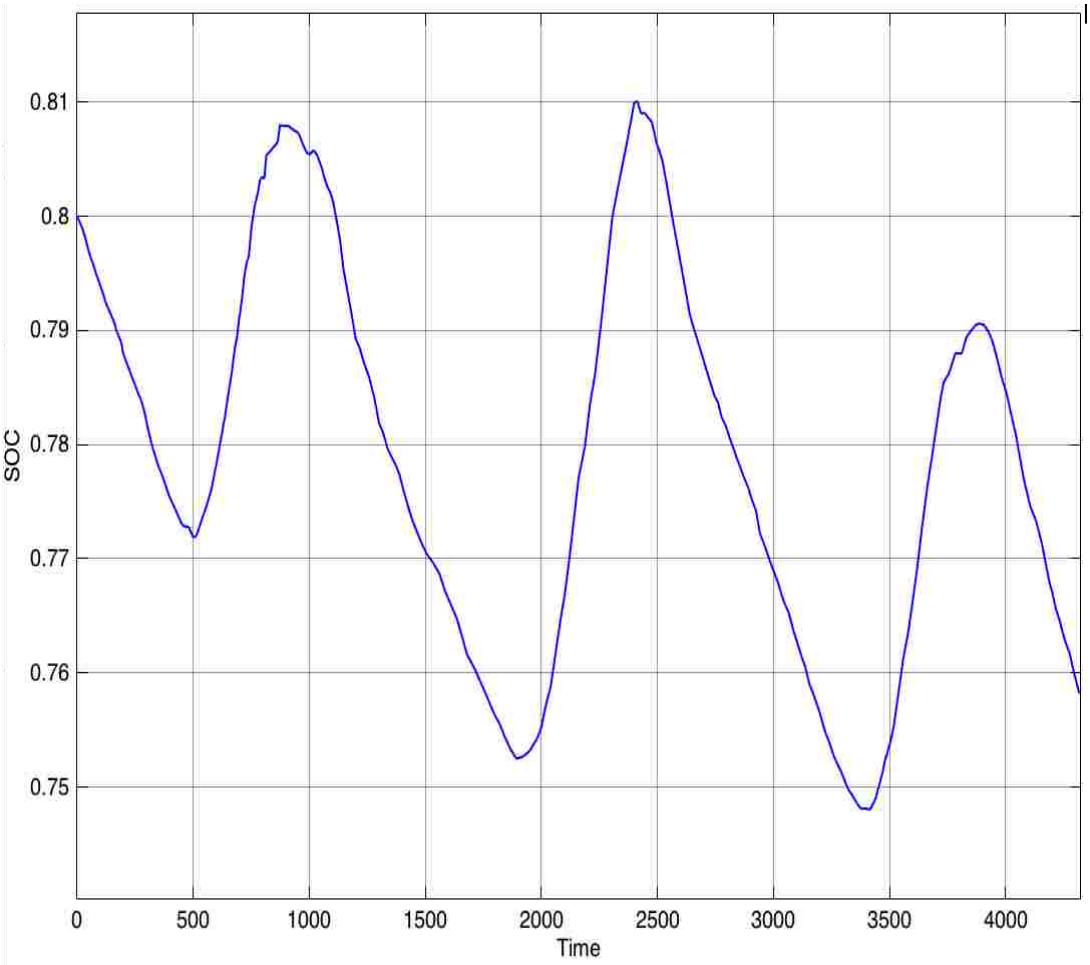

Figure 3.44. The SOC in summer.

3.5.4.2. Fall. The load and PV profiles for three days in fall are shown in Figures 3.13 and 3.14. The power supplied by the main grid in fall is shown in Figure 3.45. The power of the grid is the average of the differences between the load and PV profile the previous day. The SOC in fall is shown in Figure 3.46. The SOC is maintained between 0.8 and 0.7 except the middle of second day and the end of third day. In the middle of second day, the power of the main grid is 60% of β ,and then -2,000 for the PV peak power time when the SOC exceed the 0.8 level. At the end of the third day, the SOC decreased below 0.7 which means the grid power will return to the original β. Also, The SOC shows that the final SOC is much lower than initial SOC by approximately 12% ($\Delta\, SOC \approx -12\%$).

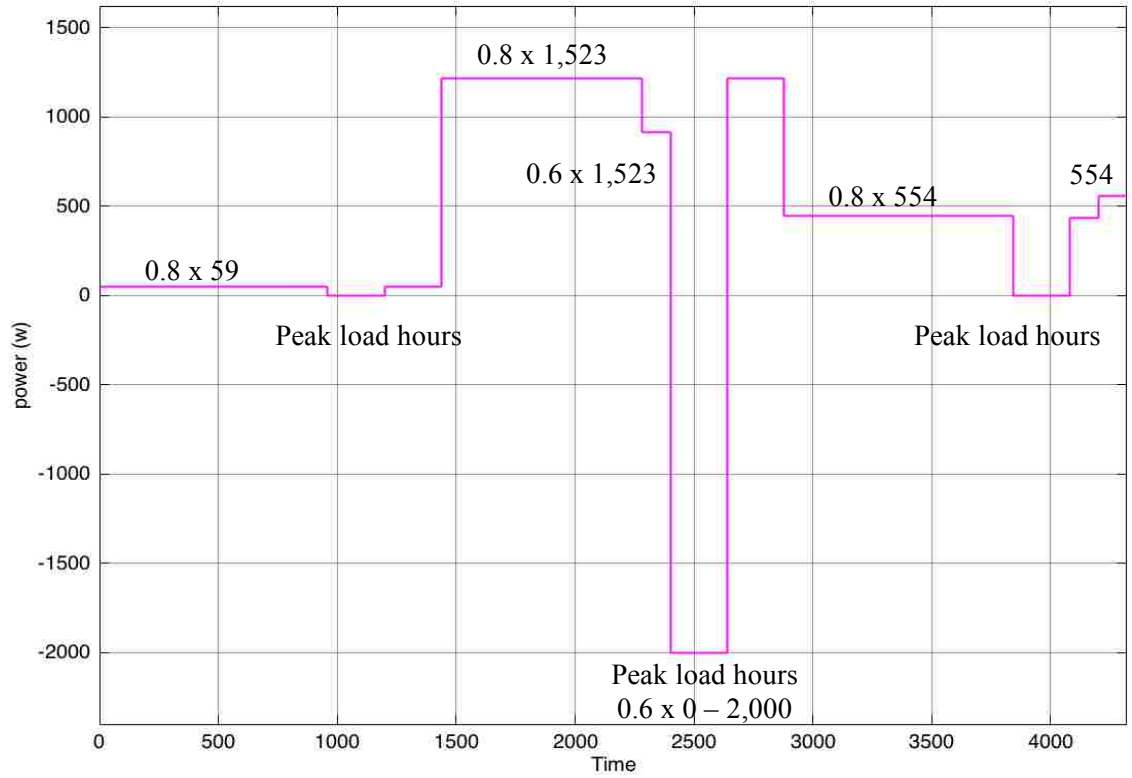

Figure 3.45. The power supplied by the main grid in fall.

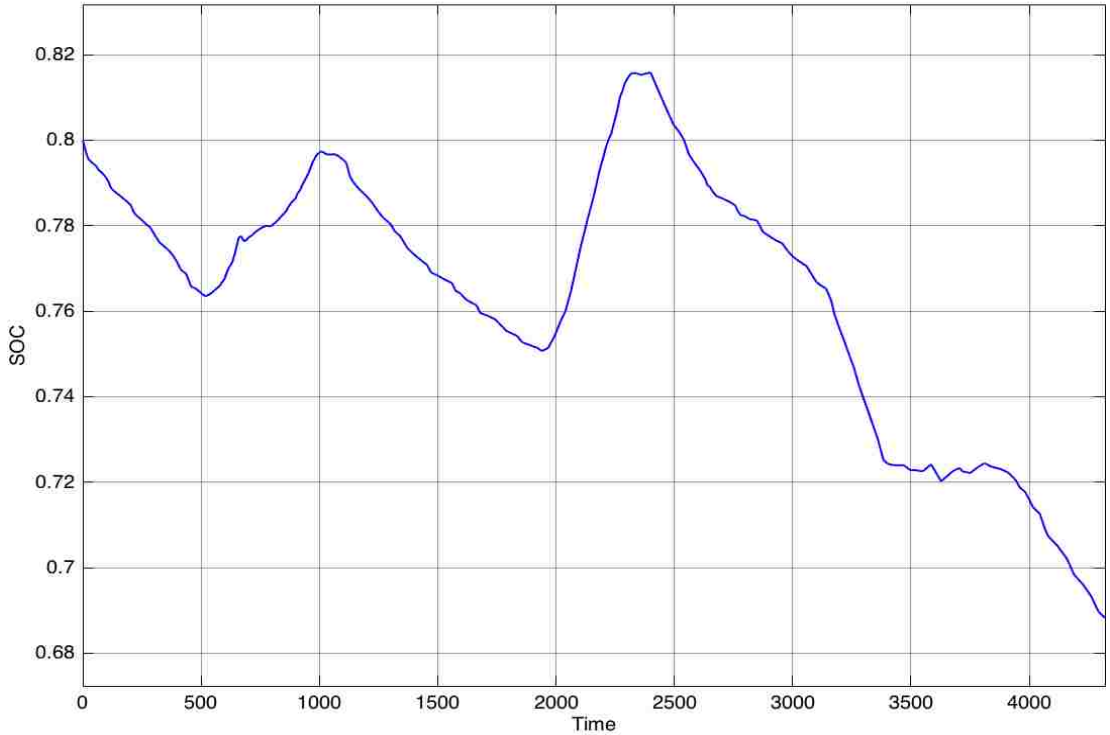

Figure 3.46. The SOC in fall.

3.5.4.3. Winter. The load and PV profiles for three days in winter are shown in Figures 3.17 and 3.18. The power of the main grid in winter is shown in Figure 3.47. The power of the grid is the average of the differences between the load and PV profile the previous day. The SOC in winter is shown in Figure 3.48. The battery SOC starts discharging with 0.8 initial value. Since the SOC within range 0.8 and 0.7, the β will be 80% of its original value. Also, once The SOC exceeds the 0.8 in the peak PV generation, the power of main grid will be -2,000. Thus, the microgrid system is sending the power to the grid. And, when the SOC below 0.7, the grid power will go back to its original value to ensure that the SOC of the battery is maintained within reasonable range. The SOC shows that the difference between the final SOC and initial SOC is around 13% ($\Delta\, SOC \approx -13\%$).

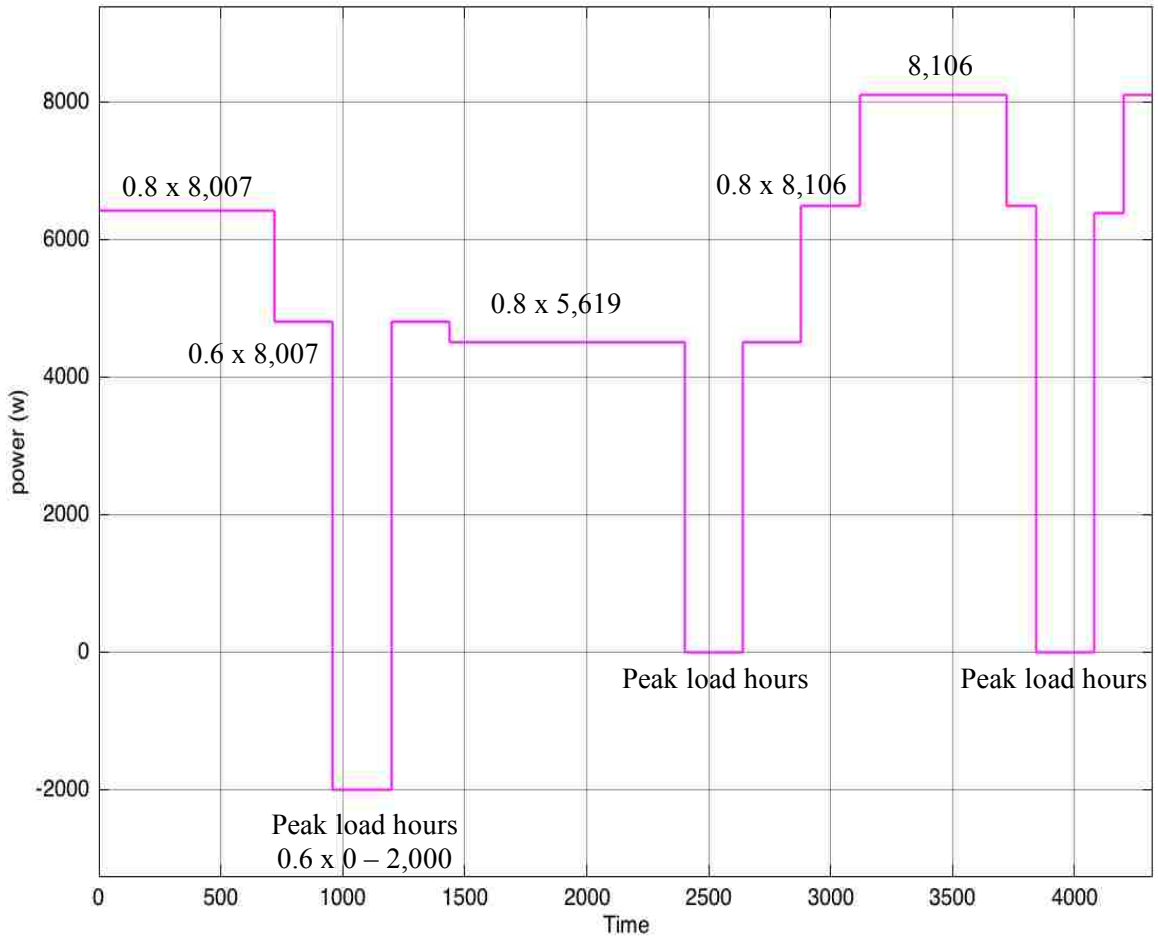

Figure 3.47. The power of the main grid in winter.

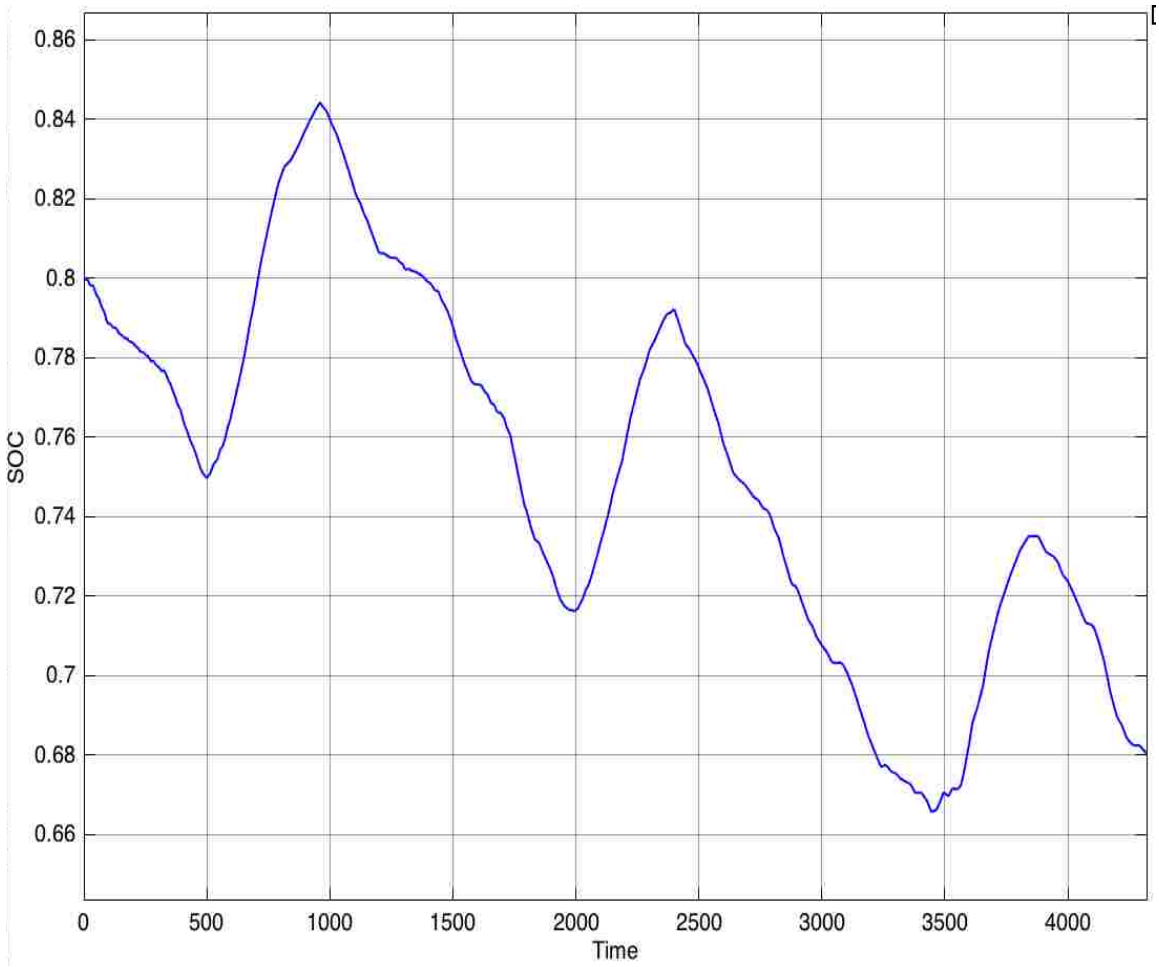

Figure 3.48. The SOC in winter.

3.5.4.4. Spring. The load and PV profiles for three days in spring are shown in Figures 3.21 and 3.22. The power supplied by the main grid in spring is shown in Figure 3.49. The power of the grid is the average of the differences between the load and PV profile the previous day. The SOC in spring is shown in Figure 3.50. The battery SOC starts discharging with 0.8 initial value. Since the SOC within range 0.8 and 0.7, the β will be 80% of its original value. Also, once The SOC exceeds the 0.8 in the peak PV generation, the power of main grid will be -2,000 which means the microgrid system is sending the power to the grid. In the third day, the β is less than 200 and the SOC within 0.8 and 0.9. therefore, the exported power to the grid will be 60% of the original β minus 2000. The SOC shows that the difference between the final SOC and initial SOC is around 1% ($\Delta\, SOC \approx -1\%$).

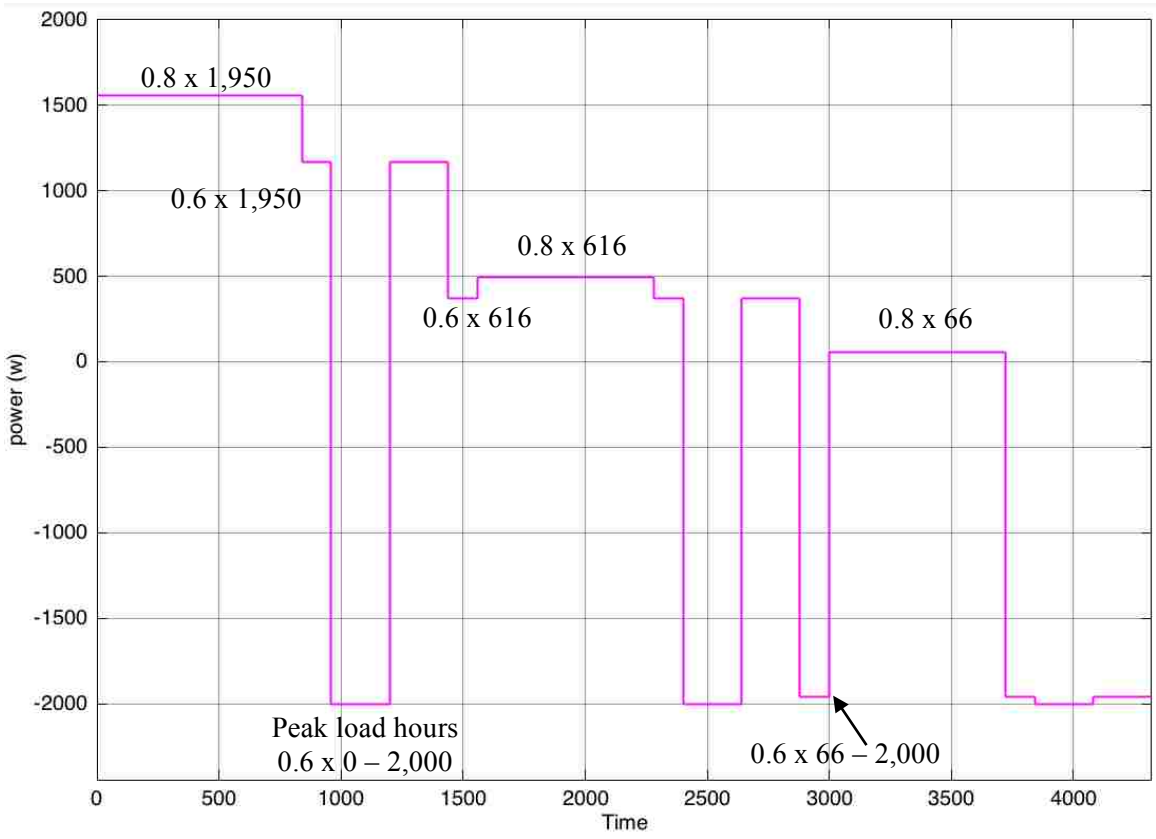

Figure 3.49. The power supplied by the main grid in spring.

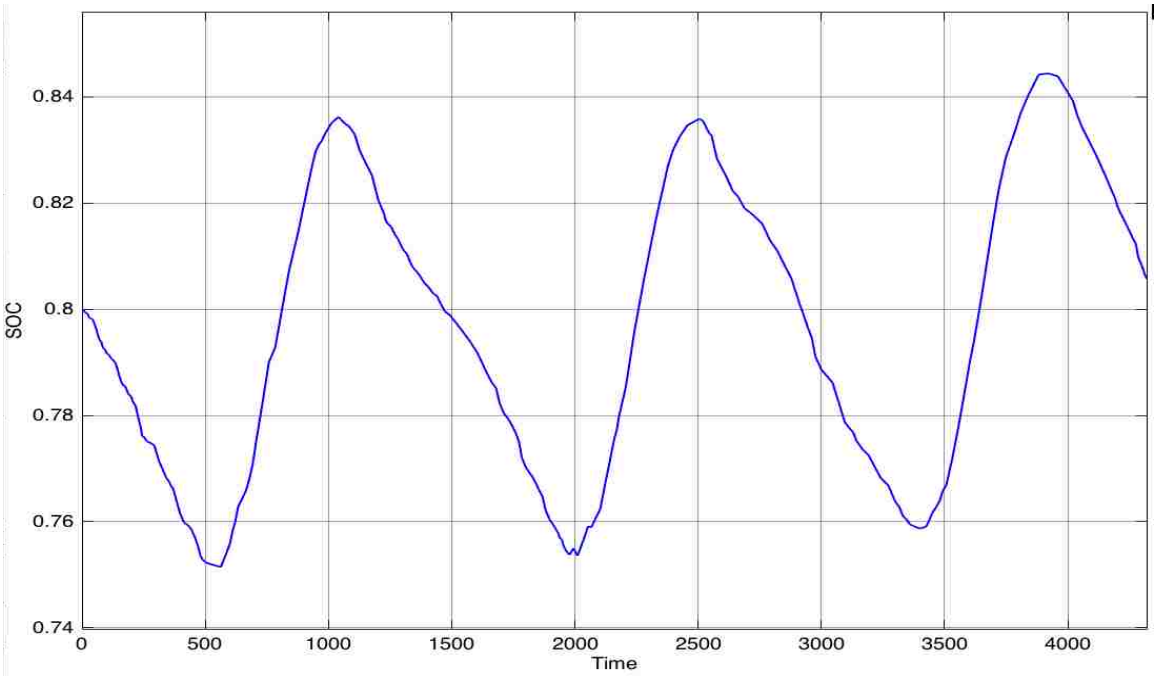

Figure 3.50. The SOC in spring.

3.6. COMPARISONS BETWEEN SCENARIOS

This section will combine all the SOCs of the scenarios in different seasons to see the differences and determine the best scenario for each season. The SOC for the scenarios in summer is shown in Figure 3.51. The SOC for fall is shown in Figure 3.52, the SOC for winter is shown in Figure 3.53, and the SOC for spring is shown in Figure 3.54. The figures show that the algorithm is controlling and managing SOC successfully. And, it is able to maintain the SOC within limits even though the initial SOC was 80%.

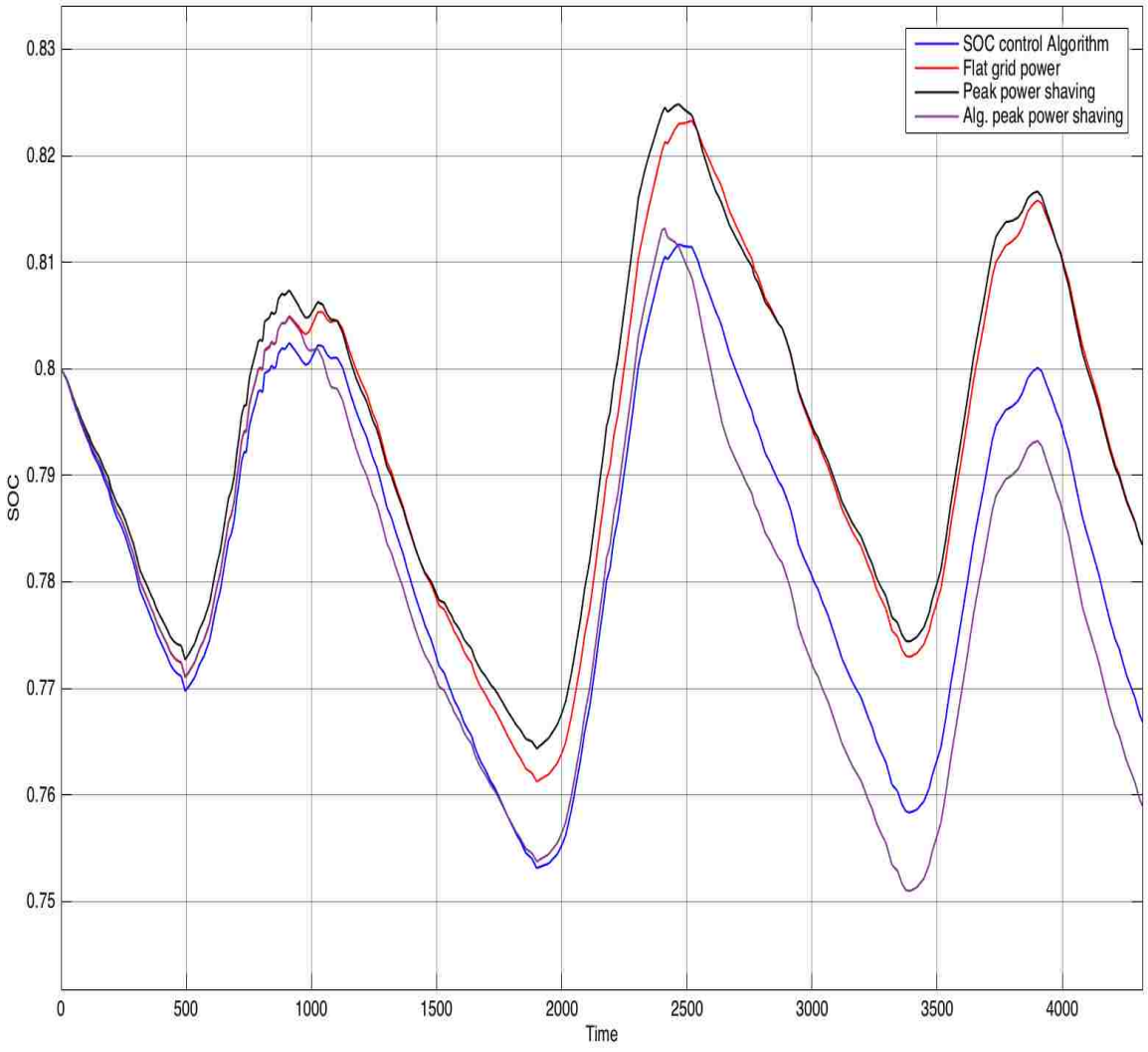

Figure 3.51. The SOC for the scenarios in summer.

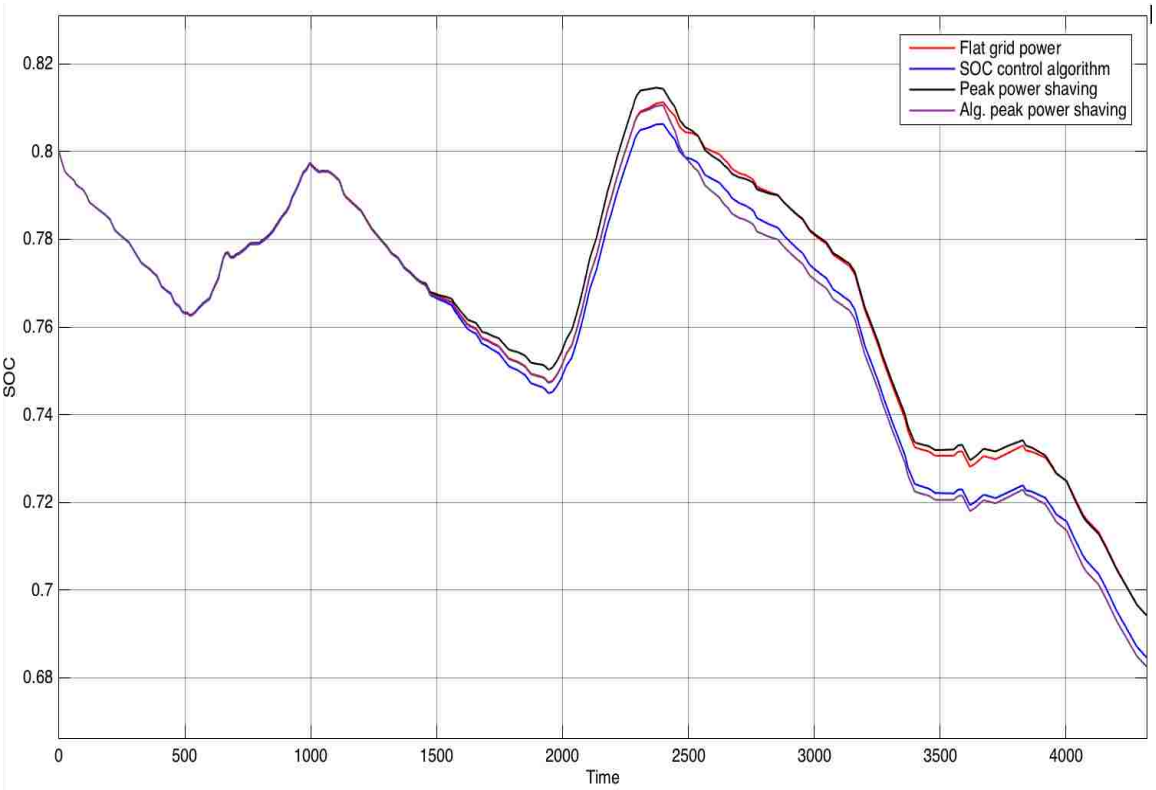

Figure 3.52. The SOC for fall.

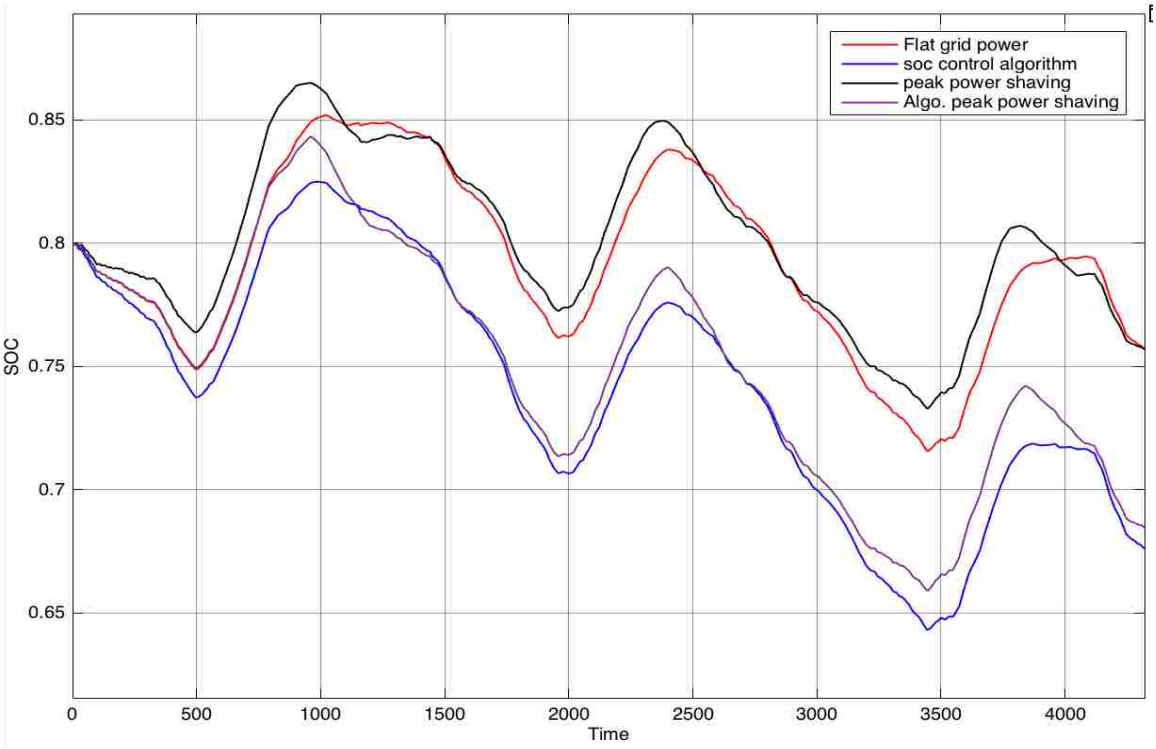

Figure 3.53. The SOC for winter.

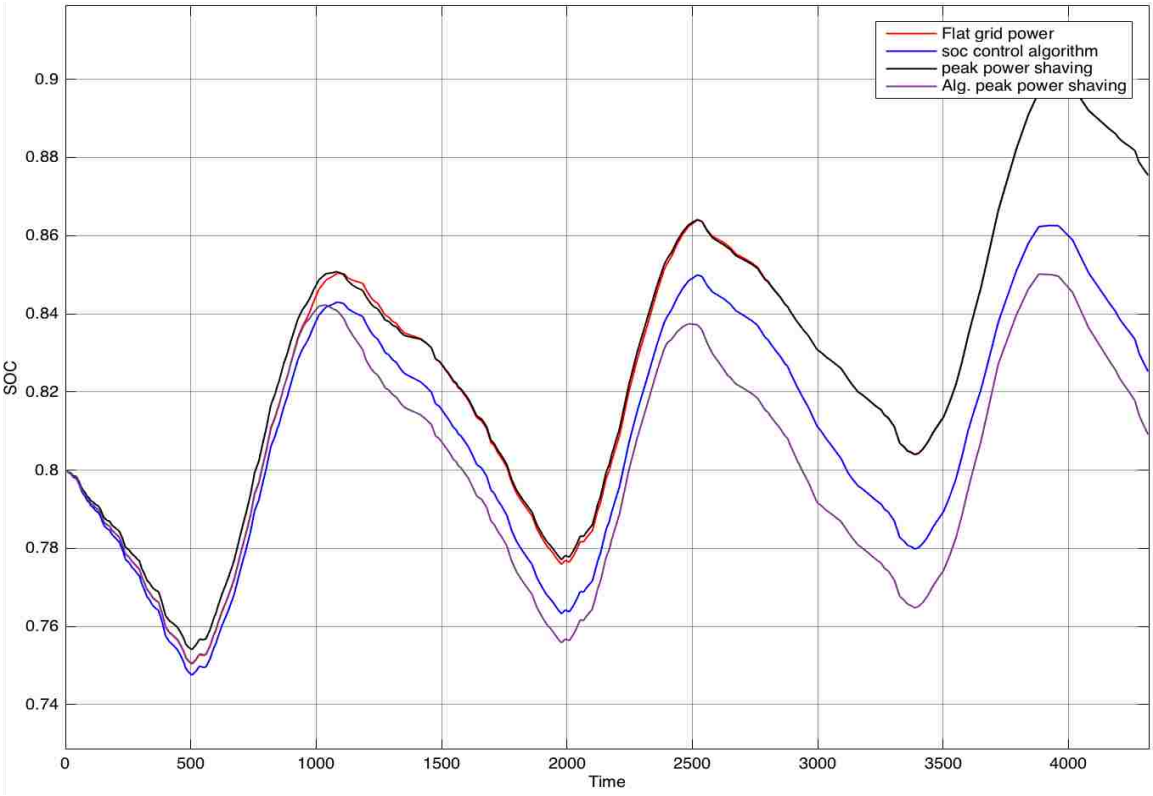

Figure 3.54. The SOC for spring.

4. CONCLUSION

This thesis presents the definition of a microgrid and how a microgrid system and distributed generators with the existence of a main grid interact with one another. In addition, the thesis also discusses certain microgrid and distributed generator components. The grid-connected and islanded modes of operation have been defined and discussed along with various types of microgrid controls. Models and simulations involving microgrids and particular scenarios allow researchers to ensure that challenges are properly addressed before new and improved microgrid systems are constructed. The simulation using the solar village constructed by the solar house team from Missouri S&T has provided a great model to enhance component functions of the system.

The main goal for this thesis is to control the battery of the microgrid system of the solar village at Missouri S&T. The thesis began with an overview involving the architecture and components of the solar village's microgrid. The Milbank Company built the microgrid system in the solar village and created very intelligent switchgear hardware. The company uses web portal software to monitor the power in the solar village.

The batteries in the solar village are currently managed by a code called SNTBatt. This code is a custom program that was written specifically by the manufacturer for the solar village at the Missouri University of Science and Technology and is used to manage and control the batteries and inverter. The code is separate from the IATS code which is responsible for reading and managing the switchgear system.

In this thesis, the simulation of the solar village was designed using MATLAB and the algorithm for energy management was written using MATLAB function. The simulation used realistic load and PV profile. They are obtained by Milbank.

Four energy management scenarios are simulated and the results of the simulations are discussed. each scenario has a specific control objective. State of charge plays a critical role in the control algorithm. The results of the simulation provide evidence regarding how certain state of charge control algorisms could play a role in charging and discharging the battery to manage grid interactions.

The solar generation and load profile of three consecutive days per season were selected for all the scenarios. In all cases, the average of load is greater than the average of solar generation. First, the flat grid power scenario objective was preferred to create a constant load to the main grid, and, therefore, the main grid provides constant power for the system. Second, the SOC control algorithm scenario aimed to manage SOC and adjust the grid power accordingly. It was controlling SOC effectively and bringing it back to limits. Third, the peak power shaving scenario is chosen to create a constant load for the main grid with the exception of the peak load power hours. Finally, SOC control algorithm for peak power shaving scenario aimed to demand a constant load to the main grid except for peak power demand hours. Also, the algorithm was efficient in this scenario to control the SOC and keep it within reasonable range.

BIBLIOGRAPHY

[1] A. Banerji, D. Sen, A. K. Bera, D. Ray, D. Paul, A. Bhakat, and S. K. Biswas, "Microgrid: a review," Global Humanitarian Technology Conference: South Asia Satellite (GHTC-SAS) IEEE, 2013, pp. 27-35.

[2] Ali Keyhani, Mohammad N. Marwali, and Min Dai, "Integration Of Green And Renewable Energy In Electric Power Systems," John Wiley & Sons, 2010.

[3] N. Hatziargyiou, H. Asano, R. Iravani, and C. Marnay, "Microgrids," IEEE Power and Energy Magazine, vol. 5, no. 4, pp.78-94, July/August 2007.

[4] R. Zamora and A. K. Srivastava, "Controls for microgrids with storage: Review, challenges, and research needs," Renewable and Sustainable Energy Reviews, vol. 14, issue 7, pp. 2009–2018, Sep. 2010.

[5] R. Lasseter, A. Akhil, C. Marnay, J. Stephens, J. Dagle, R. Guttromson, A. Sakis Meliopoulous, R. Yinger, and J. Eto, "Integration of Distributed Energy Resources – The MicroGrid Concept," CERTS MicroGrid Review Feb 2002.

[6] B. Lasseter, "Microgrids (Distributed Power Generation)," Proceedings of the IEEE PES Winter Meeting, Vol. 1, 2001, pp. 146-149.

[7] R. H. Lasseter and P. Piagi, "Microgrid: A Conceptual Solution," PESC'04, Aachen, 20-25 June 2004.

[8] M. Mahmoud, S. Hussain, and M. Abido, (2014, May). "Modeling and control of microgrid: An overview," Renewable Energy, [On-line], Available: www.sciencedirect.com. [Nov. 1, 2015].

[9] S. Najar. "Renewable energy," Internet: http://www.synergyenviron.com, Oct.25, 2014.[March. 1, 2016].

[10] M. Ferdowsi. EE 5510, Class Lecture, Topic: "Fuel cell," Electrical Engineering building, Missouri University of science and technology, Rolla, Missouri, 2014.

[11] K. Youssefi, "Altrnative Sources of energy," Internet: http://engineering.sjsu.edu/e10/wp content/uploads/Wind_Power_S13.pdf, March. 24, 2016 [April, 2015].

[12] D. Hart. Power Electronics. United States, Indiana: MC Grew Hill, 2010, pp. 65-111.

[13] S. Vazquez, S. M. Lukic, E. Galvan, L. G. Franquelo, J. M. Carrasco, "Energy Storage Systems for Transport and Grid Applications," IEEE Trans. on Industrial Electronics, vol. 57, no. 12, pp. 3881 - 3895, Dec 2010.

[14] S. Youli, Z. Litifu, and K. Nagasaka, “Efficiency of microgrid with storage battery in reliability, economy and environment assessments,” Int J Electr and Power Eng; vol.3, no. 3, pp.154–162, 2008.

[15] PJ. Hall, EJ. Bain, “Energy-storage technologies and electricity generation,” Energy Policy, vol. 36, no. 12, pp. 4352–4355, 2008.

[16] RS. Bhatia, SP. Jain, DK. Jain, and B. Singh, “Battery energy storage system for power conditioning of renewable energy sources,” In: Proceedings of the IEEE international conference on power electronics and drives systems, 2005, pp. 501–506.

[17] R. Lasseter, A. Akhil, C. Marnay, J. Stephens, J. Dagle, R. Guttromson, A. S. Meliopoulous, R. Yinger, and J. Eto, “White paper on Integration of Distributed Energy Resources,The CERTS MICROGRID Concept,” Consultant Report California Energy Commission, U.S. Department of Energy, Berkeley, CA, LBNL-50829, April 2002.

[18] R. H. Lasseter, “Microgrid,” in Proc. IEEE Power Emg. Soc. Winter Meeting, vol. 1, New York, 2002, pp. 305-308.

[19] F. Katiraei, M. R. Iravani and P. W. Lehn, “Micro-Grid Autonomous Operation During and Subsequent to Islanding Process,” IEEE Trans. Power Del., vol. 20, no. 1, Jan. 2005.

[20] P. Piagi and R. H. Lasseter, “Autonomous Control of Microgrids,” IEEE PES Meeting, Montreal, June 2006.

[21] N. Pogaku, M. Prodanovic and T. C. Green,“Modeling, Analysis and Testing of Autonomous Operation of an Inverter-Based Microgrid,” IEEE Trans.on Power Electronics, vol. 22, no. 2,pp.613-625, Mar. 2007.

[22] S. Chakraborty and M. G. Sim˜oes, “Experimental Evaluation of Active Filtering in a Single Phase High- Frequency AC Microgrid,” IEEE Trans. On Energy Conversion, vol. 24, no. 3, pp. 673 682, Sept. 2009.

[23] S. Chakraborty, M. D. Weiss, and M. G. Simões, “Distributed intelligent energy management system for a single phase high frequency AC Microgrid,” IEEE Trans. Ind. Electron., vol. 54, no.1, pp. 97-109, Feb. 2007.

[24] H. Kakigano, Y. Miura and T. Ise, T. Momose, and H. Hayakawa, “Fundamental Characteristics of DC Microgrid for Residential Houses with Cogeneration System in Each House,” in Proc. IEEE PESGM, 08GM0500, 2008.

[25] A. Kwasinski and C. N. Onwuchekwa, “Dynamic Behavior and Stabilization of DC Microgrids With Instantaneous Constant-Power Loads”, IEEE Trans. Power Electron. Vol. 26, no.3, pp. 822 834, March 2011.

[26] A. Kwasinski, "Quantitative evaluation of DC Microgrids Availability: Effect of System Architecture and Converter Topology Design Choices," IEEE Trans. Power Electron. Vol. 26, no.3, pp. 835 – 851, March 2011.

[27] R. S. Balog and P. T. Krein, "Bus selection in Multibus DC Microgrid," IEEE Trans. Power Electron, vol. 26, no.3, pp. 860-867, March 2011.

[28] H. Kakigano, Y. Miura, and T. Ise, "Loss Evaluation of DC Distribution for Residential Houses Compared with AC System," The 2010 International Power Electronics Conference- ECCE Asia-(IPECSapporo), 22A1-3, 2010, pp. 480-486.

[29] H. Kakigano, Y. Miura, and T. Ise, "Low-Voltage Bipolar-Type DC Microgrid for Super High Quality Distribution," IEEE Trans. Power Electron. Vol. 25, no. 12, pp. 3066 - 3075, Dec. 2010.

[30] H. Kakigano, Y. Miura, and T. Ise, "Configuration and control of a DC microgrid for residential houses," Transmission & Distribution Conference & Exposition: Asia and Pacific, Oct. 2009, pp.1-4.

[31] H. Kakigano, Y. Miura, and T. Ise, "Distribution Voltage Control for a DC Microgrid using Fuzzy Control and a Gain –Scheduling Technique," IEEE Trans. Power Electron., vol. 28, no. 5, pp. 2246 –2258, May 2013.

[32] K. Kawasaki, S. Matsumura, K. Iwabu, N. Fujimura, and T. Iima, "Autonomous dispersed control system for independent micro grid," Electr Eng Jpn, vol. 166, no. 1, 2009.

[33] B. Buchholz, T. Erge, and N. Hatziargyriou, "Long term European field tests for microgrids," In: Proceedings of the power conversion conference, 2007, pp.643–645.

[34] IA. Hiskens, and EM. Fleming, "Control of inverter-connected sources in autonomous microgrids," In: Proceedings of the American control conference,pp. 586–590, 2008.

[35] MA. Pedrasa and T. Spooner, (2006), "A survey of techniques used to control microgrid generation and storage during island operation," Proc Australian Universities Power Engineering Conference. [On-line]. Available: http://www.itee.uq.edu.au/_aupec/aupec06/htdocs/content/pdf/30.pdf.

[36] NL. Soultanis and ND. Hatziargyriou, "Dynamic simulation of power electronics dominated micro-grids," In: Proceedings of the IEEE PES general meeting, 2006.

[37] A. Engler, "Applicability of droops in low voltage grids," Int J Dist Energy Resour, vol. 1, no. 1, pp.3–5, 2005.

[38] S. Chakraborty, MD. Weiss, and MG. Simo˜es, “Distributed intelligent energy management for a single phase high-frequency AC microgrid,” IEEE Trans Ind Electron, vol. 54, no. 1, 2007.

[39] P. Piagi, (2005), “Microgrid control,” PSERC Tele-Seminar Presentation. [On-line]. Available: http://www.pserc.org/ecow/get/generalinf/presentati/psercsemin1/2psercsemin/piagi_seminar_slides_june_2005.pdf.

[40] JA. Pecas Lopes, CL Moreira, and FO. Resende, “Control strategies for microgrids black start and islanded operation,” Int J Distr Energy Resour, vol. 2, no. 3, pp. 211–231, 2006.

[41] JA. Pecas Lopes, CL. Moreira, AG. Madureira, FO. Resende, X. Wu, N. Jayawarna, and AL. et, “Control strategies for MicroGrids emergency operation,” In: Proceedings of the international conference on future power systems; 2005.

[42] N. Hatziargyriou. (2005) “Active distribution network.” The Effect of Distributed and Renewable Generation on Power Systems Security Round Table. [On-line]. Available: http://www.microgrids.eu/micro2000/presentations/21.pdf.

[43] N. Hatziargyriou, A. Dimeas, and A. Tsikalakis, “Centralized and decentralized control of microgrids,” Int J Dist Energy Resour, vol. 1, no. 3, pp. 197–212, 2005.

[44] AG. Tsikalakis and ND. Hatziargyriou, “Centralized control for optimizing microgrids operation,” IEEE Trans Energy Convers, vol. 23, no. 1, pp. 241–248, 2008.

[45] T. Logenthiran, D. Srinivasan, and D. Wong, “Multi-agent coordination for DER in MicroGrid,” In: Proceedings of the IEEE international conference on sustainable energy technology, 2008, pp. 77–82.

[46] K. De Brabandere, K. Vanthournout, J. Driesen, G. Deconinck, and R. Belmans, “Control of microgrids.” In: Proceedings of the IEEE PES general meeting, 2007, pp. 1–7.

[47] Microgrid examples, “Building Microgrid,” Internet: https://building-microgrid.lbl.gov/new-york-university [March 24, 2016].

[48] MST, “Missouri S&T Solar Village,” internet: http://ose3.mst.edu/ose3home/energy/solarvillage/ [March 22, 2016].

[49] A123 systems CO., “Grid Battery Rack Installation and Operation Guide,” US, 2009.

[50] Dynapower CO., “50kw/KVA Bi-directional Inverter,” US, Oct. 18, 2013.

[51] M. Ferdowsi. EE 5510, Class Lecture, Topic: “Battery,” Electrical Engineering building, Missouri University of science and technology, Rolla, Missouri, 2014.

[52] Math works, “Battery,” Internet: http://www.mathworks.com/help/physmod/sps/powersys/ref/battery.html, Mar. 27, 2016 [Mar. 25, 2016].

[53] Milbank CO. drown by J. Bridges, “MST Solar Village one line,” US, Sep. 3, 2013.

[54] R. Zamora and A. K. Srivastava, “Energy Management and Control Algorithms for Integration of Energy Storage Within Microgrid” 2014 IEEE 23rd International Symposium on Industrial Electronics (ISIE), 2014, pp. 1805–1810.

[55] K. N. Hasan, M. E. Haque, M. Negnevitsky, and K. M. Muttaqi, "Control of Energy Storage Interface with a Bidirectional Converter for Photovoltaic Systems," presented at 2008 Australasian Universities Power Engineering Conference (AUPEC'08), Dec. 2008.

[56] Clear Edge power CO., “Product Data and Applications Guide, The pure Cell Model 5 Fuel Cell System,” US, June 7, 2013.

[57] Dr. Jonathan Kimball. “Bi-directional Inverter” Personal e-mail (June 2, 2016).

VITA

Hamad Ahmed Alharkan was born on July 2, 1988 in Al-Qassim, Saudi Arabia. He received his Bachelor of Engineering degree in Electrical Engineering from Alqassim University located in Alqassim, Saudi Arabia in June 2012. Since 2013, he has been a teaching assistant in the Electrical Engineering Department at Alqassim University. In 2014, he began working toward his M.Sc. degree in Electrical Engineering at Missouri University of Science and Technology under the direction and guidance of his advisor Prof. Mehdi Ferdowsi. He has obtained his Master's degree in July 2016.